

**LMI-BASED CONTROL OF NONLINEAR TIME-
DELAY MODEL FOR "TYPE 1-DIABETIC
PATIENT"**

BY

HOSAM ABDUL RAHIM FAREED ARABASY

A Thesis Presented to the
DEANSHIP OF GRADUATE STUDIES

KING FAHD UNIVERSITY OF PETROLEUM & MINERALS
DHAHRAN, SAUDI ARABIA

In Partial Fulfillment of the
Requirements for the Degree of

MASTER OF SCIENCE
In
SYSTEMS ENGINEERING

JUNE 2009

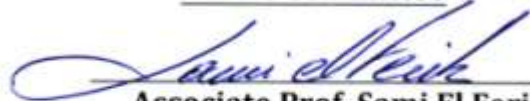
KING FAHD UNIVERSITY OF PETROLEUM & MINERALS

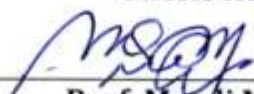
Dhahran 31261, Saudi Arabia

DEANSHIP OF GRADUATE STUDIES

This thesis, written by **HOSAM ABDUL RAHIM ARABASY** under the direction of his advisor and approved by his thesis committee, has been presented to and accepted by the Dean of Graduate Studies, in partial fulfillment of the requirements for the degree of **MASTER OF SCIENCE IN SYSTEM ENGINEERING**

Thesis Committee


Associate Prof. Sami El Ferik
Thesis Advisor



Prof. Magdi Mahmoud
Thesis Co-Advisor



Associate Prof. Laltouari Cheded
Member


Assistant Prof. Samir Al-Amer
Member


Assistant Prof. Muhammad
Mysorewala
Member


Prof. Fouad Al-Sunni
Department Chairman


Dr. Salam A. Zummo
Dean Of Graduate Studies


Date

DEDICATION

To all of my family, wife and son.

ACKNOWLEDGEMENTS

All praise to Allah, the Cherisher and Sustainer of the worlds, none is worthy of worship but Him. Blessings and peace upon Prophet Mohammad, the mercy for all the creatures. I would like first to sincerely thank my advisor, Dr. Sami El Ferik, and the co-advisor, Prof. Magdi Mahmoud, for their unlimited and invaluable support, help and continuous guidance. They have been encouraging me to develop new research field and interested control techniques.

Many thanks to all the thesis committee members, Dr. Lahouari Cheded, Dr. Samir Al-Amer, and Dr. Muhammad Mysorewala, for their valuable comments and suggestions that enhance the quality of the work.

Thanks are also due to the Systems Engineering Department faculty members, from whom I have learned remarkable topics. I gratefully acknowledge the support and help of all my colleagues, especially Eng. Ali Elrayyah who has spent his valuable time giving me some important hints and guidelines.

Above the all, I would like to express my deep appreciation to my lovely wife and son for their patience, continuous encouragement, and valuable support till I finished this work.

Finally, I would like to express my utmost gratitude to my parents and all my family members for their support and prayers that have helped me throughout my study.

TABLE OF CONTENTS

DEDICATION.....	iii
ACKNOWLEDGEMENTS	iv
TABLE OF CONTENTS	v
LIST OF TABLES.....	viii
LIST OF FIGURES	ix
THESIS ABSTRACT (English).....	xii
THESIS ABSTRACT (Arabic).....	xiii
Chapter 1 MEDICAL BACKGROUND	1
1-1 Introduction	1
1-2 Blood Glucose Classification	2
1-3 Types of diabetes.....	3
1-4 Insulin-Glucose Control in Healthy Individuals.....	6
1.5 Insulin Therapy for Type-1 Diabetic patients.....	12
Chapter 2 GLUCOSE-INSULIN MODELS	17
2-1 Introduction	17
2-2 Ordinary Differential Equations (ODEs).....	18
2-2-1 Nonlinear Model	19
2-2-2 Bergman Minimal Model	21
2-2-3 Six-Dimensional model ODEs.....	25
2-3 Models in the form of Delay Differential Equations (DDEs).....	28
2-3-1 Single explicit time delay DDEs model.....	29
2-3-2 Two explicit time delay DDEs models.....	30
2-3-3 Alternative explicit time delay DDEs models.....	33
2-4 Models in the form of Integral Differential Equations (IDEs).....	34
2-5 Models in the form of Partial Differential Equations (PDEs).....	37

Chapter 3 CONTROLLERS	39
3-1 Introduction	39
3-2 Control Strategies	40
3-3 Run to Run (R2R) or Iterative Learning Control (ILC)	43
3-4 PD and PID Controllers	45
3-5 Biostator & Nonlinear PID Controllers	46
3-6 Dynamic Neural Networks (DNN) Controller with State Observer	47
3-7 Pole Placement Controller	47
3-8 Optimal Control	50
3-9 H_∞ Robust Control	53
3-10 Adaptive Control.....	54
3-11 Model Predictive Control (MPC).....	56
3-12 Nonlinear Predictive Control	59
3-13 Nonlinear Neural Networks.....	62
3-14 Stochastic Control.....	64
3-15 Fuzzy Control	67
Chapter 4 LMI-BASED CONTROL DEVELOPMENT	72
4-1 Introduction	72
4-2 Symbols and their definitions.....	73
4-3, H_2 and H_∞ Controllers Performance.....	74
4-4 H_∞ Control Problem	76
4-5 Nominally Linear Time Delay (NLTD) System	77
4-5-1 Theoretical Background.....	77
4-5-2 Mathematical formulation	79
4-6 \mathcal{L}_2 Gain Analysis.....	81
4-7 State Feedback Control Scheme.....	89
4-8 Dynamic Output Feedback Control Scheme	97

Chapter 5 RESULTS AND CONCLUSIONS.....	105
5-1 Introduction	105
5-2 Patient Data Simulation using AIDA Software.....	106
5-3 MPC Simulation for Bergman Model.....	107
5-4 New Stabilizing Methodology Results	108
5-4-1 Stability Results based on \mathcal{L}_2 Gain Analysis	112
5-4-2 State-Feedback Results.....	113
5-4-3 Dynamic Output Feedback Results.....	113
5-5 New Stabilizing Method Simulation Results.....	115
5-6 Control Schemes Robustness and Sensitivity Analysis.....	122
5-7 Discussion and Conclusions	142
5-8 Future research topics	145
NOMENCLATURE	146
BIBLIOGRAPHY	147
Vita.....	

LIST OF TABLES

Table 1.1: Pharmacokinetics of available insulin products.	14
Table 2.1: Bergman model parameter values.....	23
Table 2.2: The parameter values for both Six-dimensional ODE model and DDE models.	28
Table 5.1: The time delay effect on the internal asymptotic stability parameters.	112
Table 5.2: The time delay effect on the State feedback system parameters.	113
Table 5.3: The time delay effect on the Dynamic Output Feedback system parameters.	114
Table 5.4: The effect of sampling time on the system output for the State Feedback and the Dynamic Output Feedback.	115
Table 5.5: Sensitivity analysis and robustness test.	123

LIST OF FIGURES

Figure 1.1: Insulin-Glucose regulatory system diagram.....	9
Figure 1.2: Time course of plasma insulin concentration after a subcutaneous injection (10 U) of regular (solid), Lispro (dash-dot), and NPH insulin (dotted).	14
Figure 2.1: Bergman's Minimal Model describing the glucose and insulin kinetics in an IVGTT study.....	21
Figure 2.2: Physiological Insulin Glucose regulatory system.....	25
Figure 2.3: The DDEs model Functions f_i , $i= 1, 2, 4, 5$	28
Figure 2.4: Two explicit time delay glucose–insulin regulatory system model	31
Figure 3.1: The partially closed-loop control strategy of conventional and intensified insulin therapy	41
Figure 3.2: The closed-loop control strategy with SC glucose measurement and SC insulin injection	42
Figure 3.3: The compartmental model of SC insulin absorption and kinetics for pole placement strategy	48
Figure 3.4: The self-tuning adaptive control scheme.....	54
Figure 3.5: The basic Linear MPC.....	57
Figure 3.6: The setting used to test the neural predictive control scheme	64
Figure 3.7: A single time transition Bayesian network.....	66
Figure 3.8: Control diagram for blood glucose regulation in Type-1 diabetes patients by subcutaneous route.	70
Figure 5.1: AIDA data entry screen.....	106
Figure 5.2: AIDA graphical simulator display: blue glucose graph before insulin increase, and the black is after.	107
Figure 5.3: MPC Response for Bergman Model	108
Figure 5.4: System Open loop simulation.....	111
Figure 5.5: Response to reference value without disturbance	117
Figure 5.6: Response to initial conditions without disturbance	118
Figure 5.7: Response to initial conditions with added disturbance through Γ_o	119

Figure 5.8: State feedback Response for all the three cases.....	120
Figure 5.9: Dynamic Output feedback Response for all the three cases	120
Figure 5.10: Response for all the cases	121
Figure 5.11: Meal disturbance signals	122
Figure 5.12: State feedback with V_g variation	124
Figure 5.13: State feedback with V_g variation and meal disturbance	124
Figure 5.14: Dynamic Output feedback with V_g variation	125
Figure 5.15: Dynamic output feedback with V_g variation and meal disturbance.....	125
Figure 5.16: State feedback with C_3 variation	126
Figure 5.17: State feedback with C_3 variation and meal disturbance	126
Figure 5.18: Dynamic Output feedback with C_3 variation.....	127
Figure 5.19: Dynamic output feedback with C_3 variation and meal disturbance.....	127
Figure 5.20: State feedback with V_p variation	128
Figure 5.21: State feedback with V_p variation and meal disturbance	128
Figure 5.22: Dynamic Output feedback with V_p variation	129
Figure 5.23: Dynamic output feedback with V_p variation and meal disturbance.....	129
Figure 5.24: Dynamic Output feedback with V_i variation	130
Figure 5.25: Dynamic output feedback with V_i variation and meal disturbance	130
Figure 5.26: Dynamic Output feedback with E variation	131
Figure 5.27: Dynamic output feedback with E variation and meal disturbance	131
Figure 5.28: State feedback with U_m variation	132
Figure 5.29: State feedback with U_m variation and meal disturbance	132
Figure 5.30: Dynamic Output feedback with U_m variation	133
Figure 5.31: Dynamic output feedback with U_m variation and meal disturbance.....	133
Figure 5.32: Dynamic Output feedback with β_1 variation	134

Figure 5.33: Dynamic output feedback with β_1 variation and meal disturbance.....	134
Figure 5.34: Dynamic Output feedback with C_4 variation.....	135
Figure 5.35: Dynamic output feedback with C_4 variation and meal disturbance.....	135
Figure 5.36: State feedback with R_g variation	136
Figure 5.37: State feedback with R_g variation and meal disturbance	136
Figure 5.38: Dynamic Output feedback with R_g variation	137
Figure 5.39: Dynamic output feedback with R_g variation and meal disturbance.....	137
Figure 5.40: Dynamic Output feedback with α_1 variation.....	138
Figure 5.41: Dynamic output feedback with α_1 variation and meal disturbance.....	138
Figure 5.42: State feedback with C_5 variation.....	139
Figure 5.43: State feedback with C_5 variation and meal disturbance	139
Figure 5.44: Dynamic Output feedback with C_5 variation.....	140
Figure 5.45: Dynamic output feedback with C_5 variation and meal disturbance.....	140
Figure 5.46: Dynamic Output feedback with t_i variation	141
Figure 5.47: Dynamic output feedback with t_i variation and meal disturbance	141

THESIS ABSTRACT

Name: Hosam Abdul Rahim Fareed Arabasy

Title: LMI-based control of nonlinear time-delay model for “type 1-diabetic patient”

Major: Systems Engineering

Date: June 2009

Diabetes mellitus is one of the worst diseases with respect to the size of the affected population. It is very difficult to maintain the Normoglycemia for type 1 diabetic patient. This motivates many researchers to study the glucose-insulin endocrine regulatory system and try to find a proper controllable mathematical model. These models are in the form of ordinary differential, partial-differential, delay-differential, and integral-differential equations. Partial closed-loop and closed-loop control strategies were found in the literature for this task. These strategies did not consider the presence of time delay in the model, which may affect systems' performance and stability.

In this thesis, new criteria for LMI-based characterization of Nominally Linear Time Delay system and \mathcal{L}_2 gain analysis based on Lyapunov-Krasovskii Functional will be developed. Later on, this method will be extended to design feedback controllers, which ensure robustness against disturbances and parameter variations. All the developed theorems are verified through simulations, and compared with each other, with partial closed-loop, and with Model Predictive Control technique using Bergman model.

ملخص الرسالة

الاسم: حسام عبد الرحيم فريد عرباسي

عنوان الرسالة: التحكم المبني على المتراجحة المصفوفية الخطية لنظام غير خطي مصحوب بالتأخير الزمني

"لمريض البول السكري من النوع الأول"

التخصص: هندسة النظم

التاريخ: يونيو ٢٠٠٩

يعتبر مرض البول السكري أحد أسوأ الأمراض في الوقت الحاضر نظرا لحجم الإصابات في السكان، إنه من الصعب السيطرة على مستوى سكر الدم في الحدود الطبيعية لمرض السكر من النوع الأول، هذا كان دافعا لكثير من فرق البحث العلمي لدراسة الغدد الصماء و علاقة السكر في الدم مع هرمون الأنسولين و ذلك من أجل إيجاد نموذج تحكم رياضي، لقد توصل الباحثون إلى نماذج معادلات تفاضلية اعتيادية و تفاضلية جزئية و تفاضلية محتوية على تأخير زمني و تفاضلية تكاملية ، استراتيجيات التحكم الموجودة في الأبحاث تشمل على طرق الحلقة شبه المغلقة و الحلقة المغلقة، لكن كل هذه الاستراتيجيات لم تأخذ بعين الاعتبار وجود تأخير زمني في النموذج و الذي من الممكن أن يؤثر على أداء و استقرار النظام.

في هذه الرسالة سيتم تطوير ضوابط جديدة لوصف المتراجحة المصفوفية الخطية المبنية على نظام غير خطي مصحوب بالتأخير الزمني و حساب معامل الكسب بالاعتماد على طريقة ليايونيوف آراسوفسكي، بعد ذلك سيتم تعميم هذه الطريقة بحيث تصبح صالحة لتصميم و اختبار متحكمات التغذية العكسية لضمان احتواء النظام للقلقل و الانحرافات في عوامل التجربة الخاصة بالنموذج، سيتم إجراء محاكاة للنظريات الجديدة التي تم تطويرها في هذا البحث للتأكد من صلاحيتها ، و كذلك عمل مقارنات للنتائج المتحصل عليها بعضها مع بعض و مع نتائج نموذج برجمان باستخدام التحكم التنبؤي للنموذج و باستخدام التحكم باستراتيجية الحلقة شبه المغلقة.

Chapter 1

MEDICAL BACKGROUND

1-1 Introduction

When the pancreas does not release or properly use the insulin to uptake and control the blood glucose [1], it is considered that the patient has diabetes mellitus. Thus Diabetes mellitus can be considered as a group of metabolic disorders characterized by inability of the pancreas to regulate blood glucose concentration due to defects in insulin secretion and/or insulin action.

The Insulin, discovered in 1921, is considered as a heart of blood glucose control. Development of the DNA technology leads to have pure insulin. Insulin treatment is used to mimic normal physiology in order to prevent hyperglycemia or hypoglycemia side effects. The amount of the injected insulin is typically based on the blood glucose level.

According to the American Diabetes Association [2] data [3] published in 2002, about 6.3% of the total population had type 2-diabetes in the United States. Thus, diabetes mellitus is considered as one of the worst diseases with respect to the size of affected population. The direct and indirect cost of the treatment of diabetes was \$132 billion. The world wide diabetic population is much higher, especially in underdeveloped countries.

The medical diabetic complications will be provided in this chapter to give better understanding of the models and controls that will be presented in the following chapters.

1-2 Blood Glucose Classification

The Diabetes Control and Complications Trial (DCCT) Research Group have classified the blood glucose level into three main categories: Hypoglycemia, Normoglycemia, and Hyperglycemia [4].

The normal condition with blood glucose concentrations is called Normoglycemia. The narrow range limits of Normoglycemia, after overnight fasten, is 70 mg/dl (3.9 mmol/l) to 110 mg/dl (6.04 mmol/l), and can be accepted for random test to be in the range of 60 mg/dl to 140 mg/dl as wide range limits. Inadequate secretion of insulin by the diabetic pancreas results in poor maintenance of the Normoglycemia with elevated blood glucose concentrations. The only treatment is with Subcutaneous (SC) or Intravenous (IV) insulin injections, traditionally administered in an open-loop manner. Without insulin treatment, these patients will die.

The patient will have Hypoglycemia when his blood glucose level turns out to be less than 40 mg/dl (2.2 mmol/l) [5]. The over delivery of insulin is the typical cause of this class. Hypoglycemia is a short term concern because it starves the body cells of fuel. The risk of Hypoglycemia is that it can lead to insulin shock, faint, coma, and death.

While induce insulin resistance and diabetes via increased blood glucose levels is normally called Hyperglycemia [6]. Thus, Hyperglycemia is considered when blood glucose exceeds 140 mg/dl (7.8 mmol/l) after an Oral Glucose Tolerance Test, or 100 mg/dl (5.5 mmol/l) after a Fasting Glucose Tolerance Test. In the United Kingdom Prospective Diabetes Study (UKPDS) [1] only 23% of patients allocated to diet alone attained fasting plasma glucose levels below 140 mg/dl.

According to DCCT [4] the persistent Hyperglycemia in diabetes is associated with long-term complications and dysfunction of various organs, especially the eyes, kidneys, nerves, heart, and blood vessels.

1-3 Types of diabetes

Medical researchers have classified diabetes mellitus to be in to two types: Type 1-diabetes, or Insulin Dependent Diabetes Mellitus (IDDM), and Type 2-diabetes, or Non Insulin Dependent Diabetes Mellitus (NIDDM) [7, 8].

Type 1-diabetes is characterized by the patient's immune system destroying the insulin producing β -cells in the pancreas such that exogenous insulin is required to control the disease. This type commonly develops in young people (under 20 years old) and persists throughout life [1]. Insulin dependent diabetes accounts for 5–10% of the diabetic population. It is believed that both genetic factors and virus infections are responsible for causing this type of diabetes. Risk factors for type 1-diabetes include autoimmune, genetic, and environmental factors. DCCT [4] showed that an improved metabolic control was achieved using intensive insulin treatment in type 1-diabetes patients. Even more severe defects in insulin secretion are present in patients with type 1-diabetes following islet transplantation, when Normoglycemia is maintained in the absence of exogenous insulin treatment [8]. This suggests that glucose homeostasis can be maintained despite significant loss of β -cell function when an individual has normal insulin sensitivity.

While Type 2-diabetes has been associated with defects in components of both the short term and chronic negative feedback loops [7]. Type 2-diabetes is known as a

heterogeneous disorder characterized by insulin resistance and insulin deficiency due to a deficit in the mass of β -cells, reduced insulin secretion, and resistance to the action of insulin [1]. The relative contribution and interaction of these defects in the pathogenesis of this disease remains to be clarified. About 90% to 95% of all diabetics diagnose type 2-diabetes. This type of diabetes is associated with older age, obesity, family history of diabetes, prior history of gestational diabetes, impaired glucose tolerance, physical inactivity, and race/ethnicity. Type 2-diabetes is increasingly being diagnosed in children and adolescents [5]. About 150 million individuals are estimated to have type-2 diabetes worldwide [1].

Insulin stimulated glucose disposal is reduced by 50-100% in patients with type 2-diabetes as compared to non diabetic controls. However, insulin resistance of a similar magnitude also has been documented in many non-diabetic individuals including obese subjects, or during pregnancy, puberty, and aging [7]. Thus, Normoglycemia can be maintained in subjects with insulin resistance via increases in blood insulin levels. Defects of insulin secretion have been demonstrated in some people with type 2-diabetes [9].

It was observed that the β -cell mass is reduced by 40-50% in patients with type 2-diabetes when compared with weight matched non diabetic subjects [8]. In comparison, approximately 80% to 90% of the β -cell mass is lost before the onset of hyperglycemia in individuals who develop type 1-diabetes, suggesting that a greater β -cell mass is required in the presence of insulin resistance. This is also consistent with the observation of a 43% higher β -cell mass in Normoglycemia subjects with insulin resistance due to obesity.

Although these data suggest that multiple defects are required for the onset of type 2-diabetes, it is unclear if these defects have a single causal origin or if they occur independently. Experimental induction of insulin resistance using either high fat feeding, glucocorticoid administration, or genetically induced obesity has been shown to cause type 2-diabetes under certain circumstances. This supports the hypothesis that insulin resistance can cause β -cell defects, and hence diabetes, either by overworking the β -cells or by toxic effects of hyperglycemia on the β -cells. However, the existence of Normoglycemia in humans and animals highly resistant to insulin suggests independent defects in insulin sensitivity and β -cell function are required for type 2-diabetes [8].

Moreover some women can have glucose intolerance that is diagnosed during pregnancy for Type 1-diabetes and Type 2-diabetes. These types are common among obese women and women with a family history of diabetes. Gestational diabetes requires treatment during pregnancy period to normalize maternal blood glucose levels to avoid complications in the infant. After pregnancy, 5% to 10% of women with gestational diabetes are found to have Type 2-diabetes. 20% to 50% chance of developing diabetes in the next 5-10 years can be happen with women who have had gestational diabetes [5].

Other specific types of diabetes result from specific genetic conditions (such as maturity-onset diabetes of youth), surgery, drugs, malnutrition, infections, and other illnesses. Such types of diabetes may account for 1% to 5% of all diagnosed cases of diabetes [5].

DCCT and UKPDS [1] demonstrated that tight glucose control reduces the risk of long term complications of type 1-diabetes and type 2-diabetes, and hence reducing the cost to the health care system. There is no threshold for the relationship between blood glucose,

Glycosylated Hemoglobin (HbA1C), and reduced risk. This indicates that glucose levels in subjects with type 1-diabetes or type 2-diabetes should be as close as possible Normoglycemia.

It is estimated that nearly 50% subjects with type 2-diabetes will receive insulin at some stage of their disease [5].

1-4 Insulin-Glucose Control in Healthy Individuals

For a normal subject, the liver releases glucose into the blood. This helps the body to keep cells functioning 24 hours a day. The goal of intensive insulin therapy is to mimic the natural pattern of insulin release from the pancreas so that plasma glucose levels can be kept close to normal [10].

The insulin required for the normal person can be varied from 0.5 units per kilogram per day up to 2.0 units per kilogram per day at maximal stress situations. Insulin is secreted from β -cells. A diabetic patient's response to insulin can vary significantly for a variety of reasons since the insulin sensitivity varies with the time of day and the fitness and health of the patient [11]. The normal physiologic insulin secretion has two profiles [12]:

- 1- The basal secretion: The pancreas responds by releasing a small but steady amount of insulin into the bloodstream day and night in pulsating manner, providing a background rate of insulin to the body. This constant basal insulin rate of approximately 22 mU/min [13].
- 2- The bolus secretions: The pancreas responds by releasing a large amount of insulin, after meals, to uptake the glucose produced when food is digested.

The variables that state the basal insulin needs for an individual include growth and development, hormonal status, age, gender, stress levels, health status, and activity level. In addition, the amount and composition of food dictate the meal related needs [14]. Stress and exercise levels affect the patient's insulin sensitivity. Furthermore, the timescales of the variations for a diabetic can vary from hours to months. Thus, practical automated glucose control strategies have to be adaptive to some extent in order to accommodate changing and unknown patient conditions [11]. Insulin is cleared mainly by the liver and kidney. Insulin is degraded by enzymes in the subcutaneous tissue and interstitial fluid as well.

While the glucagon, counter regulatory hormone, would be released in response to hypoglycemia to raise blood glucose concentration in a healthy individuals. This hormone is secreted from α -cells. However, the counter regulatory response in the diabetic patient is often blunted or absent, and hence it is less effective [15]. The exogenous factors that can affect the blood glucose concentration level include food intake, rate of digestion, exercise, reproductive state.

The optimum treatment strategy for insulin treatment is used for type 1-diabetes. Insulin titration, or optimum insulin dosing, is a difficult task but is at the cornerstone of the management of type 1-diabetes [1]. DCCT has shown that intensive insulin therapy leads to improved outcomes of blood glucose control. On the other hand DCCT showed that resources needed to achieve this goal are beyond the present means. Novel approaches are needed to assist patients with type 1-diabetes and healthcare professionals in achieving the

goals set by the DCCT. Information technology has an important role to play contributing to these activities [4].

It was documented that even minor glucose elevations increase the risk of complications [11]. DCCT was the landmark study of 1440 type 1-diabetic people randomized into two treatment groups: intensive insulin delivery and standard care. Those people who had mean blood glucose concentrations below 110 mg/dl had no increase risk for retinopathy, nephropathy and peripheral vascular disease. Those patients who had elevated glucose hemoglobin levels had a significant and positive correlation with increased risk [4]. However, when the blood glucose concentration was normalized, the risk of severe life threatening hypoglycemia increased up to 10 fold above the risk in those patients with hyperglycemia. Thus the goal of achieving and maintaining normal blood glucose includes accepting the risk of hypoglycemia. The recent long term study by the DCCT group has confirmed these conclusions.

As shown in Figure 1.1, the normal pancreas has two phases of insulin delivery: a first phase consisting of an immediate bolus and a second phase of prolonged insulin delivery [5], [11]. The function of the first phase is to reduce the glucagon secretion from the pancreatic α -cell and thus turn off the hepatic output of glucose, while the function of the second phase of insulin secretion is to metabolize the slower acting carbohydrates. The normal β -cell has its first priority to prevent hyperglycemia. Thus the α -cells are needed to secrete glucagon to prevent late postprandial hypoglycemia [11].

It is important to regulate diabetic patient blood glucose concentrations to be within the Normoglycemia limits [15]. When the blood glucose concentration level is high, the β -

cells release insulin which results in lowering the blood glucose concentration level by inducing the uptake of the excess glucose by the liver and other cells such as muscles, and by inhibiting hepatic glucose production [16]. The only way the β -cell can respond to a falling blood glucose concentration is to turn off the insulin secretion. There is no way the β -cell can retract the insulin once it is given.

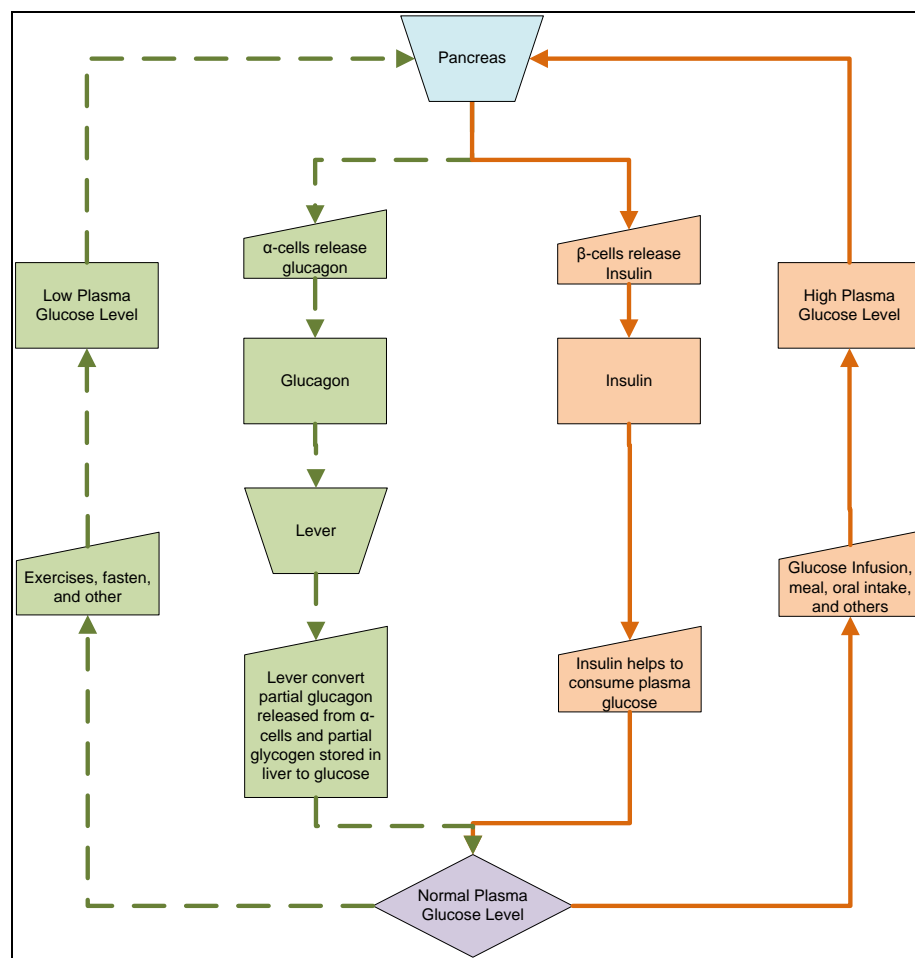


Figure 1.1: Insulin-Glucose regulatory system diagram.

When the blood glucose level is low, the α -cells release glucagon, which results in increasing the blood glucose level by acting on liver cells and causing them to release glucose into the blood [16].

The β -cell depends on the other counter regulation hormones that should be secreted to buffer the falling glucose concentration. The hormones that play a major role in counter regulation are glucagon, epinephrine, cortisol and growth hormone. This delicate balance is perfectly arranged to maintain the blood glucose within the Normoglycemia range [11]. In short, hyperglycemia stimulates a rapid increase in insulin release from the pancreatic β -cells. The associated increase in blood insulin levels causes increased glucose uptake and decreased glucose production leading to a reduction in blood glucose [7]. Recent indication proposes that chronic hyperglycemia may contribute to a second negative feedback loop by increasing the mass of insulin secreting β -cells, through changes in the rates of β -cells replication, and death. An increased β -cell mass represents an increased capacity for insulin secretion which, in turn, would lead to a decrease in blood glucose [8].

Treatment of type 2-diabetes has received little attention from the adaptive control community, except when titrating insulin dosing [1]. This may need revision given the complexities associated with the management of type 2-diabetes. It is usual to start the treatment of type 2-diabetes with non pharmacological therapies. The base effort of these therapies is to improve both good glycogenic control and to begin the process of helping patients to make healthy life style changes. Modification of the nutrition is the first task that is undertaken. If treatment goals are not achieved after a trial of dietary and lifestyle changes, an oral hypoglycemic are prescribed alone or in combination with insulin [4].

Various in-vivo and in-vitro experiments have shown that the Insulin Secretion Rate (ISR) from pancreatic islets, oscillates in a number of different time scales [17-19]:

- 1- The fastest oscillations have a period of tens of seconds and they have been shown to be in phase with oscillations in the free Ca_2^+ concentration of β -cells
- 2- The rapid oscillations have a period of 5–15 minutes, and are caused by coordinate periodic secretory insulin bursting from the β -cells.
- 3- The ultradian oscillations, or slow oscillations, have a period within the range of 50–120 minutes. These oscillations of insulin concentration are associated to similar oscillations of the plasma glucose concentration, and they are best seen after meal ingestion, oral glucose intake, continuous enteral nutrition or IV glucose infusion [19-20].

In addition to these types of oscillations, circadian rhythms have been also observed [17].

These bursts are the dominant mechanism of insulin release at basal states [18]. In some cases compound bursting occurs [17], the term referred to episodic bursts clustered together and they propose that the compound bursting is responsible for insulin oscillations with a period of approximately 5 minutes.

The most important factors that play vital role for glucose disposal are [21]:

- 1- Insulin sensitivity: the capability of insulin to increase glucose disposal to muscles, liver and adipose tissue.
- 2- Glucose effectiveness: the ability of glucose to enhance its own disposal at basal insulin level.
- 3- Pancreatic responsiveness: the ability of the pancreatic β -cells to secrete insulin in response to glucose stimuli.

Any failure in these may lead to damage the glucose tolerance. Quantitative assessment is possible [22] and may improve classification, prognosis and therapy of the disease [23].

1.5 Insulin Therapy for Type-1 Diabetic patients

DCCT [4, 5] have shown that there is an important correlation between a Normoglycemia and the prevention or delay of the complications of insulin-dependent diabetes. The DCCT has demonstrated that Intensive Insulin Therapy (IIT), consisting of three or more SC insulin injections per day or in the use of insulin pumps, significantly reduces the incidence of retinopathies, autonomic neuropathies, and other complications. Alternatively, IIT shows an increased probability of hypoglycemic events, 2 to 3 times, and a remarkable increase of the costs of patient monitoring [4].

Three control variables affecting the blood glucose level are insulin, meals, and physical exercise. Although meals and physical exercise are crucial in determining the quality of metabolic control, their quantitative evaluation still represents a major problem in home monitoring [24]. Thus, meals and physical exercise are usually considered as (known) disturbances that can be compensated for by suitable feed-forward control laws in any insulin therapy control strategies that will be presented later.

The metabolic control of type-1 diabetic patients can be evaluated by:

1. Physicians during periodical control visits, on the basis of data coming from patient home monitoring.

2. The self-monitoring procedure includes the reading of blood glucose level, by portable devices and then records the insulin dosages and the relevant events related to meals and physical exercise.
3. The medium period indicators is based on the measurement of the percentage of hemoglobin bound to glucose, that uses the HbA1c, to reflect the average glucose levels over the past 60 days.

The objective of insulin therapy is to reproduce the physiological insulin profiles of the diabetic patient. This profile is characterized by a bi-phasic pattern, in response to a meal, and by a basal level in the fasting state. This goal is nearly impossible to achieve through a small number of SC injections. Pharmaceutical research has produced various types of insulin to mimic, through their combined injection, such that the plasma insulin being similar to normal individual profile.

Various insulin analogues are available for SC injection. Each product is used for specific case and action such that [22 ,25]:

- 1- Rapid-acting insulin analogues use Lispro and Aspart Insulin.
- 2- Short-acting insulin analogues use Buffered regular insulin.
- 3- Intermediate-acting insulin analogues use Lente and NHP (Neutral Protamine Hagedorn) Insulin.
- 4- Long-acting insulin analogues use Glargine and Ultralente insulin.

Table 1.1 lists the pharmacokinetics of available insulin products such as the time needed for the onset, peak, and duration of several types of insulin. Figure 1.1.2 shows the plasma

insulin concentration after SC injection of a typical dose of the most widely used insulin preparations.

Table 1.1: Pharmacokinetics of available insulin products.

Insulin	Action since injection	Peak time (hours)	Duration (hours)	Action
Lispro	5-15 minutes	0.5-1.5	3-5	Rapid
Aspart	10-20 minutes	1-3	3-5	Rapid
Regular insulin	30-60 minutes	1-5	6-10	Short
Buffered regular insulin	30-60 minutes	1-3	8	Short
Lente	1-3 hours	6-14	16-24	Intermediate
NPH	1-2 hours	6-14	16-24 and more	Intermediate
Glargine	1.1 hours	None	24	Long
Ultralente	4-6 hours	8-20	More than 24	Long

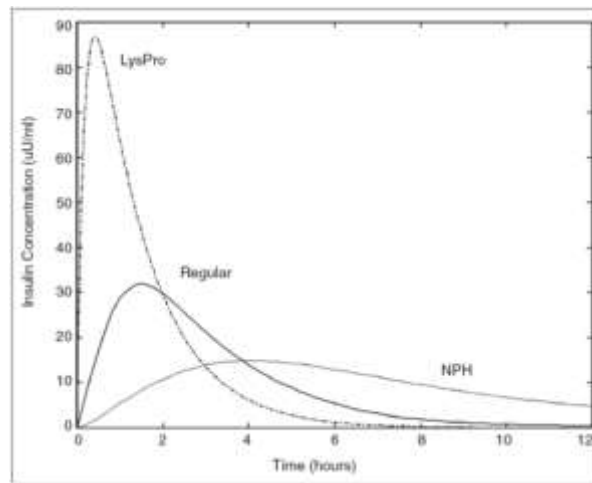


Figure 1.1.2: Time course of plasma insulin concentration after a subcutaneous injection (10 U) of regular (solid), Lispro (dash-dot), and NPH insulin (dotted).

The insulin preparations with rapid action are used to obtain post-prandial peaks in plasma insulin concentration. Delayed action (Intermediate or long) Insulin is used to satisfy the basal insulin requirement. It is not possible to reproduce exactly the physiological profile due to the suboptimal insulin profile. Using an appropriate mixture of Lispro and NPH can give good results [24].

Unfortunately, there is great variability of SC insulin absorption, especially for the delayed action insulins [26]. Large day by day plasma insulin fluctuations may be caused

by the variable SC absorption combined with errors in SC delivery (the drug is self-administered). Also, undesired side-effects may occur such that a delay in the insulin peak can produce a post-prandial hyperglycemia followed by hypoglycemia. Hence, new intermediate-acting insulin preparations, such as the Neutral Protamine Lispro (NPL), are becoming available to enhance the blood glucose control when used in conjunction with Lispro insulin [27].

Insulin therapy can be viewed as an optimization problem with constraints. Optimization requires the search in a four-dimension space [24]:

1. Number of injections: two to four per day.
2. Time of injection: usually four per day: meals and bed times.
3. Insulin type: Lispro, regular, NPH, and their mixtures.
4. Insulin dosage.

It is known that Lispro and regular insulin cannot be delivered at the same time. This will clinically limit the search to a subspace of possible combinations. Today, good evidence exists that an insulin protocol made of mealtime injections of a Lispro and NPH mixture, followed by a pre-bedtime NPH, is probably the most reliable strategy for blood glucose control [28].

Unfortunately, in addition to the intrinsic complexity of the decision space, other problems affect the design of a partially closed-loop control strategy that are:

1. Blood glucose concentration is under-sampled [29]: Patients usually measure their blood glucose 3-4 times a day, while it is required to be measured at least 8 times per day to completely reconstruct the glycemic profile.

2. Intra-individual variability is rather high, even in patients whom maintain nearly the same habits every day [30].

These difficulties have motivated the researchers to develop suboptimal control strategies for defining the best insulin therapy as will be illustrated later in Chapter 3.

Chapter 2

GLUCOSE-INSULIN MODELS

2-1 Introduction

The Insulin dose needs to be adjusted based on the blood glucose level after an initial insulin dose is given. This method of insulin delivery is fraught with continuous risk of hyperglycemia and hypoglycemia because the moment to moment fluctuations in glucose are not adequately treated with intermittent SC insulin injections. The optimal insulin delivery protocol would be performed such that the blood glucose monitoring and insulin dosing are continuously managed in real time. The meal-related insulin need is also difficult to derive and allow for the incorporation of carbohydrate into the meal plan and minimize the postprandial glucose peak.

Thus, it is important to have insulin glucose model in order to normalize the glucose levels of type 1-diabetic patients. To do so, all glucose-insulin variables are needed to be included into an algorithm for insulin delivery.

The minimal model and its siblings study the insulin sensitivity, while the proposed mathematical models aim to better understand the glucose-insulin regulatory system. Virtual patient need to be implemented using an appropriate mathematical model such that we can test the performance of the control algorithm.

During the last decades, Many Insulin glucose mathematical models have been developed in order to have better understanding of the mechanisms of the glucose insulin regulatory

system. These models differ in the way in which they formulate and mimic the process. Each of these models has its own advantages and weaknesses. Different aspects were used to deal with insulin regulatory processes. The general form of Glucose-Insulin model can be expressed by the following mass conversion law:

$$\dot{G}(t) = \text{Glucose change rate} = \text{Glucose Production Rate} - \text{Glucose Utilization Rate}$$

$$\dot{I}(t) = \text{Insulin change rate} = \text{Insulin Production Rate} - \text{Insulin Removal Rate}$$

The types of model used in the literature can be classified mathematically as: Ordinary Differential Equations (ODEs), Delay Differential Equations (DDEs), Partial Differential Equations (PDEs), Stochastic Differential Equations (SDEs), Fredholm Integral Equations (FIEs) (in the estimation of parameters problem), and Integro Differential Equations (IDEs).

In this chapter, we will present some literature surveys that discuss the most important insulin-glucose mathematical models and control of insulin-glucose regulatory system.

2-2 Ordinary Differential Equations (ODEs)

Several sets of Ordinary Differential Equations (ODEs) mathematical models have been proposed to describe the insulin-glucose action. These ODEs are classified into three main classes that are: the Nonlinear Model, the Bergman Minimal Model, and the Six-Dimensional model.

2-2-1 Nonlinear Model

The nonlinear model, that has long been identified, was demonstrably more appropriate under many circumstances particularly in the control context where the model structure should remain minimal [31]. The following set of equations describing the glucose-insulin kinetics was used for the maintenance of basal glycemia during hyperinsulinemic clamps:

$$\dot{G} = \frac{dG(t)}{dt} = -[k_o + k(t)]G(t) + RG(t) \quad (2.1-1)$$

$$\dot{k} = \frac{dk(t)}{dt} = -a_1 k(t) + a_2 i(t) \quad (2.1-2)$$

$$\dot{i} = \frac{di(t)}{dt} = -a_3 i(t) + a_4 k(t) + a_6 i_3(t) + RI(t) \quad (2.1-3)$$

$$\dot{i}_3 = \frac{di_3(t)}{dt} = -a_6 i_3(t) + a_5 i(t) \quad (2.1-4)$$

where

$G(t)$ is the plasma glucose concentration (mg/ml)

k_o is the insulin-independent fractional removal rate of glucose (min^{-1})

$k(t)$ is the insulin-dependent fractional removal rate of glucose (min^{-1})

$i(t)$ is the insulin mass in the central compartment (μU)

$i_3(t)$ is the insulin mass in a peripheral compartment non-active in glucose removal (μU)

$RG(t)$ is the glucose systemic appearance rate (mg/ml.min)

$RI(t)$ is the insulin systemic appearance rate ($\mu\text{U/min}$)

a_1 - a_6 are the fractional transfer rates of the 3-compartment model of insulin kinetics: [a_1 ,

$$a_3, a_5, a_6] = \text{min}^{-1}, [a_2] = \text{min}^{-2} \mu\text{U}, \text{ and } [a_4] = \mu\text{U/min}^{-2}$$

Equations (2.1-1 to 2.1-4) illustrates the variations in plasma glucose according to the principle of mass conservation. The term $[k_o + k(t)]G(t)$ accounts for glucose removal

while the term $RG(t)$ represents both the endogenous and the exogenous glucose input. A single compartment description is appropriate since in the euglycemic control situation, \dot{G} will be minimized. The fractional removal rate of glucose consists of a constant component k_o , added to an insulin dependent term $k(t)$.

The insulin-dependent component of the fractional removal rate of glucose $k(t)$, has been shown to be directly proportional to the presence of insulin in a compartment remote from plasma. The latter is thus assumed directly proportional to the insulin mass in a peripheral compartment of a multi-compartment model of insulin kinetics. The two-compartment description is generally considered to be minimal.

$k(t)$ appears explicitly in the Equations (2.1-2) to (2.1-4) rather than the insulin mass in the compartment acting on glucose removal. The coefficient of proportionality between these two variables is simply lumped together with the fractional rates of transfer between plasma insulin and this pool. $RI(t)$ represents the entry of both the endogenous and the exogenous insulin into the systemic circulation. Similarly, $RG(t)$ accounts for the rate of appearance of glucose in the systemic circulation from both the endogenous and the exogenous sources. At steady state, prior to the onset of the insulin signal, the basal glucose removal simply equals the endogenous production but higher levels of circulating insulin would reduce the hepatic glucose production.

This model predicts the time course of the insulin action for any insulin signal and thus allows certain flexibility in the regularity and frequency of the plasma glucose monitoring at a minimal cost in performance.

2-2-2 Bergman Minimal Model

The standard Bergman model [32] is based on an Intravenous Glucose Tolerance Test (IVGTT), where glucose and insulin concentrations in plasma are sampled after an IV glucose injection [33]. Bergman minimal model was the base for many researchers to control the glucose behavior for type-1 diabetic patients. There are now approximately 50 major studies published per year and more than 500 can be found in the literature, according to the same author, which involve the minimal model [34].

The glucose and insulin kinetics are described by two components, where the parameters traditionally have been estimated separately within each component. The glucose-insulin system is an integrated system and coupling of the components to obtain a unified model seems appropriate.

In an IVGTT study, a dose of glucose (usually 0.3 gram of glucose per kg body weight) is injected intravenously over a 60 seconds period to overnight fasted person, and subsequently the glucose and insulin concentrations in plasma are frequently sampled and evaluated (usually 30 times) over a period of 180 minutes.

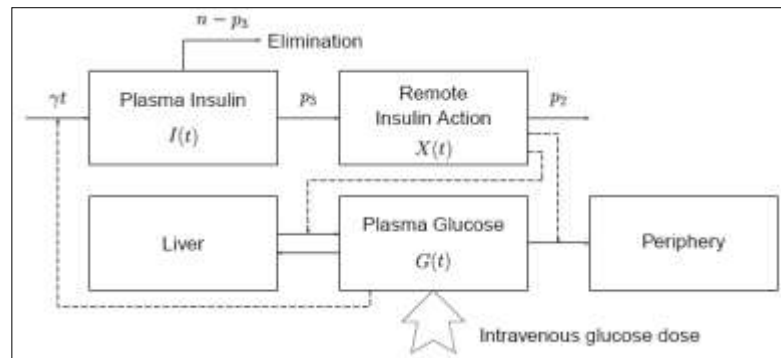


Figure 2.1: Bergman's Minimal Model describing the glucose and insulin kinetics in an IVGTT study.

The IV glucose dose immediately elevates the glucose concentration in plasma forcing the pancreatic β -cells to secrete insulin. The insulin in plasma is hereby increased, and the glucose uptake in muscles, liver and tissue is raised by the remote insulin in action. This lowers the glucose concentration in plasma, implying the β -cells to secrete less insulin, from which a feedback effect arises. This integrated glucose-insulin system is illustrated by the compartment model in Figure 2.1. Based on the measurements of the glucose level in the SC layer, a modified version of Bergman's Minimal model is used. This modified version of Bergman's Minimal Model [7, 23] can be represented by the following, five state, ODEs:

$$x = \begin{bmatrix} G \\ X_r \\ I \\ G_{sc} \\ D_m \end{bmatrix} \Rightarrow \dot{x} = \begin{bmatrix} \dot{G} \\ \dot{X}_r \\ \dot{I} \\ \dot{G}_{sc} \\ \dot{D}_m \end{bmatrix} \quad (2.2)$$

Where the system states are:

$$\dot{G} = -P_1(G(t) + G_b) - X_r(t)G(t) + D_m(t) \quad (2.2-1)$$

$$\dot{X}_r = -P_2X_r(t) + P_3(I(t) - I_b) \quad (2.2-2)$$

$$\dot{I} = -nI(t) + \frac{U(t)}{V_I} \quad (2.2-3)$$

$$\dot{G}_{sc} = \frac{G - G_{bsc}}{5} - R_{utin} \quad (2.2-4)$$

$$\dot{D}_m = -\alpha D_m(t) \quad (2.2-5)$$

and the system state variables are:

$G(t)$ is the Blood plasma glucose concentration above basal value (mg/dL).

$X_r(t)$ is the Insulin in the remote compartment (mU/L).

$I(t)$ is the Plasma insulin concentration above basal value (mU/L).

$G_{sc}(t)$ is the Glucose concentration on the SC layer (mg/dL). This state approximates

$G(t)$, and is the one which is measurable.

$D_m(t)$ is the Meal glucose disturbance (mg/dL/min).

The input is the manipulated insulin infusion rate ($U(t)$: (mU/min)). The time variable t is measured in minutes. The standard parameters for the model can be found in Table 2.1.

G_b ; X_{br} ; I_b ; G_{bsc} and D_{bm} denote the basal values for the system.

Hence, a steady-state point for the system can be represented by:

$$x_s = \begin{bmatrix} G_b \\ X_{br} \\ I_b \\ G_{bsc} \\ D_{bm} \end{bmatrix} \quad (2.3-1)$$

$$u_s = nI_b V_I \quad (2.3-2)$$

$$d_s = 0 \quad (2.3-3)$$

Table 2.1: Bergman model parameter values.

Variable	Value	Variable	Value
P_1	$0.028735 \text{ min}^{-1}$	G_b	81.3 mg/dL
P_2	$0.028355 \text{ min}^{-1}$	I_b	15 mU/L
P_3	$5.035 \cdot 10^{-5} \text{ mU/L}$	G_{sc}	$G_b - 5R_{utin}$
V_I	12 L	D_{bm}	0
R_{utin}	0.7400 mg/dL/min	X_{br}	0
α	0.05	n	$5/54 \text{ min}^{-1}$

Using the standard linearization technique, it's clear that this system of differential equations can be set up like this:

$$\dot{X} = \bar{A}X + \bar{B}U + \bar{E}D \quad (2.4)$$

where the deviation variables are:

$X = x - x_s$ is the state vector.

$U = u - u_s$ is the input variable for insulin injection.

$D = d - d_s$ is input variable for meal consumption.

\bar{A} , \bar{B} and \bar{E} are the partial derivatives of the model that produce the system matrices such that:

$$\bar{A} = \frac{\partial f}{\partial x} \Big|_{(x_s, u_s, d_s)} = \begin{bmatrix} -P_1 - X_b & -G_b & 0 & 0 & 1 \\ 0 & -P_2 & P_3 & 0 & 0 \\ 0 & 0 & -n & 0 & 0 \\ 0.2 & 0 & 0 & -0.2 & 0 \\ 0 & 0 & 0 & 0 & -\alpha \end{bmatrix} \quad (2.4-1)$$

$$\bar{B} = \frac{\partial f}{\partial u} \Big|_{(x_s, u_s, d_s)} = \begin{bmatrix} 0 & 0 & \frac{1}{V_I} & 0 & 0 \end{bmatrix}^T \quad (2.4-2)$$

$$\bar{E} = \frac{\partial f}{\partial d} \Big|_{(x_s, u_s, d_s)} = \begin{bmatrix} 1 & 0 & 0 & 0 & -\alpha \end{bmatrix}^T \quad (2.4-3)$$

It is required to have boundaries for the measured output blood glucose level, z , to keep the plasma glucose level in the Normoglycemia wide-range, avoid the Hyperglycemia or Hypoglycemia.

Moreover, input constraints that restrict the insulin injected volume and frequency to ensure that the system obeys physiological and physical limits such that:

$$0 \text{ mU/min} \leq u \leq 100 \text{ mU/min}$$

$$-16.7 \text{ mU/min} \leq \Delta u \leq 16.7 \text{ mU/min}$$

We can summarize the limitations for this model as [32]:

1. It is a highly ill-posed inverse problem and most often the reconstruction of the glucose kinetics has been done by deterministic iterative numerical algorithms.
2. The model parameters have usually been estimated by a non-linear weighted least squares estimation technique in a two-step procedure, where the parameters in \dot{G} and

\dot{X} are estimated using insulin as a forcing function and then the parameter in \dot{I} are estimated using glucose as a forcing function. However, the glucose-insulin system is an integrated system, and must be considered as a whole.

3. The oscillations resulted from the interaction between the insulin and glucose was not considered in this model. Thus this model considered improper in qualitative behavior.

2-2-3 Six-Dimensional model ODEs

To determine whether the ultradian, or slow, oscillations could result from the interaction between insulin and glucose, a parsimonious nonlinear mathematical model consisting of the six-dimensional ODEs including the major mechanisms involved in glucose regulation [5]. The four negative feedback loops, shown in Figure 2.2, describe the relation between insulin and glucose such that: glucose stimulates pancreatic insulin secretion, insulin stimulates glucose uptake and inhibits hepatic glucose production, and glucose enhances its own uptake [5], [16]. Sturis et al. [20], developed his six-dimensional ODE model.

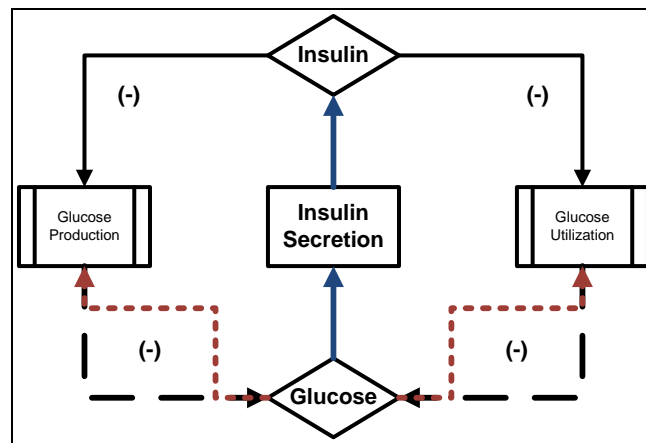


Figure 2.2: Physiological Insulin Glucose regulatory system.

This model has three main state variables in addition to three auxiliary variables [5]. The main state variables are:

- 1- G is the amount of glucose in the plasma and intercellular space.
- 2- I_p is the amount of insulin in the plasma.
- 3- I_i is the amount of insulin in the intercellular space.

While the other auxiliary variables are x_1 , x_2 , and x_3 . The following terms are included in the system state space equations:

- 1- V_p is the plasma insulin distribution volume.
- 2- V_i is the effective volume of the intercellular space.
- 3- E is the diffusion transfer rate.
- 4- t_p is insulin degradation time constants in the plasma.
- 5- t_i is insulin degradation time constants in the intercellular space.
- 6- G_{in} is the exogenous glucose supply rate to plasma (such as meal ingestion, oral glucose intake, continuous enteral nutrition or IV glucose infusion).

We can now represent our system functions f_1 , f_2 , f_3 , f_4 , and f_5 as [5]:

$f_1(G)$ is the function modeling the pancreatic insulin production as controlled by the glucose concentration, and it is given by:

$$f_1(G(t)) = \frac{R_m}{1 + \exp\left(\left(c_1 - \frac{G}{V_g}\right)/a_1\right)} \quad (2.5)$$

$f_2(G(t))$ is the insulin-independent glucose consumption by the brain, nerve cells and others. $f_2(0) = 0$, $f_2(x) > 0$ and $\dot{f}_2(x) > 0$ are bounded for $x > 0$.

$$f_2(G) = U_b \left(1 - \exp\left(-\frac{G}{c_2 V_g}\right)\right) \quad (2.6)$$

$f_3(G(t))$ is the function for glucose utilization by various body parts such as muscle and fat cells and others. $f_3(x) = k_3x$, where $k_3 > 0$ is a constant:

$$f_3(G) = \frac{G}{c_3V_g} \quad (2.7)$$

$f_4(I_i(t))$ is the functions for insulin dependent utilization/uptake by various body parts such as muscle and fat cells and others. $f_4(0) > 0$, for $x > 0$, $f_4(x) > 0$ and $\dot{f}_4(x) > 0$ are bounded:

$$f_4(I_i) = U_o + \frac{U_m - U_o}{1 + \exp\left(-\beta \ln\left(\frac{I_i}{c_4\left(\frac{1}{V_i} + \frac{1}{Et_i}\right)}\right)\right)} \quad (2.8)$$

$f_5(x_3(t))$ is a function modeling hepatic glucose production:

$$f_5(x) = \frac{R_g}{1 + \exp\left(\alpha\left(\frac{x}{V_p} - c_5\right)\right)} \quad (2.9)$$

Thus, Sturis et al. [20] Six-Dimensional model ODE can be represented as:

$$\dot{G} = \frac{dG(t)}{dt} = G_{in} - f_2(G(t)) - f_3(G(t))f_4(I_i(t)) + f_5(x_3(t)) \quad (2.10-1)$$

$$\dot{I}_p = \frac{dI_p(t)}{dt} = f_1(G(t)) - E\left(\frac{I_p(t)}{V_p} - \frac{I_i(t)}{V_i}\right) - \frac{I_p(t)}{t_p} \quad (2.10-2)$$

$$\dot{I}_i = \frac{dI_i(t)}{dt} = E\left(\frac{I_p(t)}{V_p} - \frac{I_i(t)}{V_i}\right) - \frac{I_p(t)}{t_i} \quad (2.10-3)$$

$$\dot{x}_1 = \frac{dx_1(t)}{dt} = \frac{3}{t_d}(I_p(t) - x_1(t)) \quad (2.10-4)$$

$$\dot{x}_2 = \frac{dx_2(t)}{dt} = \frac{3}{t_d}(x_1(t) - x_2(t)) \quad (2.10-5)$$

$$\dot{x}_3 = \frac{dx_3(t)}{dt} = \frac{3}{t_d}(x_2(t) - x_3(t)) \quad (2.10-6)$$

The parameter values for these functions that used in the Six-Dimensional model ODE are given in Table 2.2. The graphs of the above functions, f_i , $i = 1, 2, 4$, and 5 are shown in Figure 2.3. The importance of these functions is in their shapes rather than in their forms.

Table 2.2: The parameter values for both Six-dimensional ODE model and DDE models.

Parameters	Unit	Values	Parameters	Unit	Values
V_g	1	10	U_0	mg. min ⁻¹	40
R_m	μUmin^{-1}	210	U_m	mg. min ⁻¹	940
a_1	mg.l ⁻¹	300	β		1.77
C_1	mg.l ⁻¹	2000	C_4	μUI^{-1}	80
U_b	mg. min ⁻¹	72	R_g	mg. min ⁻¹	180
C_2	mg.l ⁻¹	144	α	$\text{l}\mu\text{UI}^{-1}$	0.29
C_3	mg.l ⁻¹	1000	C_5	μUI^{-1}	26
t_p	Min	6	E	lmin^{-1}	0.2
t_i	Min	100	t_d	Min	36
V_p	1	3	V_i	1	11

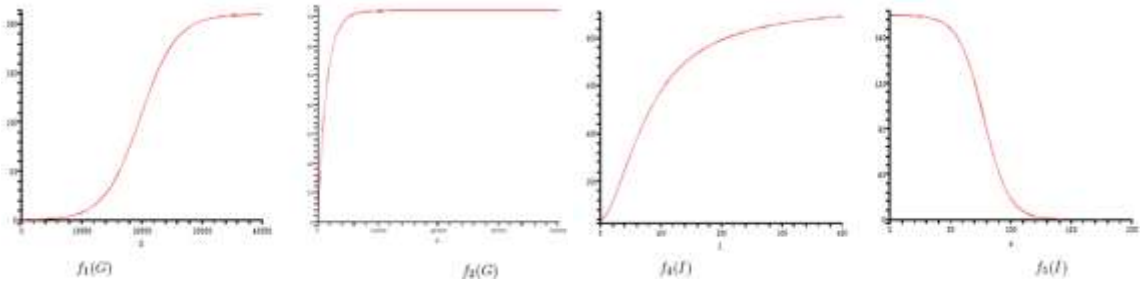


Figure 2.3: The DDEs model Functions f_i , $i = 1, 2, 4$, and 5.

2-3 Models in the form of Delay Differential Equations (DDEs)

Several models were published based on the Six-Dimensional ODEs model (2.10) for ultradian insulin secretion oscillation analysis. These models take into consideration the effect of time delay in Insulin-Glucose system allowing them to mimic the real situation and make them more realistic than the previous models. Some models have glucose triggered insulin production delay is missing that have the single and two explicit time delay. The auxiliary variables may be assigned as third order delay state time delay

because they are representing the delay between insulin in plasma and its effect on the hepatic glucose production with total time t_d .

2-3-1 Single explicit time delay DDEs model

Engelborghs et al [35] replaced the auxiliary variables (x_1 , x_2 , and x_3) and introduced a single time delay, τ , in the negative feedback loop model and proposed following DDE model. With the above notations: the Single explicit time delay DDE model takes the form of:

$$\dot{G}(t) = \frac{dG(t)}{dt} = E_g - f_2(G(t)) - f_3(G(t))f_4(I(t)) + f_5(I(t - \tau)) \quad (2.11-1)$$

$$\dot{I}(t) = \frac{dI(t)}{dt} = f_1(G(t)) - \frac{I(t)}{t_i} \quad (2.11-2)$$

where:

f_1 , f_2 , f_3 , and f_4 are the same as that in the six dimensional ODE model, while

$$f_5(I) = \frac{R_g}{1 + \exp\left(\alpha\left(\frac{I}{V_p} - C_5\right)\right)} \quad (2.12)$$

E_g stands for the glucose infusion rate.

$1/t_i$ is the insulin degradation rate.

The positive constant delay τ (5-15 min) mimics the hepatic glucose production delay. On the other hand, this model ignores the second time delay that represents the glucose stimulating insulin secretion time delay. Due to the complex chemical reactions on the β -cells, the insulin secretion occurs a few minutes after the plasma glucose concentration rises. This significant time delay is not negligible in physiology [5].

2-3-2 Two explicit time delay DDEs models

This system contains two significant delays. The first delay, τ_1 , (5-15 minutes) is related to the fact that the physiological action of insulin on the utilization of glucose is correlated with the concentration of insulin in a slowly equilibrating intercellular compartment rather than with the concentration of insulin in the plasma [31, 36]. The second delay, τ_2 , (25-50 minutes) is associated with the time lag between the appearance of insulin in the plasma and its inhibitory effect on the hepatic glucose production [37, 38].

The two explicit time delay DDE insulin–glucose regulatory model is shown in Figure 2.4 [5]. The purpose of this model is to provide a possible mechanism for the origin of ultradian oscillations in pancreatic insulin secretion with appropriate analysis and numerical simulations with suitable software packages.

The following indicators should memorize to have better understanding of this diagram:

- 1- The insulin inhibits hepatic glucose production with time delay is indicated by the dash-dot-dot lines.
- 2- The insulin secretion from the β -cells stimulated by elevated glucose concentration level indicated by dash-dot lines.
- 3- The insulin caused acceleration of glucose utilization in cells with time delay indicated by the short dashed line.
- 4- The low glucose concentration level triggering α -cells in the pancreas to release glucagon indicated by dashed lines.

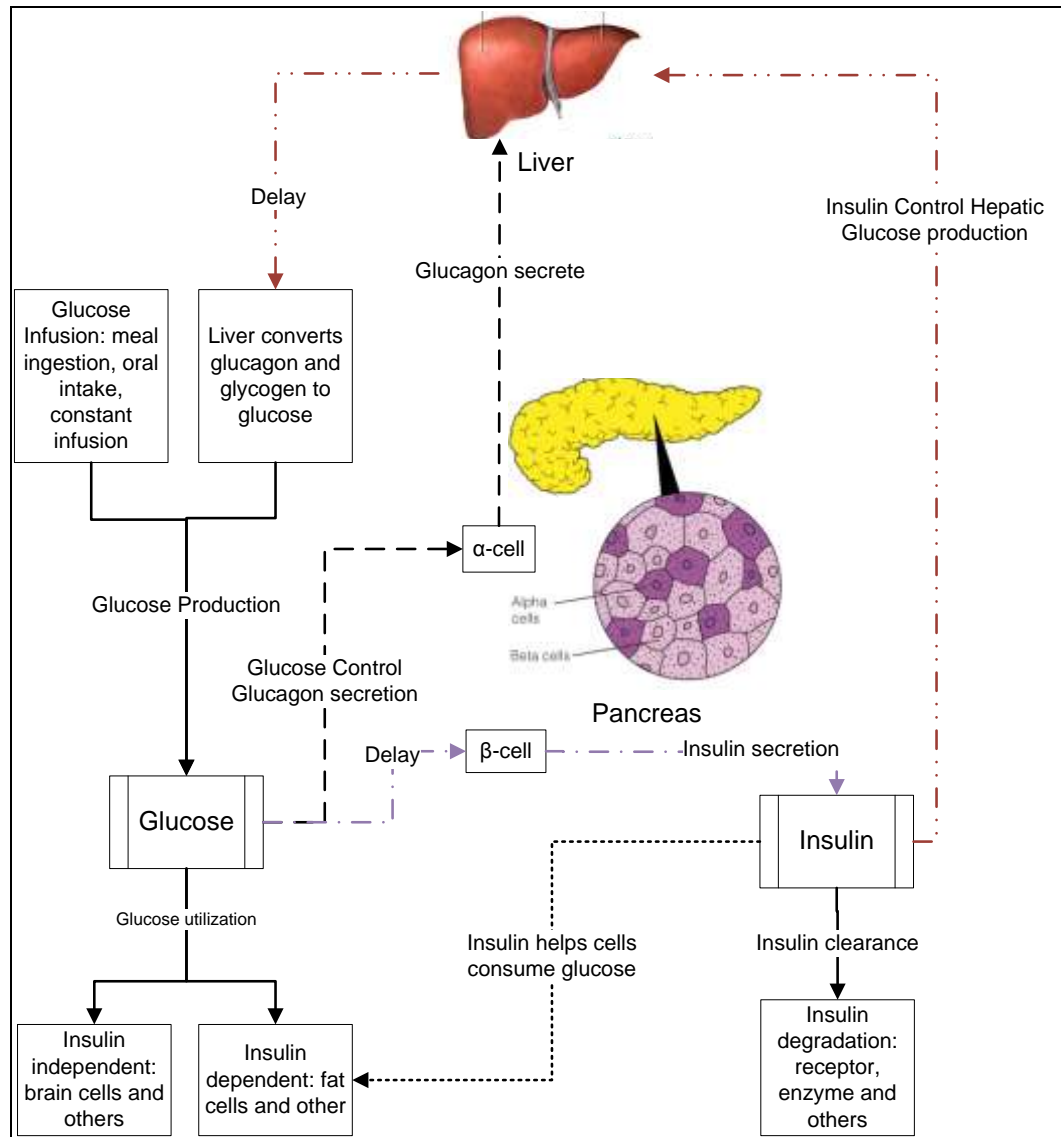


Figure 2.4: Two explicit time delay glucose–insulin regulatory system model.

These models comprised of two major negative feedback loops describing the effects of insulin on glucose utilization and glucose production, respectively, and both loops include the stimulatory effect of glucose on insulin secretion.

Observing the time delay of glucose triggered insulin production recently applied time delay in the insulin response to the glucose stimulation and presented the following model called two time delay model.

Several research papers have deal with this two explicit time DDEs models. Now, we will present some of these models:

Engelborghs et al. [35] try to model the exogenous insulin infusion by assuming that the exogenous insulin infusion function takes the same form as internal insulin production, which was too artificial. There new model takes the form of:

$$\dot{G}(t) = G_{\text{in}} - f_2(G(t)) - f_3(G(t))f_4(I(t)) + f_5(I(t - \tau_2)) \quad (2.13-1)$$

$$\dot{I}(t) = \alpha f_1(G(t)) - \frac{I(t)}{t_1} + (1 - \alpha)f_1(G(t - \tau_1)) \quad (2.13-2)$$

Later on, Li et al [39] have proposed his model based on the mass conservation law. This model was used for better understanding the self constrained regulatory mechanism of the system. With the explicit delays, the model is more accurate to depict the glucose-insulin endocrine metabolic dynamics. The model is given as follows.

$$\dot{G}(t) = G_{\text{in}} - f_2(G(t)) - f_3(G(t))f_4(I(t)) + f_5(I(t - \tau_2)) \quad (2.14-1)$$

$$\dot{I}(t) = f_1(G(t - \tau_1)) - d_i I(t) \quad (2.14-2)$$

where

$f_1(G(t - \tau_1))$ stands for insulin secretion from the pancreas. The delay is due to the complex electric processes inside of the islet.

$f_5(I(t - \tau_2))$ indicates for hepatic glucose production that is dependent on insulin in the plasma with time delay $\tau_2 > 0$. The time delay $\tau_2 > 0$ reflects that the liver does not convert the stored glucose and glycogen into glucose immediate when the insulin concentration level decreases. When insulin concentration level increases, the liver converts glucagon and glycogen to glucose decreasingly.

d_i is the degradation rate constant, and $d_i I(t)$ is the insulin degradation.

2-3-3 Alternative explicit time delay DDEs models

Li et al [39] and Bennett et al. [40] try to develop some alternative explicit time delay DDE models. In this subsection, we will show these models.

In 2004, Bennett et al. [40] have modified model 2.10 by removing the three auxiliary linear chain equations and their associated artificial parameters and introducing one time delay, τ , into the model explicitly. Again, this time delay stands for the hepatic glucose production and is the same as that in model 2.11. On the other hand, Bennett et al. [40] kept Sturis et al. [20] and Tolic et al. [41] ideas, given in model (2.10), of breaking the insulin into two compartments to simulate the delayed insulin-dependent glucose uptake.

This alternative DDE model takes the following form:

$$\dot{G}(t) = G_{\text{in}} - f_2(G(t)) - f_3(G(t))f_4(I_i(t)) + f_5(I_p(t - \tau)) \quad (2.15-1)$$

$$\dot{I}_p(t) = f_1(G(t)) - E \left(\frac{I_p(t)}{V_p} - \frac{I_i(t)}{V_i} \right) - \frac{I_p(t)}{t_p} \quad (2.15-2)$$

$$\dot{I}_i(t) = E \left(\frac{I_p(t)}{V_p} - \frac{I_i(t)}{V_i} \right) - \frac{I_i(t)}{t_i} \quad (2.15-3)$$

In 2006, Li et al [39] have develop two alternative approaches, based on their previous model 2.14, for modeling the glucose–insulin regulatory system in the form of there first explicit time delay DDEs. These approaches are:

1. First explicit time delay τ_1 is keep, but mimic the hepatic glucose production time delay by variable chain as in 2.10 model. This alternative model is expressed by:

$$\dot{G}(t) = G_{\text{in}} - f_2(G(t)) - f_3(G(t))f_4(I_i(t)) + f_5(x_3(t)) \quad (2.16-1)$$

$$\dot{I}(t) = \frac{dI(t)}{dt} = f_1(G(t - \tau_1)) - d_i I(t) \quad (2.16-2)$$

$$\dot{x}_1(t) = \frac{dx_1(t)}{dt} = \frac{3}{t_d}(I(t) - x_1(t)) \quad (2.16-3)$$

$$\dot{x}_2(t) = \frac{dx_2(t)}{dt} = \frac{3}{t_d}(x_1(t) - x_2(t)) \quad (2.16-4)$$

$$\dot{x}_3(t) = \frac{dx_3(t)}{dt} = \frac{3}{t_d}(x_2(t) - x_3(t)) \quad (2.16-5)$$

2. The effect of the first time delay τ_1 in glucose utilization was modeled by

$f_3(G(t))f_4(I_i(t - \tau_1))$. Thus, the new alternative model is represented by:

$$\dot{G}(t) = G_{in} - f_2(G(t)) - f_3(G(t))f_4(I_i(t - \tau_1)) + f_5(x_3(t - \tau_2)) \quad (2.17-1)$$

$$\dot{I}(t) = f_1(G(t)) - d_i I(t) \quad (2.17-2)$$

2-4 Models in the form of Integral Differential Equations (IDEs)

Bergman minimal model (2.2) is considered improper in qualitative behavior since it requires the parameter b_5 to equal the basal glucose level G_b . Thus it was required to introduce IDEs models. In 2000, De Gaetano et al. [42] developed there, so called dynamic, model by performing proper mathematical analysis on model 2.2 and established a more realistic delay integral differential equation model:

$$\dot{G}(t) = \frac{dG(t)}{dt} = -b_1 G(t) - b_4 I(t)G(t) + b_7 \quad (2.18-1)$$

$$\dot{I}(t) = \frac{dI(t)}{dt} = -b_2 I(t) + \frac{b_6}{b_5} \int_{t-b_5}^t G(s)ds \quad (2.18-2)$$

where:

t is time [min].

G is the glucose plasma concentration [mg/dl].

G_b is the basal, pre-injection, plasma glucose concentration [mg/dl].

I is the insulin plasma concentration [$\mu\text{U/ml}$]

I_b is the basal, pre-injection, insulin plasma concentration [pM].

b_0 is the theoretical increase in plasma concentration over basal glucose concentration at time zero after instantaneous administration and redistribution of the I.V. glucose bolus [mg/dl].

b_1 is the spontaneous glucose first order disappearance rate constant [min^{-1}].

b_2 is the apparent "1st-order disappearance rate constant for insulin [min^{-1}].

b_3 is the 1st phase insulin concentration increase per (mg/dl) increase in the concentration of glucose at time zero due to the injected bolus [$\text{pM}/(\text{mg/dl})$].

b_4 is the constant amount of insulin-dependent glucose disappearance rate constant per pM of plasma insulin concentration [$\text{min}^{-1} \text{pM}^{-1}$].

b_5 is the length of the past period whose plasma glucose concentrations influence the current pancreatic insulin secretion [min]

b_6 is the constant amount of second-phase insulin release rate per (mg/dl) of average plasma glucose concentration throughout the previous b_5 minutes [$\text{min}^{-1} \text{pM}/(\text{mg/dl})$].

b_7 is the constant increase in plasma glucose concentration due to constant baseline liver glucose release [$(\text{mg/dl}) \text{min}^{-1}$].

$$G(t) = G_b(t), t \in [-b_5, 0], G(0) = G_b + b_0, I(0) = I_b + b_3 b_0$$

This model describes how the glucose concentration changes in blood based on spontaneous, insulin-independent net glucose tissue uptake, on insulin-dependent net glucose tissue uptake and on constant baseline liver glucose production. The term net glucose uptake indicates that the changes in tissue glucose uptake and liver glucose

delivery are considered together. Due to insulin catabolism, Insulin plasma concentration changes are considered to depend on spontaneous constant rate decay, and pancreatic insulin secretion. The delay term, $\dot{I}(t)$, refers to the pancreatic secretion of insulin: effective pancreatic secretion at time t is considered to be proportional to the average value of glucose concentration in the b_5 preceding time t .

This model is considered the closest to real representation of the insulin-glucose system.

Li et al [43] introduced their more generic model in 2001. Their model was in the form:

$$\dot{G}(t) = -f(G(t)) - g(G(t), I(t)) + b_7 \quad (2.19-1)$$

$$\dot{I}(t) = -p(I(t)) + q(L(G_t)) \quad (2.19-2)$$

where

$$G(t) = G_b(t), t \in [-b_5, 0],$$

$$G(0) = G_b + b_0, I(0) = I_b + b_3 b_0,$$

$$G_t(\theta) = G_t(t + \theta), t > 0, \theta \in [-b_5, 0]$$

This model (2.19) is considered as general form, thus the following two special cases for $L(G_t)$ can be considered. The models in these two special cases are as follows:

Case1: when $L(G_t) = G(t - b_5)$, the model for this special case is:

$$\dot{G}(t) = -b_1 G(t) - \frac{b_4 I(t) G(t)}{\alpha G(t) + 1} + b_7 \quad (2.20-1)$$

$$\dot{I}(t) = -b_2 I(t) + b_6 G(t - b_5) \quad (2.20-2)$$

Case2: when $L(G_t) = \frac{1}{b_5} \int_{-b_5}^0 G(t + \theta) d\theta$, the model for this special case is:

$$\dot{G}(t) = -b_1 G(t) - \frac{b_4 I(t) G(t)}{\alpha G(t) + 1} + b_7 \quad (2.21-1)$$

$$\dot{I}(t) = -b_2 I(t) + \frac{b_6}{b_5} \int_{-b_5}^0 G(t + \theta) d\theta \quad (2.21-2)$$

Limitation: The reason for assuming that the insulin-dependent glucose uptake has a unit of time, a unit of insulin can only process a limited amount of glucose. The mass action law in this situation is not quite realistic.

Later on, Mukhopadhyay et al. [43] develop the following model (for IVGGT) in 2004.

This model can be assumed as a subfamily of Li et al model (2.19):

$$\dot{G}(t) = -b_1 G(t) - b_4 I(t)G(t) + b_7 \quad (2.22-1)$$

$$\dot{I}(t) = -b_2 I(t) + b_6 \int_0^\infty w(s)G(t-s)ds \quad (2.22-2)$$

where

$$G(t) = G_b, t \in (-\infty, 0),$$

$$G(0) = G_b + b_0,$$

$$I(0) = I_b + b_3 b_0$$

$$w(s) = \alpha^2 s e^{-\alpha s}$$

2-5 Models in the form of Partial Differential Equations (PDEs)

Models in the form of partial differential equations (PDE) were introduced to address the oscillatory nature of the in vitro insulin secretion by the β -cells. Searching the Literatures, many models in the form of PDEs were found. Some of the papers that presents these models are: Bertram et al. [17], Boutayeb et al. (2002) [44], Boutayeb et al (2004) [45], Aslanidi et al. [46], Wach et al. [47], and Keener [48]. We will selected some literatures for discussion.

Wach et al. model [47] assumed that injected soluble insulin is present in the SC tissue in hexametric and diametric form. Only diametric molecules can penetrate the capillary membrane:

$$\frac{\partial h}{\partial t} = P(Qd^3 - h) + D\nabla^2 h \quad (2.23-1)$$

$$\frac{\partial d}{\partial t} = -P(Qd^3 - h) + D\nabla^2 h - Bd \quad (2.23-2)$$

where

h is the concentration of hexameric insulin, P is a rate constant,
 d is the concentrations of diametric insulin, D is a diffusion constant,
 Q is a chemical equilibrium constant, B is an absorption rate constant.

This model has been solved numerically by dividing the SC region into spherical shells for the space discretization. Moreover, the authors for this model have extended this model to be used with monomeric insulin.

Other example is that what Keener [48] has done. In his first model, the situation of a one-dimensional reactor was assumed based on the assumption that a mechanism of insulin secretion identical to that assumed by Maki et al. [49]. Later, it was shown that for certain large values of the ratio of the flow rate to the volume of the reaction islet bed, there are no oscillations. In the second model diffusion was introduced. The model predicts that oscillations occur if there is sufficient diffusion to create adequate concentrations mixing in the reacting layers of the cells. With insufficient such mixing, the oscillations are inhibited. An ‘unsolved dilemma’ having to do with difficulty to produce large enough δ values ($\delta > 0.1$) from experimental values of the scaling parameters V, L_{bed} , where L_{bed} is the length of the islet bed and V is the velocity of the steady flow of the solution along the 1-dimensional reactor, and large physical diffusion (large DI coefficient) which is needed for the model to predict oscillations.

Chapter 3

CONTROLLERS

3-1 Introduction

The traditional type-1 diabetic patients' therapy allows substantial fluctuations in the blood glucose levels. Since such injections can be accumulated and lead to different complications of diabetes, there is an opportunity to reduce this effect by improving the control of the blood glucose.

Early diabetes control papers in the 1960s involved clinical studies using both glucose and insulin infusions that were calculated using on-off control or special nonlinear control algorithms (e.g., the "Biostator" algorithm). The nonlinear control algorithms can be interpreted as Nonlinear Proportional-Derivative controllers that are related to standard gain scheduling technique. Later on, many diabetes control papers have been concerned with automated insulin infusion using standard or modified PID control algorithms. These feedback control strategies are often enhanced by feed-forward control action based on a known meal challenge: an insulin bolus is calculated assuming that the meal time and content are known.

The challenge of automating insulin delivery for diabetic patients using implantable pumps and glucose sensors has received considerable attention over the last 10-20 years. Almost all type-1 diabetic patients live with a traditional or intensified insulin therapy

regimen such that the insulin is injected subcutaneously three to four times a day. The injected insulin dose must be adjusted based on three to seven capillary blood glucose concentration measurements. The use of SC route for insulin delivery is superior to that of IV route. The management and safety of SC route make it ideal for insulin control.

Recent surveys and tutorials provide excellent overviews of diabetes control strategies from a control engineering perspectives. We will start this chapter with the general form of a Partially Closed-Loop and Closed-Loop control schemes to have better understanding of the controller. Later on, the most important control schemes will be discussed such as Run to Run (R2R) or Iterative Learning Control, Standard Proportional Integral Derivative (PID) Controller, Biostator & Nonlinear PID, Dynamic Neural Networks State Observer, Pole Placement Strategy, Optimal Control, H_∞ Robust Control, Bayesian Approach, Model Predictive Control, Adaptive Control, and Self-Tuning Adaptive Control.

3-2 Control Strategies

Control strategies of diabetes therapy can be classified as open loop control, semi closed-loop, and closed-loop control.

The current treatment involves open loop control in which physicians inject a predetermined dose of insulin subcutaneously based on three or four time daily glucose measurements, usually by an invasive method of finger prick. This method not only is painful and inconvenient, but also unreliable because of approximation involved in type and the amount of insulin delivered.

The classical form for the insulin therapy regimen, shown in Figure 3.1, can be presented as a partially closed-loop scheme such that the insulin infusion rate is adjusted according to intermittent blood glucose readings [24]. The feed-forward control, defined by the physician according to the patient's lifestyle (activity level, meals, and occasional self-administered serum glucose tests), is coupled with a feedback control action to utilize the available plasma glucose measurements. The partially closed loop strategy found to be not capable of optimally controlling the blood glucose profile, but can lead to acceptable results from a clinical point of view [50].

The limitations of using partially closed loop strategy are:

1. The lack of appropriated sensors.
2. The absence of any appropriate control algorithm.
3. Suffering from long sampling time problem that lead to miss fast or inter-sample disturbances.

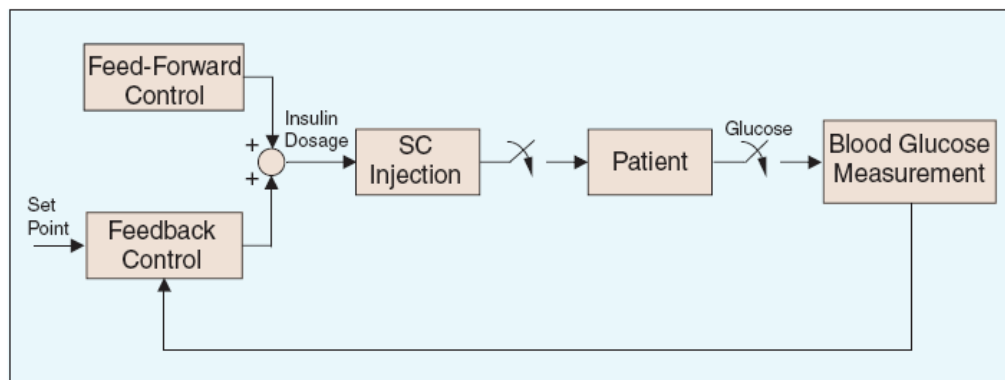


Figure 3.1: The partially closed-loop control strategy of conventional and intensified insulin therapy.

However, the closed-loop control method [51, 52, 53], shown in Figure 3.2, acts as an artificial pancreas is the most effective way of diabetes treatment and could improve the quality of life and life expectancy of patients.

The closed-loop realizations elect the SC route for insulin delivery, with glucose concentration being continuously monitored by an implanted glucose sensor. An implantable blood glucose sensor is definitely the ideal solution for blood glucose measurement [26]. Given this situation, the closed-loop scheme based on an implanted SC glucose sensor becomes widely used [51, 54].

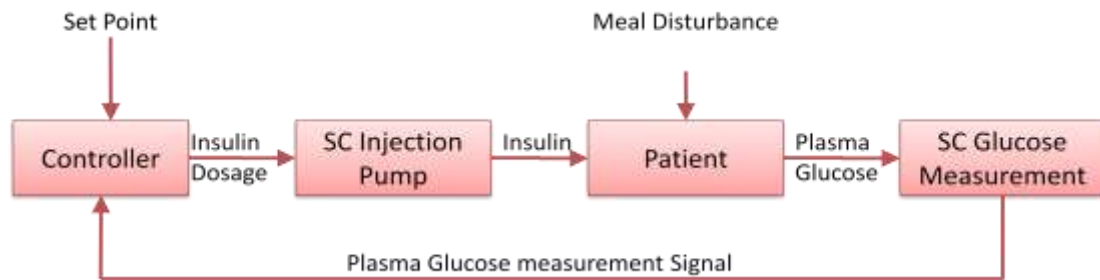


Figure 3.2: The closed-loop control strategy with SC glucose measurement and SC insulin injection.

On the other hand, it is not easy to obtain a satisfactory insulin-glucose control by SC insulin infusion, even in a closed-loop configuration, because of the time delay in absorption by this route. This difficulty is even more distinct in a partially closed-loop configuration where, in addition to regular insulin, an insulin preparation with a delayed action is needed to cope with the basal requirement of the diabetic patient. The recent introduction of the monomeric insulin analogs, such as Lispro insulin, which is absorbed two to three times faster after SC injection than regular insulin [55], has significantly improved the quality of control obtainable through this route.

Some of closed-loop strategies, called model-based systems, deal with the therapy selection problem by combining a set of heuristics for the reduction of the search space with a mathematical model of the glucose-insulin system for the choice of optimal dose. Other approaches, called algorithmic-based systems, only exploit heuristic algorithms for

the therapy definition. Here, we will review some model-based approaches that have been presented in the insulin-glucose control papers. Almost all the systems discussed below were designed before the advent of Lispro insulin. There is no doubt that updating these systems with the new short- and intermediate-acting analogs will improve their usability and performance.

3-3 Run to Run (R2R) or Iterative Learning Control (ILC)

Run to Run control (R2R) or iterative learning control (ILC) is a methodology for dealing with engineering systems that exhibit a cyclic behavior [56]. This control strategies have been successfully used to provide improved control based on experience with one or more recent industrial processes batches. The key idea is that certain disturbances are persistent across repeated “cycles” in a process. R2R have been developed for diabetes control, by considering glucose data for a meal response or an entire day to be the “batch” of interest [11].

Instead of repeatedly correcting for the persistence disturbance from an initial (incorrect) conditions, this algorithmic approach formulates an update on a time scale of the entire cycle, one correction allowed at the end of the batch, which minimizes the effect of the persistent disturbance. Viewed from another perspective, the R2R algorithm starts on a cycle that is poorly controlled, and refines to the control action over the course of multiple cycles until a nearly perfect controlled cycle is obtained [56].

Unlike other techniques; the R2R control strategy is measurements based and its independent variable of the control loop is the batch number, while other control

strategies are model based. Srinivasan et al. [56] and Zisser et al. [57] reported an experimental R2R application. We can now summarize the R2R algorithm as follow [58, 59]:

1. The input profile is parameterize for k run, $u_k(t)$, as $U(t, v_k)$. by considering the ψ_k as a sample version of the measured output $y_k(t)$ such that both input parameter vector v_k and sample output ψ_k (controlled variable).

$$\psi_k = F(v_k)$$

2. Choose an initial random estimate for v_k , $k = 1$
3. Complete the run using the $u_k(t)$ corresponding to v_k .
4. Determine ψ_k from the measurement $y_k(t)$.
5. Input parameters are updated using the following formula

$$v_{k+1} = v_k + K(\psi^r - \psi_k)$$

(3.1)

where:

K : is appropriate gain matrix.

ψ_k : is the reference value.

6. Set $k = k + 1$ and repeat the steps 3-5 until the algorithm converge.

Thus a solution is implemented as an open-loop strategy for each batch (24 hour cycle), and the feedback allows refinement over successive batches (or days) [58, 59]. The Advantage of this technique is that it is almost independent because it translates the limited information about glucose level in the patient into any time of particular interest. In the present context, the limited measurement information of the patient's blood glucose

level is translated into quality measurements (max/min glucose) and resultant quality variables are of the same type of variables that are used to evaluate the effectiveness of a particular insulin regimen.

The results Zisser et al. [57] experiment shows that the glucose control was improved significantly over a two week period based on infrequent glucose measurements (60 and 90 minutes) after the start of a meal.

The clinical trial results of Zisser et al. [58] showed that most of the patients responded positively to the algorithm, and the algorithm's predictions were in line with the medical doctors' recommendations.

3-4 PD and PID Controllers

As stated in the introduction of this chapter, several control algorithms were used since 1960 in medical treatment by injecting both glucose and insulin to control glucose level in the diabetes patient [11].

For most of the Proportional Integral Derivative (PID) control papers, the proposed controllers were evaluated in simulation studies of post-prandial responses. Few experimental applications were evaluated on dogs or humans in different experimental conditions (IV vs. SC sensors and pumps, different types of insulin and insulin analogs, etc.).

The limitation for PID controllers is that the direct comparisons of latter papers can be difficult due to differences in the experimental conditions. Insulin injection were considered in the algorithms using standard or modified PID control with some

enhancement to the feedback control such feed forward action to compensate for the meal disturbance. Assuming that the meal time and content are known, the calculations were performed [11].

During and after meals, Integral control action can lead to insulin overdosing, wind up, and subsequent hypoglycemia; hence, Proportional Derivative (PD) controllers have received considerable attention and being preferred over the standard PID controller.

The limitation for PD controller is that the potential problem can be overcome reduced by judicious use of “anti-reset windup” with the integral control action [11].

3-5 Biostator & Nonlinear PID Controllers

Early diabetes regulation Biostator works to the Glucose Controlled Insulin Infusion System (GCIIS) [60] and later to the On-off control and Biostator algorithm [11] and device of Clemens [52, 61]. The Biostator algorithm feedback controller uses a low-volume continuous-flow blood glucose sampling mechanism with a dual infusion system (insulin and glucose) to maintain blood glucose concentration at a user-defined value. The control algorithm structure was Nonlinear PD type; using a five-point moving average of glucose measurements to minimize noise effects. This control type was excellent for the hospital indoor, bedside, implementation.

The limitation of this controller is the difficulty of implantation due to the additional size associated with the dual-reservoir system necessary for a device of this type. Patient specificity was also an issue, as the algorithm would require individualization prior to its use [60].

3-6 Dynamic Neural Networks (DNN) Controller with State Observer

Alejandro et al. [62] have analyzed Bergman model using the modern observability theory and derived the observability conditions. The glucose concentration measurements in plasma or any of its combinations with the others components are shown to provide the observability property: they contain the complete information about the considered state space dynamic model. The Dynamic Neural Networks (DNN) state observer is suggested to obtain immeasurable state estimates, since this model has several unknown parameters and the measurable data may have noises. The significant advantage of the DNN with respect to the traditional control used in the normal insulin infusion pumps is the present opportunity to avoid any active patient actions [63].

The corresponding numerical simulations show that the suggested technique can be successfully used to realize the insulin doses administration in infusion pumps [62].

Developed the observability analysis for this system have been done. Three output structures turn out to be observable and can be considered in the practical experiments. This means that the glucose concentration as well as its linear combination with any other state contains enough information to realize the adequate on-line control process [62].

3-7 Pole Placement Controller

The pole placement strategy requires the plasma insulin concentration of the diabetic subject follows the same dynamics of the normal subject. Based on SC measurements obtained through a needle-type glucose sensor and on an insulin pump with SC access; the

relationship between plasma insulin and blood glucose concentration in a normal subject during an oral glucose load has been described by a proportional derivative control law [51, 64]:

$$I(t) = aG(t) + b \frac{dG(t)}{dt} + c \quad (3.2)$$

where

I denotes plasma insulin concentration;

G is the blood glucose concentration;

a , b , and c are the parameters responsible for insulin secretion.

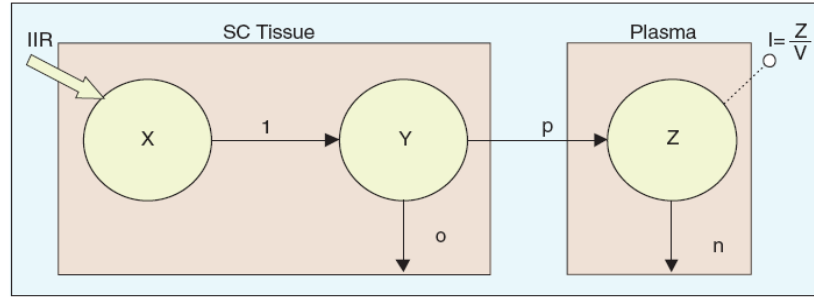


Figure 3.3: The compartmental model of SC insulin absorption and kinetics for pole placement strategy.

Hashiguchi et al. [65] have estimated the parameter values by nonlinear least squares. The pharmacokinetics of SC-injected insulin is described by the three-compartment linearized model of Figure 3.3:

$$\dot{X} = \frac{dX(t)}{dt} = IIR(t) - lX(t) \quad (3.3)$$

$$\dot{Y} = \frac{dY(t)}{dt} = lX(t) - (p + o)Y(t) \quad (3.4)$$

$$\dot{Z} = \frac{dZ(t)}{dt} = pY(t) - nZ(t) \quad (3.5)$$

$$I(t) = \frac{Z(t)}{V} \quad (3.6)$$

where

IIR is the insulin infusion rate.

X , Y , and Z are the insulin masses in the two SC compartments and in plasma, respectively.

V is plasma volume.

The model parameters have been estimated by nonlinear least squares from data obtained in ten diabetic subjects treated with both regular and Lispro insulin. The pole-assignment strategy requires that the plasma insulin concentration of the diabetic subject follows the same dynamics of the normal subject; i.e., the control law is obtained by substituting equation (3.3) into equation (3.4), and neglecting higher-order derivatives:

$$IIR(t) = K_p G(t) + K_d \frac{dG(t)}{dt} + K_c \quad (3.7)$$

where

$$K_p = \frac{amnV}{p}$$

$$\frac{K_d}{K_p} = \frac{1}{l} + \frac{1}{m} + \frac{1}{n} + \frac{b}{a}$$

$$K_c = d + \frac{c}{a}K_p$$

$$m = o + p,$$

d accounts for the IV basal infusion rate.

This system has been tested in venous input venous output (vivo) on ten hospitalized insulin-dependent diabetic patients both in response to a 75g oral glucose load and to a standard meal. Three therapeutic regimens were employed: regular insulin-injected SC,

Lispro-injected SC, and regular insulin- injected IV. The results obtained with SC Lispro were similar to those achieved with IV regular insulin, with the only statistical difference being plasma insulin concentration values between 100-180 minutes (which were higher in the SC case). On the other hand, the results obtained by injecting SC regular insulin were significantly worse than by IV: the total dose of insulin was significantly higher and plasma insulin concentrations were lower at 30 minutes and higher from 90 to 300 minutes, with consequent presence of hyperglycemic peaks followed by hypoglycemic episodes.

Limitations of this controller are:

1. It is not very robust.
2. It requires a repeated assessment of the model parameters, which is usually difficult in clinical practice.

3-8 Optimal Control

Kikuchi et al. [66, 67] solved the glucose control problem for the optimal insulin infusion rate using an approximate solution to the Riccati equation. Swan [68] has solved the glucose control problem for the optimal insulin infusion rate, using a linear diabetic patient model and a quadratic performance criterion:

$$J_1 = \int_0^{\infty} (x_1^2(t) + pu^2(t))dt \quad (3.8)$$

This approach uses optimal control theory and solution of a nonlinear algebraic Riccati equation and it improves the results of Kikuchi et al. [66, 67]. The insulin delivery rate is a function of both the current insulin and glucose concentrations. Assuming that no

glucose-dependent endogenous insulin release, the insulin state can be removed to yield a solution only in terms of the glucose concentration. The limitation of this control was that it focused on the initially hyperglycemic diabetic patient, so meal disturbance attenuation was not treated.

Later on, Fisher et al. [69] have studied the Normalization of patient blood glucose in response to both meal consumption and initial hyperglycemia. Thus, the performance criterion is:

$$J = \int_0^T x_1^2 dt \quad (3.9)$$

where $T = 240$ minutes.

Various infusion protocols were tested to minimize the sum-squared glucose tracking error. Impulse control was found to provide superior control in both cases, with perfect reference tracking achievable if a good estimate of the meal was available (under certain assumptions regarding the shape of the meal disturbance and insulin effects). This impulse control (a single injection at time = 0 minute) is given by:

$$u(t) = \begin{cases} \frac{u_0}{t_b} & \text{if } 0 \leq t \leq t_b \\ 0 & \text{if } t > t_b \end{cases} \quad (3.10)$$

where

t_b is the time taken for the injection.

u_0 is the total amount of insulin injected.

This trial showed superior control in both cases, with perfect reference tracking achievable if a good estimate of the meal was available under the assumption that the glucose injection rate into the blood $p(t)$ takes the following form:

$$p(t) = \begin{cases} B & \text{if } 0 < t < t_a \\ B \exp(-\beta(t - t_a)) & \text{if } t \geq t_a \end{cases} \quad (3.11)$$

where B , β , t_a are constant.

The limitation of this control was that this form was not practical because $p(t)$ differ from patient to patient.

To overcome this problem Lim et al. [41] studied impulse control for the same situations, but in the presence of fuzzy model parameters (patient uncertainty). The results of this method found to be robust and numerically stable for the chosen uncertainty set, and again under assumptions about the dynamic behavior of meals and insulin injection.

Application of the optimal control theory to Bergman model (2.2) was undertaken in two studies using Integral Squared Error (ISE) cost function:

- 1- Ollerto [70] utilized his cost function based on deviation from the desired glucose value. He evaluates the system using (10 and 180) minutes sampling times. The results of using 180 minutes sampling time shows that the system was less sensitive to noise about the basal state, but it had a longer rise time and could also miss significant disturbances that occurred within the inter-sample window. On the other hand, using 10 minutes sampling time on discrete Bergman system shows that the controller was sensitive to glucose profile oscillation around the basal state, and it resulted in physiologically unrealistic profiles characterized by high amplitude sustained oscillations. An insensitive model was introduced, based on a type of dead-band control, but no method for its development was discussed.
- 2- Fisher [71] utilized his cost function based on two objectives: the deviations in glucose concentration from a reference value, and the amount of insulin to perform

the corrective action. Three insulin infusion profiles were evaluated: determining that an initial injection plus optimal hourly infusion minimized the cost function for an initially hyperglycemic patient. The limitation of this algorithm was that it is not robust to patient uncertainty, and suffered from the long sampling time problem of missing fast or inter-sample important disturbances.

3-9 H_∞ Robust Control

Kienitz et al. [72] was evaluated the robust control using the H_∞ control methodology for model 2.2 such that the model containing patient-dependent parameters was governing the glucose and insulin dynamics. The design of this controller was based on two assumptions:

1. Nominal patient model
2. Set of frequency-dependent weighting functions. The frequency-dependent weighting functions were tuned to capture the entire expected patient population (parameter variations).

Since the H_∞ controllers bound worst-case performance, this controller can manage the patient glucose level within the assigned range of variation and sustain meal disturbance for the nominal patients. Compared to the previous controllers, this is a very good improvement.

The limitation of this controller using Bergman model that was robust to a small range of variation and required to be retuning outside this range.

3-10 Adaptive Control

Adaptive control was developed to overcome the limitations of the pole-placement strategy. Several adaptive control literatures were developed and tested based on SC Lispro injections and SC measurements using closed-loop strategies such as Candas et al. [31], Shimoda et al. [51], Fabietti et al. [60], Brunetti et al. [61], Hovorka et al. [73], and Fisher et al. [74]. Simplified adaptive control block diagram is illustrated in Figure 3.4.

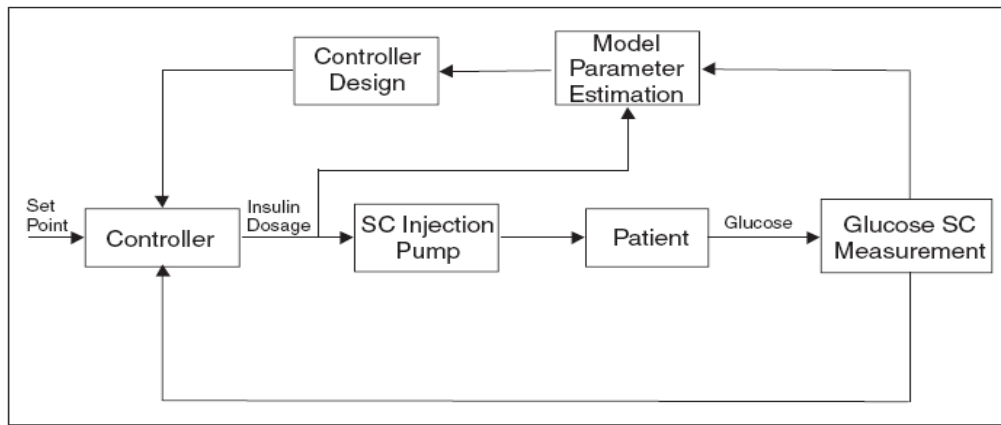


Figure 3.4: The self-tuning adaptive control scheme.

Candas et al. [31] have developed an adaptive controller based on the nonlinear model (2.1) such that the prediction of the insulin-dependent glucose-removal will be more reliable and hence provide better control over a wide spectrum of insulin signals such as IV and SC injections. The performance of the controller is presented for various IV or SC rapid injections and staircase infusions of insulin. The controller reacts promptly to large and rapid variations in insulin action. Although control improves with the number of glucose measurements, the prediction of glucose removal allows for some flexibility in the monitoring of the plasma glucose. Sampling frequency varied from a 2 minutes interval during transient periods to 7 minutes as steady states were reached.

Hovorka et al. [73] has published a detailed review of adaptive control strategies for both diabetes types. Strategies for the following types of situations were considered:

- 1- Infrequent glucose measurements are available (e.g., four to seven measurements per day).
- 2- Frequent glucose measurements are available (e.g., every five minutes). This survey paper contains an extensive bibliography.

The work of Shimoda et al. [51] is an important example of a successful use of the SC route for the closed loop control of insulin-dependent diabetic patients. The reason is mainly due to the use of Lispro insulin, which is better suited for SC closed-loop control than regular insulin since it behaves like IV-injected insulin.

The following discrete-time model M describe the glucose-insulin system:

$$G_k = M(G_{k-1}, \dots, G_{k-h}, ID_{k-1}, ID_{k-p}, \Theta) \quad (3.12)$$

where

G_k is blood glucose concentration at time k ,

ID_k is insulin dose at time k ,

Θ is a set of unknown parameters,

h and p known time delays.

The parameter set is recursively estimated at each time k , on the basis of G_k measurement, which allows one to obtain a one-step-ahead prediction, G_{k+1} , which is used in the on-line regulator design. In fact, the choice of the next dose, ID_{k+1} , is done so as to minimize a suitable cost function, J , which in the case of a minimum variance controller is:

$$J_k = (G_{k+1} - G_b)^2 - rID_{k+1}^2 \quad (3.13)$$

where

G_b is the set point

r is a weighting factor that penalizes insulin dosage

Thus compromising between amount of infused insulin and hyper/hypoglycemia is performed. One can assume that M is linear, so that both the recursive estimation and the minimization problem can be solved in closed form. Given the adaptive capability of the algorithm, the choice of a linear model with time-varying parameters seems appropriate.

These strategies do not require periodical re-evaluation of the patient parameters, and they have been shown to be at least as good, if not superior, to a pole-placement strategy with repeated estimations.

3-11 Model Predictive Control (MPC)

Recently, model-based control strategies have been proposed for the diabetes control, with Model Predictive Control (MPC) receiving considerable attention [15, 75, 76]. Since MPC strategies been successful in the process industries for many reasons, they become attractive for diabetes control:

1. The ability to control both linear and nonlinear processes.
2. Inherent handling of inequality constraints.
3. Prediction of future behavior.
4. Ease of model parameter updating.

The availability of a dynamic model that is reasonably accurate for the current patient conditions is required.

MPC evaluations for diabetes control problems showed improvement in glucose control compare with conventional PID control strategies. Most of these evaluations were simulation studies only. However, European consortium has reported successful clinical applications based on a nonlinear compartmental model [73]. The basic idea for the Linear MPC will now be introduced as illustrated in Figure 3.5 such that:

z , y , u , r and d are the actual output, the measured output, the controller input, the set point and the meal disturbance respectively.

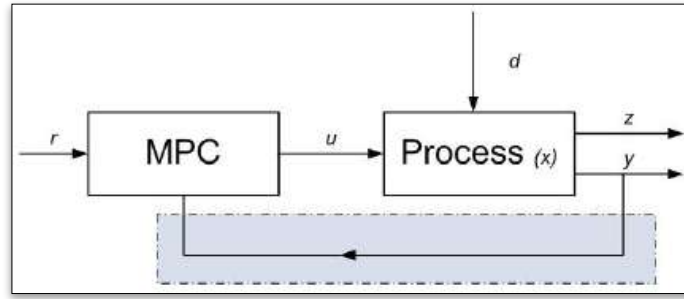


Figure 3.5: The basic Linear MPC.

This approach is developed based on a chain of control actions that minimizes a certain cost function, J , over a selected time horizon such that the difference between the output, z_k , and the reference, r_k , be minimal using a least squares problem [24]. At each sampling time, the control policy is revised by moving the time window used for the cost function calculation. Thus, the cost function, J , can be represented as follow:

$$J = \sum_{i=1}^P (r_{k+i} - \hat{y}_{k+i})^2 + \lambda \sum_{i=1}^M \Delta u_{k+i-1}^2 \quad (3.14)$$

where:

$k, P, r, \hat{y}, \lambda, M$ and Δu are the sample time index, the prediction horizon, the desired set-point, the predicted output, the weight on the manipulated input, the control horizon, and the manipulated input increment respectively.

Parker et al. [77] were the first to publish MPC approach for the management of glucose levels in type-1 diabetic patients. Their research was a simulation study that employed the Sorensen [13] model as the “virtual patient”. The following approaches were used in the model development:

1. Direct identification from patient data using rich signals.
2. Reduced order numerical models that were derived from the original compartmental model.
3. Linearized versions of the compartmental model coupled with a state estimator.

The state estimator was used to identify the unmeasured meal disturbance, providing a form of feed-forward control without the need for direct knowledge of the meal [77]. Kalman filter was used estimate the key physiologic parameters on-line. Thus, the MPC with state estimation approach show the following results:

1. The meals disturbance can be compensated without the direct knowledge of meal contents and/or its timing.
2. The blood glucose levels were controlled well within Normoglycemia.
3. The estimation of key patient parameters was managed and tested for measurement noise and patient (parametric) uncertainty

The limitation of the MPC algorithm is that:

1. It requires a good model that almost matches the real process in all the patients which is difficult. This is because the model parameters depend on many factors, as stated in the first chapter, such as patient age, weight, and health. These parameters are different from patient to patient and also affected by secondary conditions such as patient anger, sleep, sport which is reflected on glucose level in the blood.
2. It wasn't tested in detailed clinical trials involving multiple meals. Thus, the physical system, including the pump and controller, should be evaluated for each case. Hence, the controller and model parameters should be tuned for each patient.

3-12 Nonlinear Predictive Control

Several simulation trials for using the Nonlinear Predictive Control strategy for the closed-loop control with the SC route, for Lispro insulin delivery and glucose measurement, have been proposed by Trajanoski et al. [52, 53]. The scheme of the predictive controller proposed is similar to the adaptive control, shown in Figure 3.4, with the model parameter estimation block being substituted for by the nonlinear predictor.

This MPC approach runs as follow:

1. Minimizing a certain cost function over a selected time horizon by chain of control actions.
2. The cost function is independent on the chain of control actions that predict the controlled variable, but is used to utilize an appropriate model for prediction purpose.
3. The control policy, at each sampling time, is corrected by moving the time window used to calculate the cost function.

Comparing with adaptive control, this control strategy is the same but have following main differences:

1. The model parameters for adaptive control may not change for the selected time window.
2. Since the optimization problem to be solved changes in dependence with the progressive shifts of the time window, thus the control policy requires to be recalculated.

The model used for the prediction of the future blood glucose levels is a Nonlinear Auto-Regressive Model (NARX) such that:

$$G_k = f(x_k) + e_k \quad (3.15)$$

where

$$x_k = \left[G_{k-1}, \dots, G_{k-n_y}, ID_{k-1}, \dots, ID_{k-n_u} \right]^T \quad (3.16)$$

G_k is the blood glucose concentration at time k

ID_k is the insulin dose at time k

n_y is the maximum lags for G_k

n_u is the maximum lags for ID_k

Hovorka et al. [73] have developed a nonlinear model predictive controller with parameter estimator to maintain Normoglycemia in subjects with type-1 diabetes during fasting conditions such that the output trajectory $y(t + k|t)$, $k = 1, \dots, N$ is estimated for any given control sequence $u(t + k|t)$ over a prediction horizon N . The controller employs a compartment model, which represents the glucose control system and includes sub-models representing absorption of SC administered short-acting insulin Lispro and gut

absorption. The controller uses Bayesian parameter estimation to determine the time-varying model parameters. Moving target trajectory facilitates slow, controlled normalization of elevated glucose levels and faster normalization of low glucose values. The model primary use is to determine the optimum control sequence, which results in a desired trajectory. In this strategy, the following steps were used:

1. Linearization around the operating point.
2. The full model was retained.
3. The following components were kept in the controller:
 - a. Parameter optimizer.
 - b. Target projector.
 - c. Dose optimizer
 - d. Safety schemes.

As we have shown in Chapter 2, the parameters of the Insulin-Glucose system differ considerably between subjects and exhibit diurnal variations, although exact quantification of the variation (amplitude and frequency) within a subject is yet to be determined. In recognition of the variation between and within subjects, the controller adapts itself to the changing environment. This is carried out by:

1. Re-estimating parameters at each control step.
2. The parameter optimizer estimates model parameters employing glucose measurements from a ‘learning window’ or time period immediately proceeding the control time. Three lengths of the learning window are predefined, short, medium, and long, to be able to deal with both a time-invariant underlying system.

In conclusion, adaptive nonlinear model predictive control is promising for the control of glucose concentration during fasting conditions in subjects with type-1 diabetes. Its major advantages, which make it an appealing alternative to adaptive control approaches, are:

1. Its capability of handling constraints in the control space.
2. The possibility of ensuring stability to the controlled system.

3-13 Nonlinear Neural Networks

The nonlinear function $f(x(t))$ has been selected from among a class of neural networks with one layer of hidden units, called regularization networks. In particular, a Radial Basis Function (RBF) network was selected:

$$f(x(t)) = \sum_{i=1}^n w_i H(\|x - x_i^0\|) \quad (3.17)$$

where

H is a continuous function from $R^{n_y+n_u} \rightarrow R$,

$\| \cdot \|$ is the Euclidean norm,

x_i^0 are the n -centers of the RBFs.

Fabietti et al. [60] have selected H such that:

$$H(\|x - x_i^0\|) = \frac{1}{((x - x_i^0)^2 + \beta)^2} \quad (3.18)$$

where β is a dispersion parameter.

If β and x_i^0 are known, the estimation of $f(x(t))$ becomes a linear estimation problem of the unknown weights w_i . The RBF functions are known to possess a number of desirable

properties, such as the universal approximation property and the best approximation property in the case of linear estimation (β and x_i^0 known).

According to Trajanoski et al. [53], the RBF has been identified using simulated data obtained by a model of insulin-dependent diabetes that accounts for SC insulin absorption, glucose/insulin interactions, and SC glucose dynamics. The identification of RBF weights and centers was done using the method of Regularized Orthogonal Least Squares (ROLS). Thanks to ROLS, it is possible to take the minimum number of RBFS, so that $f(x(t))$ is able to fit the data under some regularity constraints.

Once the RBF predictor has been identified, the nonlinear predictive controller was synthesized through the moving horizon approach. At each step, the control input (i.e., the SC insulin infusion rate) corresponds to the solution of the minimization problem:

$$\arg \min_{ID} J = \left[\sum_{j=N_1}^{N_p} \left(e_j^T \Gamma_{e_j} \right) + \sum_{j=0}^{N_c-1} \Delta ID^T(t+j) \Gamma_u \Delta ID^T(t+j) \right] \quad (3.19)$$

where

$$ID = [ID_k, ID_{k-1}, \dots, ID_{k-N_c+1}]^T$$

N_c , N_p , N_1 , Γ_e , and Γ_u are tuning parameters of the controller, selected by trial and error.

The data for testing the controller have been obtained by simulating an OGTT of 15 and 75 g in different pathophysiological conditions, by using the same model employed for RBF identification as illustrated in Figure 3.6. The controller was able to maintain blood glucose levels within normal range for the 15 g OGTT (a small perturbation), but not for the 75 g. The authors suggested a combined strategy consisting of adding to the controller a fixed increase in injected insulin dose that would regulate glucose effects corresponding to a meal.

This study has some interesting aspects:

1. The predictive control scheme seems flexible enough to deal with blood glucose control, even in presence of disturbances and pathophysiological variations (i.e., variations in the time constants of the system).
2. The proposed controller may be easily modified to be used in real time.

Unfortunately, the results are not completely satisfactory; in particular, in the presence of meals, and the lack of in vivo validation hampers a complete appraisal of this control scheme.

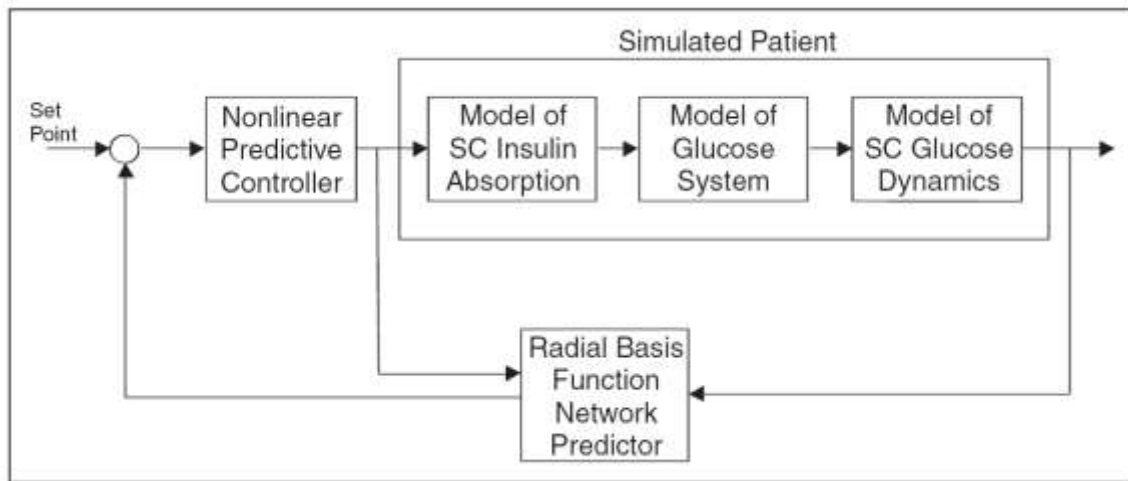


Figure 3.6: The setting used to test the neural predictive control scheme.

3-14 Stochastic Control

Hejlesen et al. [78] have suggested the insulin dosages on the basis of predictions of a discrete-time finite-state stochastic control of the glucose-insulin system. This can be done by optimizing the insulin dosages on the basis of blood glucose measurements, meal intakes, and past insulin injections. Thus, the decision space is limited to the sub-problem

of assessing dosages in a scheme that is fixed in terms of number and type of insulin injections. The state variables (X) are:

1. The blood glucose concentration.
2. The Carbohydrate content of the gut.
3. The insulin action in a compartment remote from plasma.

The output variable (Y) is the blood glucose,

The inputs are:

1. The insulin dosages.
2. Meal intakes (equivalent carbohydrates).

The model has two unknown parameters:

1. Insulin sensitivity
2. Peak time of NPH insulin.

The system dynamics are described through a Markovian process, characterized by transition probabilities

$$P(X_{k+1}|X_k, U_k, \theta) \tag{3.20}$$

where

θ is the parameter vector

$P(Y_{k+1}|X_{k+1})$ is the distribution.

Given a set of observations $D = Y_1, Y_2, \dots, Y_k$

This strategy forms a Bayesian estimate of the posterior probability distribution of the unknown parameters $P(\theta|D)$, and then uses this estimate to find the predictive distribution of blood glucose concentration: $P(Y_{k+1}|U, D)$. Since probability calculations

in a Bayesian framework are not straightforward, and particularly so the transition probability matrix, stochastic control has been built by resorting to a Bayesian network [79].

A Bayesian network is a directed acyclic graph in which every node is a stochastic variable, and the arcs express the conditional dependencies among variables. Such conditional dependencies are quantified through the conditional probability distributions of the nodes, given their parents. Moreover, finite-state Bayesian networks possess powerful algorithms for the calculation of posterior estimates. The sampling time is taken equal to one hour. A single time transition is shown in Figure 3.7.

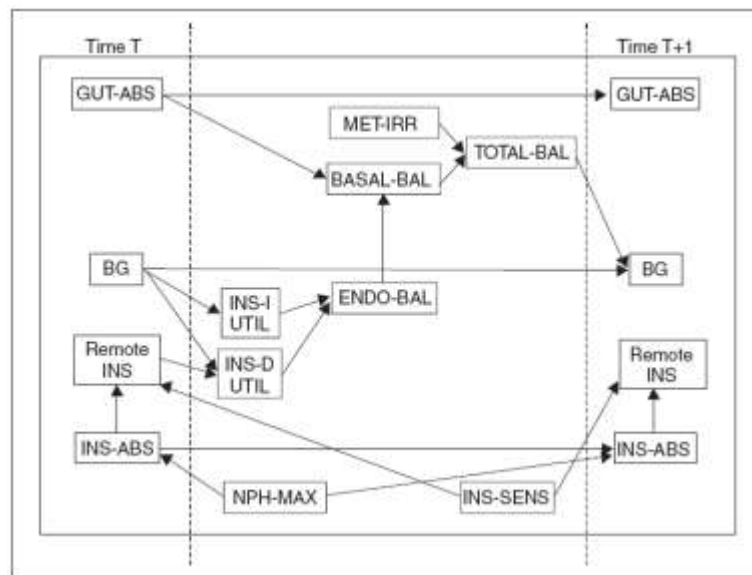


Figure 3.7: A single time transition Bayesian network.

The transition probabilities are implicitly expressed by a series of local conditional models. The blood glucose concentration (node BG) is only indirectly dependent on the quantity of carbohydrates present in the gut (node Gut-Abs), since the relationship is mediated by the balance between insulin-dependent and insulin-independent glucose utilization (node Basal-Bal). The probability distributions needed to specify the network

have been derived from data in the literature. Once $P(Y_{k+1}|U, D)$ has been derived, the optimal dosages is calculated by minimizing the Expected Value (EV) of a cost function $C(Y)$:

$$EV = \sum_{j=k+1}^{k+T} \sum_{i=1}^n P(Y_j = y_i|U, D)C(Y_i) \quad (3.21)$$

where

Y_1, \dots, Y_n are the n -states in which the blood glucose levels have been discretized ($n = 8$)

T is the time horizon of interest.

In brief, this strategy has limited predictive capability for the system but appear to be safe and able to both stabilize blood glucose levels and limit the risk of hypoglycemia. The advantages related to the use of this control are:

1. Its ability to account for intra-individual variability of patients.
2. The particular shape of the cost function naturally minimizes the hypoglycemic risks.

The limitations of this control strategy are:

1. The number of conditionals used in the model seems unnecessarily high considering the rather low accuracy of predictions.
2. It requires the precise quantification of meal intakes in terms of carbohydrate equivalents, which can be somewhat difficult during home monitoring of diabetic patients.

3-15 Fuzzy Control

Zadeh [80, 81] was the one who introduced the Fuzzy logic that is simply a conclusion reached by a computer program which considered as an extension of conventional logic

that models the uncertainties of natural language, handling the concept of partial truth that is the true value between “completely true” and “completely false”. Since the fuzzy control did not require any mathematical model to follow, we can classify this type of control as non model base, or model-free, type. Thus, fuzzy control can be used to monitor biological systems that would be difficult or impossible to model with simple, linear mathematics. Neural network, software that simulates human neural processing capabilities, has been used to apply fuzzy logic theoretical principles and to extrapolate rules (neuro-fuzzy control system).

Blood Glucose control using fuzzy logic control was attractive for many research groups and received high attention on the recent century. Selective literatures, which were published in the 2000s, will be presented in this review.

In 2001, Davide D. et al. [82] have applied fuzzy logic principles and neural network techniques to modify IV insulin administration rates during glucose infusion. Forty critically ill, fasted diabetic subjects submitted to glucose and potassium infusion entered the study. They were randomly assigned to two treatment groups:

- A. Insulin infusion rates were adjusted, every 4 hours at (0 ± 1.5) U/h step size, according to a neuro-fuzzy nomogram.
- B. Insulin infusion rates were modified according to a conventional algorithm.

In group A, Blood Glucose was lowered below 10 mmol/l faster than in group B. Mean Blood Glucose was (7.8 ± 0.2) mmol/l in group A and (10.6 ± 0.3) mmol/l in group B. Blood Glucose values below 4.4 mmol/l were: A= 5.8% and B = 10.2%. Blood Glucose values lower than 2.5 mmol/l had never been observed.

The advantages of this control strategy is that it was found to be effective and safe in improving the Blood Glucose control in critically ill diabetic patients without increasing either the number of Blood Glucose determinations or the risk of hypoglycemia.

In 2006, Campos et al. [83] have developed a fuzzy based advisory/control algorithm for type-1 diabetes patients based on multiple daily insulin injections regimen. A Mamdani-type fuzzy logic controller was used to regulate the blood glucose level. This algorithm does not rely on a direct glucose prediction or estimation to evaluate the insulin adjustments. The overall control strategy was based on a two-loop feedback strategy, as shown in Figure 3.8, to overcome the variability in the glucose-insulin dynamics from patient to patient and to add robustness to the overall control scheme:

- 1- An inner-loop provides the amount of both rapid/short and intermediate/long acting insulin formulations that are programmed on a three-shots daily basis before meals. The combined preparation is then injected by the patient through a SC route.
- 2- The outer-loop controller aims to work as a supervisor of the inner-loop controller such that it adjusts the maximum amounts of insulin provided to the patient in a time-scale of days.

Extensive closed-loop simulations are illustrated, using a detailed compartmental model of the insulin-glucose dynamics in a type 1-diabetic patient with meal intake.

Also Ibbini [84] demonstrated, in 2006, how a fuzzy PI controller was constructed using a simplified design scheme and then subjected to simulations of the two common diabetes disturbances: sudden glucose meal and system parameter variations, such as metabolic

stress. The performance of the proposed fuzzy PI controller was compared to that of the conventional PID and optimal techniques and was shown to be superior to both of them.

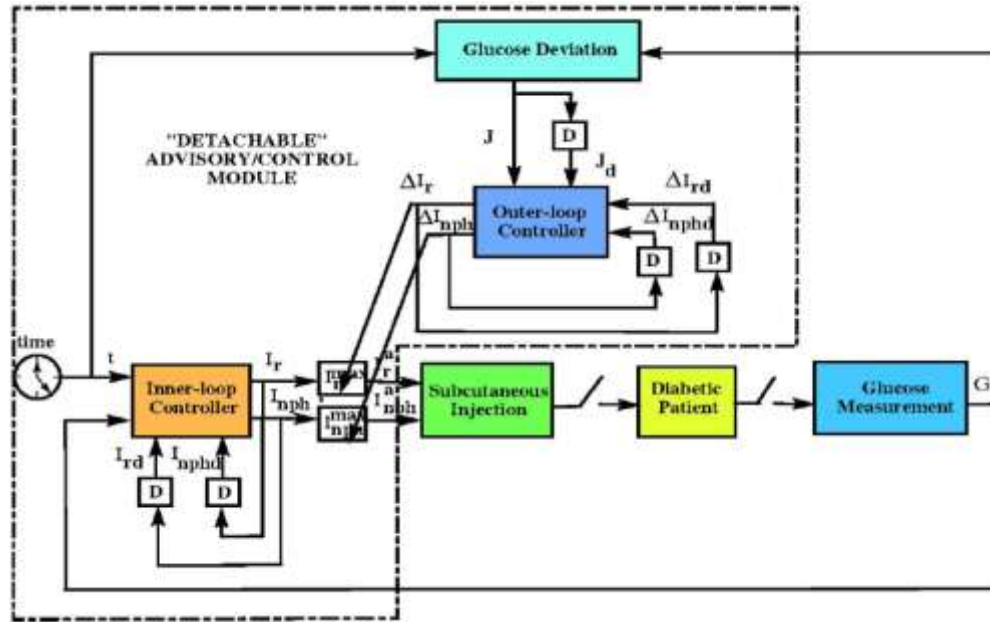


Figure 3.8: Control diagram for blood glucose regulation in Type-1 diabetes patients by subcutaneous route.

The advantage of using fuzzy PI controller is that it was more effective than previously proposed fuzzy logic controllers, especially with respect to the overshoot and settling time.

Recently in 2008, Yasini et al. [85] have developed a closed-loop control algorithm for blood glucose regulation in type-1 diabetes mellitus patients based on Bergman minimal model. The control technique incorporates expert knowledge about treatment of disease by using Mamdani-type fuzzy logic controller with two input linguistic variables and one output variable to stabilize the blood glucose concentration to the Normoglycaemic level. Controller performance is assessed in terms of its ability to reject the multiple meal disturbances resulting from food intake, on an averaged nonlinear patient model.

Robustness of the controller is tested over three patients with model parameter varying considerably from the average model.

The advantage of this controller is that it provides the possibility of more accurate control of blood glucose level in the patient in spite of uncertainty in model and measurement noise. Simulation results show the superiority of the proposed scheme in terms of robustness to uncertainty in comparison with other approaches.

Thus we can summarize the advantages of the Fuzzy logic control as follows:

- 1- It provides a simple and dynamic approach to sensitive, safety-critical problems by means of monitoring a patient's vital signs; discrete adjustments are made to reach a desired output based on straightforward linguistic rules.
- 2- It could serve as a valuable tool for teaching diabetic patients about how their body responds to insulin, as a clinical research platform for the study of drug interactions.
- 3- It offers a fast, efficient and safe mechanism for supporting anaesthetized patients peri-operatively.
- 4- It has the ability to learn and adapt, giving it far more potential than fixed Boolean computer algorithms

While the limitations of the fuzzy control can be summarized by:

1. Inadequate programming when the fuzzy logic systems do not match standard human performance.
2. It lacks innate intuition; humans are still good at acting beyond set rules. However, failures of Fuzzy logic systems are rare and they remain as good as their programmed goals.

Chapter 4

LMI-BASED CONTROL DEVELOPMENT

4-1 Introduction

Based on the understanding of the previous chapters, it is clear that we have to design a controller that is able to deal with nonlinear time-delay systems. The designed controller should be robust to uncertainty in model parameters and meal disturbances because of the parameter variations in the glucose-insulin models vary from patient to patient.

In this chapter, we will start with introduction about the time-delay systems. Then, the LMI control performance of both H_2 and H_∞ will be shown briefly. Later on, further development of robust stability and feedback stabilization methods of the Nominally Linear Time Delay (NLTD) systems will be carried out in the following sequence:

- 1- Design LMI to check the delay effects on the system stability for “type 1-diabetic patient” model with single time delay.
- 2- Mathematical development of two feedback stabilization controller schemes starting with state-feedback controller then subsequently turn to dynamic output feedback controller using linear state delay LMI technique.

The parameter uncertainties are convex-bounded and the unknown nonlinearities are time-varying perturbations satisfying Lipschitz conditions in the state and delayed-state. An

appropriate Lyapunov functional is constructed to exhibit the delay-independent dependent nonlinear dynamics.

4-2 Symbols and their definitions

Important notes that will be used in the analysis and design during this chapter:

- The Euclidean norm is used for vectors.
- W^t denotes the transpose of any matrix W
- W^{-1} denotes the inverse of any square matrix W .
- $W > 0$ ($\geq, <, \leq 0$) denotes a symmetric strictly positive definite (positive semidefinite, strictly negative definite, negative semidefinite) matrix W
- I denotes the $n \times n$ identity matrix.
- \mathbb{R}^+ denotes the set of non-negative real numbers.
- \mathbb{N} denotes the finite set of integers $\{1; \dots; N\}$.
- Symbol (\bullet) used in some matrix expressions to induce a symmetric structure, that is if given matrices $L = L^t$ and $R = R^t$ of appropriate dimensions, then

$$\begin{bmatrix} L & N \\ N^t & R \end{bmatrix} = \begin{bmatrix} L & N \\ \bullet & R \end{bmatrix}$$

- Schur Complement

$$L + NR^{-1}N^t < 0 \rightarrow \begin{bmatrix} L & N \\ N^t & R \end{bmatrix} < 0$$

Sometimes, the arguments of a function will be omitted when no confusion can arise.

4-3, H_2 and H_∞ Controllers Performance

Given a general state-space realization of the plant [86]

$$\dot{x} = Ax + B_1w + B_2u \quad (4.1-1)$$

$$z_\infty = C_1x + D_{11}w + D_{12}u \quad (4.1-2)$$

$$z_2 = C_2x + D_{22}u \quad (4.1-3)$$

where

x , z , u , w , A , B , C , and D are the state vector, the controlled output vector, the control input vector, the disturbance input vector, the states matrix, the inputs matrix, the matrix that relates the states to the outputs, and the matrix relates the inputs to the controlled outputs respectively.

The closed-loop system is given in state-space form by

$$\dot{x} = (A + B_2K)x + B_1w \quad (4.2-1)$$

$$z_\infty = (C_1 + D_{12}K)x + D_{11}w \quad (4.2-2)$$

$$z_2 = (C_2 + D_{22}K)x \quad (4.2-3)$$

where

x , z , u , w , K , A , B , C , and D are the state vector, the controlled output vector, the control input vector, the disturbance input vector, the close-loop control gain, the states matrix, the inputs matrix, the matrix that relates the states to the outputs, and the matrix relates the inputs to the controlled outputs respectively.

Taken separately, our design objectives have the following LMI formulation:

H_∞ performance: the closed-loop RMS gain from w to z_∞ does not exceed γ if and only if there exists a symmetric matrix X_∞ such that [87]

$$\begin{bmatrix} (A + B_2K)X_\infty + X_\infty(A + B_2K)^T & B_1 & X_\infty(C_1 + D_{12}K)^T \\ B_1^T & -I & D_{11}^T \\ (C_1 + D_{12}K)X_\infty & D_{11} & -\gamma^2 I \end{bmatrix} < 0 \quad (4.3-1)$$

$$X_\infty > 0 \quad (4.3-2)$$

H₂ performance: the closed-loop H₂ norm of T₂ (the closed-loop transfer functions from w to z_2) does not exceed ν if there exist two symmetric matrices X_2 and Q such that:

$$\begin{bmatrix} (A + B_2K)X_2 + X_2(A + B_2K)^T & B_1 \\ B_1^T & -I \end{bmatrix} < 0 \quad (4.4-1)$$

$$\begin{bmatrix} Q & (C_2 + D_{22}K)X_2 \\ X_2(C_2 + D_{22}K)^T & X_2 \end{bmatrix} > 0 \quad (4.4-2)$$

$$\text{Trace}(Q) < \nu^2 \quad (4.4-3)$$

These sets of conditions add up to the nonconvex optimization problem with variables Q , K , X_∞ , and X_2 . For tractability in the LMI framework, Matlab seeks a single Lyapunov matrix

$$X := X_\infty := X_2 \quad (4.5)$$

that enforces all the objectives. With the change of variable

$$Y := KX \quad (4.6)$$

This leads to the following suboptimal LMI formulation of our multi-objective state-feedback synthesis problem. Minimize $\alpha \gamma^2 + \beta \text{Trace}(Q)$ over Y , X , Q , and γ^2 satisfying the following [88-90]:

$$\begin{bmatrix} AX + XA^T + B_2Y + Y^T B_2^T & B_1 & XC_1^T + Y^T D_{12}^T \\ B_1^T & -I & D_{11}^T \\ C_1X + D_{12}Y & D_{11} & -\gamma^2 I \end{bmatrix} < 0 \quad (4.7-1)$$

$$\begin{bmatrix} Q & C_2X + D_{22}Y \\ XC_2^T + Y^T D_{22}^T & X \end{bmatrix} > 0 \quad (4.7-2)$$

$$[\lambda_{ij} + \mu_{ij}(AX + B_2Y)X_{pol} + \mu_{ij}(XA^T + Y^TB_2^T)]_{1 \leq j \leq m} < 0 \quad (4.7-3)$$

$$\text{Trace}(Q) < \nu_o^2 \quad (4.7-4)$$

$$\gamma^2 < \gamma_o^2 \quad (4.7-5)$$

Denoting the optimal solution by $(X^*, Y^*, Q^*, \gamma^*)$, the corresponding state-feedback gain is given by

$$K^* = Y^*(X^*)^{-1} \quad (4.8)$$

and this gain guarantees the worst-case performances:

$$\|T_\infty\|_\infty \leq \gamma^*, \|T_2\|_2 \leq \sqrt{\text{Trace}(Q^*)} \quad (4.9)$$

Note that K^* does not yield the globally optimal trade-off in general due to the conservatism of assumption $X := X_\infty := X_2$.

4-4 H_∞ Control Problem

Almost all practical systems are subject to the external disturbances that can in some situations degrade system performance if their effects are not considered during the design phase. There are many ways to reduce the effect of the external disturbances. One of them is the H_∞ control technique. It consists of designing a suboptimal control that minimizes the effect of the disturbances on the output. In other words, the problem can be explained as follows: given a dynamical time delay system with exogenous input that belongs to $\mathcal{L}_2[0, \infty]$, design a controller that minimize the H_∞ -norm of the transfer function between the controlled output and the external disturbance, or at least guarantees that H_∞ -norm will not exceed a given level $\gamma > 0$ (γ is the disturbance rejection ratio level). All

the design algorithms in this chapter are based on LMI formalism which makes them more useful:

$$\frac{\|z(t)\|_2^2}{\|w(t)\|_2^2} < \gamma^2 \quad (4.10)$$

Our goal in addressing the H_∞ Control problem consists of:

- 1- Developing sufficient conditions under which the unforced NLTD system, that is $u(t) \equiv 0$, will be stable and will guarantee $\gamma > 0$.
- 2- Designing controller schemes that stabilize the class of system with time delay and guarantee $\gamma > 0$.

4-5 Nominally Linear Time Delay (NLTD) System

4-5-1 Theoretical Background

A system whose future state values depend on both the present and the history of the system can be called time-delay system [86]. Nonlinear time-delay systems are frequently encountered to describe propagation, transport phenomena and population dynamics in various engineering and biological applications such as glucose response to insulin injection for type-1 diabetic patients. Presence of time delay complicates the system analysis and, in some cases, may affect the system behavior and performance. It turns out that delays are, perhaps, the main causes of instability and poor performance in dynamic systems [91, 92].

Many papers, example [89, 93], have discussed the stability analysis and control design of time-delay systems. We can classify the stability criteria for linear state-delay systems into two main categories:

- 1- Delay-independent: which are applicable to delays of arbitrary size [94, 95].
- 2- Delay-dependent: which include information on the size of the delay [92, 94-99].

The contemporary research activities can be classified two main methods:

- 1- The choice of an appropriate Lyapunov-Krasovskii Functional (LKF) for stability and performance analysis within the framework of linear matrix inequalities [100]. General LKF forms might lead to a complicated system of inequalities [99] and the selection of new and effective LKF forms is becoming crucial for deriving less-conservative stability criteria.
- 2- The introduction of additional parameters for developing improved sufficient stability conditions by importing some basic system identities [94, 96-99, 101-111].

A fundamental problem arises when estimating the upper bound of cross product terms when dealing with time-varying delays. Algebraic inequalities [112] and majorization procedures [91] have been used. This introduces a source of overdesign conservatism.

There have been different approaches to reduce the level of conservatism such as:

- 1- Full-size quadratic functions [107]
- 2- Discretized LKF [103]
- 3- Free-weighting matrices techniques [97-99, 104-115]. In particular, the significance of bypassing extra conservatism introduced after enlarged integration time-span in some LKF terms was pointed out in [99].

From the published results, it appears that further reduction of design conservatism can be achieved with:

1. Appropriate LKF with moderate number of terms.
2. Avoiding bounding methods.
3. Effective use of parameterized relations and variables to avoid redundancy.

Recently, control theory and techniques for nonlinear time-delay systems were developed and different methods generalizing some aspects of the, so-called, differential geometric approach have been made [116]. These include back-stepping, adaptive, observer-based and state-predictors for controlling nonlinear time-delay systems can be found in [117-123].

New and less conservative solutions to the stability and stabilization problems in terms of feasibility-testing of new parameterized linear matrix inequalities (LMIs) will be developed. We consider the time-delay factor as a fixed time-varying function and derive the solution criteria for nominal and poly-topic models. All the developed results are expressed in terms of convex optimization over LMIs.

The development of solutions to the stability and feedback stabilization problems are the main objectives of the next sections.

4-5-2 Mathematical formulation

The original general class of Nominally Linear Time Delay (NLTD) system is in this form:

$$\dot{x}(t) = f(x(t), x(t - \tau), u(t)) + \Gamma_o w(t)$$

$$\begin{aligned}
&= f(x(t), x(t - \tau), u(t)) + A_o x(t) - A_o x(t) + A_{do} x(t - \tau) - A_{do} x(t - \tau) + \Gamma_o w(t) \\
&= A_o x(t) + A_{do} x(t - \tau) + B_o u(t) + f_o(x(t), t) + h_o(x(t - \tau), t) + \Gamma_o w(t)
\end{aligned} \tag{4.11-1}$$

$$y(t) = C_o x(t) + C_{do} x(t - \tau) + F_o u(t) + \psi_o w(t) \tag{4.11-2}$$

$$z(t) = G_o x(t) + G_{do} x(t - \tau) + D_o u(t) + \Phi_o w(t) \tag{4.11-3}$$

where

$x(t) \in \mathfrak{R}^n$ is the state vector,

$u(t) \in \mathfrak{R}^m$ is the control input,

$w(t) \in \mathfrak{R}^q$ is the disturbance input which belongs to $\mathcal{L}_2 [0, \infty)$,

$y(t) \in \mathfrak{R}^p$ is the measured output,

$z(t) \in \mathfrak{R}^q$ is the controlled output.

The initial condition $w(\phi)$ is a differentiable vector-valued function on $[-\tau, 0]$ where $\tau > 0$ is a time delay factor.

The matrices $A_o \in \mathfrak{R}^{n \times n}$, $B_o \in \mathfrak{R}^{n \times m}$, $C_o \in \mathfrak{R}^{p \times n}$, $D_o \in \mathfrak{R}^{q \times m}$, $F_o \in \mathfrak{R}^{p \times m}$, $G_o \in \mathfrak{R}^{q \times n}$, $A_{do} \in \mathfrak{R}^{n \times n}$, $C_{do} \in \mathfrak{R}^{p \times n}$, $G_{do} \in \mathfrak{R}^{q \times n}$, $\Gamma_o \in \mathfrak{R}^{n \times q}$, $\psi_o \in \mathfrak{R}^{p \times q}$, $\Phi_o \in \mathfrak{R}^{q \times q}$ are real and known constant matrices.

For our model (2.11), we will consider $\tau(t)$ to be a constant time delay, then $\tau(t) = \tau$ where $0 < \tau \leq \varrho$; (ϱ is constant scalar (5-15 minutes))

The unknown functions $f_o = f_o(x(t), t) \in \mathfrak{R}^n$ and $h_o = h_o(x(t - \tau), t) \in \mathfrak{R}^n$ are vector-valued time-varying nonlinear perturbations with $f_o(0, t) = 0$, $h_o(0, t) = 0 \forall t$ and satisfy for the following Lipschitz conditions for all $(x, t), (\hat{x}, t) \in R^n \times R$:

$$\|f_o(x(t), t) - f_o(\hat{x}(t), t)\| \leq \alpha \|F[x(t) - \hat{x}(t)]\| \tag{4.12}$$

$$\|h_o(x(t - \tau), t) - h_o(\hat{x}(t - \tau), t)\| \leq \beta \|H[x(t - \tau) - \hat{x}(t - \tau)]\| \quad (4.13)$$

where

$F \in R^n \times R^n$ the upper bounds constant matrices of f_o .

$H \in R^n \times R^n$ the upper bounds constant matrices of h_o .

α and β are scalars > 0

Then from the properties of the Euclidean norms, it follows $\|f_o\| \leq \alpha \|Fx(t)\|$, and hence

$$\|f_o^t f_o - \alpha^2 x^t(t) F^t F x(t)\| \leq 0 \quad (4.14)$$

and in the same way $\|h_o\| \leq \beta \|Hx(t - \tau)\|$, and

$$\|h_o^t h_o - \beta^2 x^t(t - \tau) H^t H x(t - \tau)\| \leq 0 \quad (4.15)$$

4-6 \mathcal{L}_2 Gain Analysis

New criteria for LMI-based characterization of delay-dependent asymptotic stability and \mathcal{L}_2 gain analysis will be proposed in this section. The criterion includes some parameter matrices which aim at expanding the range of applicability of the developed conditions.

The following theorem establishes the main result for the NLTD system (4.11):

Theorem 1:

Given $\varrho > 0$, The NLTD system (4.11) with $u(.) \equiv 0$ is delay-independent ($\tau(t) = \tau$) asymptotically stable with \mathcal{L}_2 performance bound γ if there exist symmetric positive definite weighting matrices P, W, Q ; appropriate relaxation parameter matrices injected to facilitate the delay dependence analysis $\Theta \in \mathbb{R}^{n \times n}$, $\Upsilon \in \mathbb{R}^{n \times n}$; and scalars $\gamma > 0, \sigma > 0, \kappa > 0$ that satisfy the following LMI:

$$\mathcal{E} = \begin{bmatrix} \mathcal{E}_{11} & \mathcal{E}_{12} & -\tau\Theta & P & P & P\Gamma_o & G_o^t & -\varrho A_o^t W \\ \bullet & \mathcal{E}_{22} & -\tau Y & 0 & 0 & 0 & G_{do}^t & -\varrho A_{do}^t W \\ \bullet & \bullet & -\tau W & 0 & 0 & 0 & 0 & 0 \\ \bullet & \bullet & \bullet & -\sigma I & 0 & 0 & 0 & -W \\ \bullet & \bullet & \bullet & \bullet & -\kappa I & 0 & 0 & -W \\ \bullet & \bullet & \bullet & \bullet & \bullet & -\gamma^2 I & \Phi_o^t & -\varrho \Gamma_o^t W \\ \bullet & \bullet & \bullet & \bullet & \bullet & \bullet & -I & 0 \\ \bullet & \bullet & \bullet & \bullet & \bullet & \bullet & \bullet & -\varrho W \end{bmatrix} < 0 \quad (4.16-1)$$

where

$$\mathcal{E}_{11} = PA_o + A_o^t P^t + \Theta + \Theta^t + Q + \sigma \alpha^2 F^t F \quad (4.16-2)$$

$$= PA_o + A_o^t P + \Theta + \Theta^t + Q + \sigma \alpha^2 F^t F \quad (4.16-3)$$

$$\mathcal{E}_{12} = PA_{do} - \Theta + Y^t \quad (4.16-4)$$

$$\mathcal{E}_{22} = -Y - Y^t - Q + \kappa \beta^2 H^t H \quad (4.16-5)$$

Proof:

Consider the Lyapunov-Krasovskii Function:

$$V(t) = V_o(t) + V_a(t) + V_m(t) \quad (4.17-1)$$

$$V_o(t) = x^t(t) P x(t) \quad (4.17-2)$$

$$V_a(t) = \int_{t-\varrho}^t \int_{t+s}^t \dot{x}^t(\alpha) W \dot{x}(\alpha) d\alpha ds \quad (4.17-3)$$

$$V_m(t) = \int_{t+\tau(t)}^t x^t(s) Q x(s) ds = \int_{t-\tau}^t x^t(s) Q x(s) ds \quad (4.17-4)$$

where

$V_o(t)$ is standard to the delayless nominal system

$V_a(t)$ and $V_m(t)$ correspond to the delay-dependent conditions.

A straightforward computation gives the time-derivative of $V(t)$ along the solutions of the

NLTD with $w(t) = 0$ as:

$$\dot{V}(t) = \dot{V}_o(t) + \dot{V}_a(t) + \dot{V}_m(t) \quad (4.18)$$

$$\begin{aligned}
\dot{V}_o(t) &= \dot{x}^t(t)Px(t) + x^t(t)P\dot{x}(t) = 2x^t(t)P\dot{x}(t) \\
&= 2x^t(t)P[A_o x(t) + A_{do} x(t - \tau) + f_o + h_o] \\
&= 2x^t(t)P[A_o x(t) + A_{do} x(t - \tau)] + 2x^t(t)Pf_o + 2x^t(t)Ph_o \\
&\quad + 2x^t(t)\Theta \int_{t-\tau}^t \dot{x}(s) ds + 2x^t(t - \tau)Y \int_{t-\tau}^t \dot{x}(s) ds \\
&\quad - \left[2x^t(t)\Theta \int_{t-\tau}^t \dot{x}(s) ds + 2x^t(t - \tau)Y \int_{t-\tau}^t \dot{x}(s) ds \right] \\
&= 2x^t(t)P[A_o x(t) + A_{do} x(t - \tau)] + 2x^t(t)Pf_o + 2x^t(t)Ph_o \\
&\quad + 2x^t(t)\Theta[x(t) - x(t - \tau)] + 2x^t(t - \tau)Y[x(t) - x(t - \tau)] \\
&\quad - \left[2x^t(t)\Theta \int_{t-\tau}^t \dot{x}(s) ds + 2x^t(t - \tau)Y \int_{t-\tau}^t \dot{x}(s) ds \right] \\
&= 2x^t(t)[PA_o + \Theta]x(t) + 2x^t(t)[PA_{do} - \Theta + Y^t]x(t - \tau) \\
&\quad + 2x^t(t - \tau)(-Y)x(t - \tau) - 2x^t(t)\Theta \int_{t-\tau}^t \dot{x}(s) ds - 2x^t(t - \tau)Y \int_{t-\tau}^t \dot{x}(s) ds \\
&\quad + 2x^t(t)Pf_o + 2x^t(t)Ph_o \\
\dot{V}_o(t) &= x^t(t)PA_o x(t) + x^t(t)A_o^t P^t x(t) + x^t(t)\Theta x(t) + x^t(t)\Theta^t x(t) \\
&\quad + 2x^t(t)[PA_{do} - \Theta + Y^t]x(t - \tau) + 2x^t(t - \tau)(-Y)x(t - \tau) \\
&\quad - 2x^t(t)\Theta \int_{t-\tau}^t \dot{x}(s) ds - 2x^t(t - \tau)Y \int_{t-\tau}^t \dot{x}(s) ds + 2x^t(t)Pf_o \\
&\quad + 2x^t(t)Ph_o
\end{aligned}$$

$$\begin{aligned}
\dot{V}_o(t) = & \frac{1}{\tau} \int_{t-\tau}^t \left(x^t(t) P A_o x(t) + x^t(t) A_o^t P^t x(t) + x^t(t) \Theta x(t) + x^t(t) \Theta^t x(t) \right. \\
& + 2x^t(t) [P A_{do} - \Theta + Y^t] x(t - \tau) - 2x^t(t - \tau) Y x(t - \tau) \\
& \left. - 2x^t(t) \tau \Theta \dot{x}(s) - 2x^t(t - \tau) \tau Y \dot{x}(s) + 2x^t(t) P f_o + 2x^t(t) P h_o \right) ds
\end{aligned} \tag{4.19}$$

$$V_a(t) = \int_{t-\varrho}^t \int_{t+s}^t \dot{x}^t(\alpha) W \dot{x}(\alpha) d\alpha ds$$

Using Leibniz Rule:

$$\begin{aligned}
F(x) &= \int_{\phi_1(x)}^{\phi_2(x)} f(x, s) ds \\
\dot{F}(x) &= \frac{dF(x)}{dx} = \int_{\phi_1(x)}^{\phi_2(x)} \frac{df(x, s)}{dx} ds + \frac{d\phi_2(x)}{dx} f(x, \phi_2(x)) - \frac{d\phi_1(x)}{dx} f(x, \phi_1(x))
\end{aligned}$$

Yields to:

$$\begin{aligned}
\dot{V}_a(t) &= \int_{t-\varrho}^t \frac{d}{dt} \left(\int_{t+s}^t \dot{x}^t(\alpha) W \dot{x}(\alpha) d\alpha \right) ds \\
&= \int_{t-\varrho}^t (\dot{x}^t(t) W \dot{x}(t) - \dot{x}^t(t+s) W \dot{x}(t+s)) ds \\
&= \varrho \dot{x}^t(t) W \dot{x}(t) - \int_{-\varrho}^0 (\dot{x}^t(t+s) W \dot{x}(t+s)) ds
\end{aligned}$$

Using integration by part, and let $t + s = \alpha$ then $ds = d\alpha$. when $s = -\varrho$ then $\alpha = t - \varrho$, and when $s = 0$ then $\alpha = t$. Thus:

$$\begin{aligned}
\dot{V}_a(t) &= \int_{-\varrho}^0 (\varrho \dot{x}^t(t) W \dot{x}(t) - \dot{x}^t(s) W \dot{x}(s)) ds \\
&= \frac{1}{\tau} \int_{t-\tau}^t (\varrho \dot{x}^t(t) W \dot{x}(t) - \tau \dot{x}^t(s) W \dot{x}(s)) ds
\end{aligned} \tag{4.23}$$

$$\begin{aligned}
\dot{V}_m(t) &= x^t(t) Q x(t) - x^t(t - \tau) Q x(t - \tau) \\
&= \frac{1}{\tau} \int_{t-\tau}^t (x^t(t) Q x(t) - x^t(t - \tau) Q x(t - \tau)) ds
\end{aligned} \tag{4.24}$$

where

P, Q, W are symmetric weighting matrices such that $0 < P, 0 < W, 0 < Q$,

$\varrho = \tau > 0$ is the time delay,

$\Theta \in \mathfrak{R}^{n \times n}$, and $Y \in \mathfrak{R}^{n \times n}$ are appropriate relaxation parameter matrices injected to facilitate the delay dependence analysis

Combing (4.19) – (4.24) and appending (4.14) – (4.15) through scalars $\kappa > 0, \sigma > 0$ we arrive at:

$$\chi(t, s) = \begin{bmatrix} x^t(t) & x^t(t - \tau) & \dot{x}^t(s) & f_o^t & h_o^t \end{bmatrix}^t \tag{4.25}$$

$$\dot{V}(t)|_{(2)} \leq \frac{1}{\tau} \int_{t-\tau}^t (\chi^t(t, s) \Xi_h \chi(t, s)) ds < 0 \tag{4.25}$$

where $\dot{V}(t)|_{(2)}$ defines the Lyapunov derivative along the solutions of our LNDT system

along with $\hat{\Theta}W = \Theta$, and $\hat{Y}W = Y$

$$\mathcal{E}_h = \begin{bmatrix} \mathcal{E}_{11} & \mathcal{E}_{12} & \mathcal{E}_{13} & \mathcal{E}_{14} & \mathcal{E}_{15} \\ \bullet & \mathcal{E}_{22} & \mathcal{E}_{23} & \mathcal{E}_{24} & \mathcal{E}_{25} \\ \bullet & \bullet & \mathcal{E}_{33} & \mathcal{E}_{34} & \mathcal{E}_{35} \\ \bullet & \bullet & \bullet & \mathcal{E}_{44} & \mathcal{E}_{45} \\ \bullet & \bullet & \bullet & \bullet & \mathcal{E}_{55} \end{bmatrix} < 0 \quad (4.26)$$

From (4.18), (4.22), (4.23), and (4.24) we can conclude:

$$\mathcal{E}_h = \begin{bmatrix} \mathcal{E}_{h11} & \mathcal{E}_{h12} & -\tau\Theta & P & P \\ \bullet & \mathcal{E}_{h22} & -\tau Y & 0 & 0 \\ \bullet & \bullet & -\tau W & 0 & 0 \\ \bullet & \bullet & \bullet & -\sigma I & 0 \\ \bullet & \bullet & \bullet & \bullet & -\kappa I \end{bmatrix} < 0 \quad (4.27-1)$$

where

$$\mathcal{E}_{h11} = PA_o + A_o^t P + \Theta + \Theta^t + Q + \sigma\alpha^2 F^t F \quad (4.27-2)$$

$$\mathcal{E}_{h12} = PA_{do} - \Theta + Y^t \quad (4.27-3)$$

$$\mathcal{E}_{h22} = -Y - Y^t - Q + \kappa\beta^2 H^t H \quad (4.27-4)$$

but the following term $(\varrho \dot{x}^t(t) W \dot{x}(t))$ was not included in the \mathcal{E}_h LMI (4.27-1), and since

$\dot{x}(t) = A_o x(t) + A_{do} x(t - \tau) + f_o + h_o$, we can rewrite $\dot{x}(t)$ in the matrix form:

$$\dot{x}(t) = \begin{bmatrix} A_o & A_{do} & 0 & 1 & 1 \end{bmatrix} \begin{bmatrix} x(t) \\ x(t - \tau) \\ \dot{x}(s) \\ f_o \\ h_o \end{bmatrix} \quad (4.28-1)$$

$$= \bar{A}\chi(t, s) \triangleq \bar{A}\chi \quad (4.28-2)$$

Then

$$\varrho \dot{x}^t(t) W \dot{x}(t) = \varrho \chi^t \bar{A}^t W \bar{A} \chi \quad (4.29)$$

Thus:

$$\dot{V}(t) = \frac{1}{\tau} \int_{t-\tau}^t (\dot{\chi} \mathcal{E}_h \chi + \varrho \chi^t \bar{A}^t W \bar{A} \chi) ds = \frac{1}{\tau} \int_{t-\tau}^t (\dot{\chi} [\mathcal{E}_h + \varrho \bar{A}^t W \bar{A}] \chi) ds$$

$$\begin{aligned}
&= \frac{1}{\tau} \int_{t-\tau}^t (\dot{\chi}[\mathcal{E}_h + \varrho \bar{A}^t W W^{-1} W \bar{A}] \chi) ds \\
&= \frac{1}{\tau} \int_{t-\tau}^t (\dot{\chi}[\mathcal{E}_h + \varrho \bar{A}^t W \varrho^{-1} W^{-1} W \bar{A} \varrho] \chi) ds < 0
\end{aligned}$$

(4.30-1)

or

$$\dot{V}(t) < \frac{1}{\tau} \int_{t-\tau}^t (\dot{\chi} \mathcal{E} \chi) ds < 0$$

(4.30-2)

Using the Schur Complement yield to transform the LMI from the equation form into the matrix form yield to:

$$\begin{bmatrix} \mathcal{E}_h & \varrho \bar{A}^t W \\ \varrho W \bar{A} & \varrho W \end{bmatrix} < 0 \quad (4.31)$$

But $\mathcal{E} < 0$, hence

$$\mathcal{E} = \begin{bmatrix} \mathcal{E}_{11} & \mathcal{E}_{12} & \mathcal{E}_{13} & \mathcal{E}_{14} & \mathcal{E}_{15} & \mathcal{E}_{16} & \mathcal{E}_{17} & \mathcal{E}_{18} \\ \bullet & \mathcal{E}_{22} & \mathcal{E}_{23} & \mathcal{E}_{24} & \mathcal{E}_{25} & \mathcal{E}_{26} & \mathcal{E}_{27} & \mathcal{E}_{28} \\ \bullet & \bullet & \mathcal{E}_{33} & \mathcal{E}_{34} & \mathcal{E}_{35} & \mathcal{E}_{36} & \mathcal{E}_{37} & \mathcal{E}_{38} \\ \bullet & \bullet & \bullet & \mathcal{E}_{44} & \mathcal{E}_{45} & \mathcal{E}_{46} & \mathcal{E}_{47} & \mathcal{E}_{48} \\ \bullet & \bullet & \bullet & \bullet & \mathcal{E}_{55} & \mathcal{E}_{56} & \mathcal{E}_{57} & \mathcal{E}_{58} \\ \bullet & \bullet & \bullet & \bullet & \bullet & \mathcal{E}_{66} & \mathcal{E}_{67} & \mathcal{E}_{68} \\ \bullet & \bullet & \bullet & \bullet & \bullet & \bullet & \mathcal{E}_{77} & \mathcal{E}_{78} \\ \bullet & \bullet & \bullet & \bullet & \bullet & \bullet & \bullet & \mathcal{E}_{88} \end{bmatrix} < 0 \quad (4.32)$$

$$\dot{V}(t)|_{(2)} < \frac{1}{\tau} \int_{t-\tau}^t (\chi^t(t, s) \mathcal{E} \chi(t, s)) ds = -\omega \|x(t)\|_2 < 0$$

(4.33)

We can rewrite the LMI as

$$\Xi = \begin{bmatrix} \Xi_{11} & \Xi_{12} & -\tau\Theta & P & P & P\Gamma_o & G_o^t & -\varrho A_o^t W \\ \bullet & \Xi_{22} & -\tau Y & 0 & 0 & 0 & G_{do}^t & -\varrho A_{do}^t W \\ \bullet & \bullet & -\tau W & 0 & 0 & 0 & 0 & 0 \\ \bullet & \bullet & \bullet & -\sigma I & 0 & 0 & 0 & -W \\ \bullet & \bullet & \bullet & \bullet & -\kappa I & 0 & 0 & -W \\ \bullet & \bullet & \bullet & \bullet & \bullet & -\gamma^2 I & \Phi_o^t & -\varrho \Gamma_o^t W \\ \bullet & \bullet & \bullet & \bullet & \bullet & \bullet & -I & 0 \\ \bullet & \bullet & \bullet & \bullet & \bullet & \bullet & \bullet & -\varrho W \end{bmatrix} < 0$$

where

$$\Xi_{11} = PA_o + A_o^t P^t + \Theta + \Theta^t + Q + \sigma \alpha^2 F^t F$$

$$= PA_o + A_o^t P + \Theta + \Theta^t + Q + \sigma \alpha^2 F^t F$$

$$\Xi_{12} = PA_{do} - \Theta + Y^t$$

$$\Xi_{22} = -Y - Y^t - Q + \kappa \beta^2 H^t H$$

Thus the internal asymptotic stability has been established and the first part of the proof of LMI (4.16) is done.

Now, consider the performance measure:

$$J = \int_0^\infty (z^t(s)z(s) - \gamma^2 w^t(s)w(s))ds \quad (4.34)$$

For any $w(t) \in \mathcal{L}_2 [0, \infty) \neq 0$ and zero initial condition $x(t) = 0$, then we can rewrite the performance measure as follow:

$$\begin{aligned} J &= \int_0^\infty \left(z^t(s)z(s) - \gamma^2 w^t(s)w(s) + \dot{V}(x)|_{(2)} - \dot{V}(x)|_{(2)} \right) ds \\ &\leq \int_0^\infty \left(z^t(s)z(s) - \gamma^2 w^t(s)w(s) + \dot{V}(x)|_{(2)} \right) ds \end{aligned} \quad (4.35)$$

Using the same development as before, we can easily find that

$$z^t(s)z(s) - \gamma^2 w^t(s)w(s) + \dot{V}(x)|_{(2)} = \bar{\chi}^t(t, s) \bar{\Xi} \bar{\chi}(t, s) \quad (4.36-1)$$

where

$$\bar{\chi}(t, s) = \begin{bmatrix} x^t(t) & x^t(t - \tau) & \dot{x}^t(s) & f_o^t & h_o^t & w^t(s) \end{bmatrix}^t \quad (4.36-2)$$

and $\bar{\mathcal{E}}$ correspond to \mathcal{E} by Schur Complement.

For any arbitrary $s \in [t, \infty)$, which implies for any $w(t) \in \mathcal{L}_2 [0, \infty) \neq 0$ that $J < 0$

leading to equation (4.10): $\|z(t)\|_2 < \gamma \|w(t)\|_2$ or $\frac{\|z(t)\|_2^2}{\|w(t)\|_2^2} < \gamma^2$

This complete the proof of (4.16)

4-7 State Feedback Control Scheme

Applying the state-feedback control $u(t) = K_s x(t)$ to the NLTD (4.11), and define

$$A_s = A_o + B_o K_s \text{ and } G_s = G_o + D_o K_s \quad (4.37)$$

It then follows from the previous analysis (theorem 1) that the resulting closed-loop system is delay-independent asymptotically stable with \mathcal{L}_2 performance bound γ , if there exist symmetric positive definite weighting matrices P ; Q ; W ; appropriate relaxation parameter matrices injected to facilitate the delay dependence analysis $\Theta \in \Re^{n \times n}$, $Y \in \Re^{n \times n}$; and scalars $\gamma > 0, \sigma > 0, \kappa > 0$ that satisfy the following LMI:

$$\mathcal{E}_\varrho = \begin{bmatrix} \mathcal{E}_{\varrho 11} & \mathcal{E}_{\varrho 12} & -\varrho \Theta & P & P & P \Gamma_o & G_s^t & -\varrho A_s^t W \\ \bullet & \mathcal{E}_{\varrho 22} & -\varrho Y & 0 & 0 & 0 & G_{do}^t & -\varrho A_{do}^t W \\ \bullet & \bullet & -\varrho W & 0 & 0 & 0 & 0 & 0 \\ \bullet & \bullet & \bullet & -\sigma I & 0 & 0 & 0 & -W \\ \bullet & \bullet & \bullet & \bullet & -\kappa I & 0 & 0 & -W \\ \bullet & \bullet & \bullet & \bullet & \bullet & -\gamma^2 I & \Phi_o^t & -\varrho \Gamma_o^t W \\ \bullet & \bullet & \bullet & \bullet & \bullet & \bullet & -I & 0 \\ \bullet & \bullet & \bullet & \bullet & \bullet & \bullet & \bullet & -\varrho W \end{bmatrix} < 0 \quad (4.38-1)$$

where

$$\mathcal{E}_{\varrho 11} = P A_s + A_s^t P + \Theta + \Theta^t + Q + \sigma \alpha^2 F^t F \quad (4.38-2)$$

$$\mathcal{E}_{\varrho 12} = PA_{do} - \theta + Y^t \quad (4.38-3)$$

$$\mathcal{E}_{\varrho 22} = -Y - Y^t - Q + \kappa\beta^2 H^t H \quad (4.38-4)$$

The main state-feedback design results are established by the following theorem:

Theorem 2:

Given scalar ϱ and matrix $W > 0$, the LNDT System (4.11) with the state-feedback control $u(t) = K_s x(t)$ is delay independent asymptotically stable with \mathcal{L}_2 performance bound γ if there exist symmetric positive define weighting matrices $X, \mathcal{Y}, Q_1, S_{x1}, S_{x2}$; and parameter matrices θ_1, Y_1 ; and scalars $\sigma > 0, \kappa > 0, \gamma > 0, \varepsilon > 0$ satisfying the following LMI:

$$\mathcal{E}_3 = \begin{bmatrix} \mathcal{E}_{s311} & \mathcal{E}_{s312} & -\varrho\theta_1 & S_{x1} & 0 & I & I & \Gamma_o & XG_o^t + \mathcal{Y}^t D_o^t - \varrho XA_o^t - \varrho \mathcal{Y}^t B_o^t \\ \bullet & \mathcal{E}_{s322} & -\varrho Y_1 & 0 & S_{x2} & 0 & 0 & 0 & XG_{do}^t & -\varrho XA_{do}^t \\ \bullet & \bullet & -\varrho \varepsilon X & 0 & 0 & 0 & 0 & 0 & 0 & 0 \\ \bullet & \bullet & \bullet & -\sigma I & 0 & 0 & 0 & 0 & 0 & 0 \\ \bullet & \bullet & \bullet & \bullet & -\kappa I & 0 & 0 & 0 & 0 & 0 \\ \bullet & \bullet & \bullet & \bullet & \bullet & -\kappa I & 0 & 0 & 0 & -I \\ \bullet & \bullet & \bullet & \bullet & \bullet & \bullet & -\sigma I & 0 & 0 & -I \\ \bullet & \bullet & \bullet & \bullet & \bullet & \bullet & \bullet & -\gamma^2 I & \Phi_o^t & -\varrho \Gamma_o^t \\ \bullet & \bullet & \bullet & \bullet & \bullet & \bullet & \bullet & \bullet & -I & 0 \\ \bullet & \bullet & \bullet & \bullet & \bullet & \bullet & \bullet & \bullet & \bullet & -\varrho \varepsilon^{-1} X \end{bmatrix} < 0 \quad (4.39-1)$$

where

$$\mathcal{Y} = K_s X \quad (4.39-2)$$

$$\theta_1 = X\theta_c X \quad (4.39-3)$$

$$Q_1 = XQX \quad (4.39-4)$$

$$Y_1 = XY_c X \quad (4.39-5)$$

$$\mathcal{E}_{s311} = A_o X + B_o \mathcal{Y} + XA_o^t + \mathcal{Y}^t B_o^t + \theta_1 + \theta_1^t + Q_1 \quad (4.39-6)$$

$$\mathcal{E}_{s312} = A_{do} X - \theta_1 + Y_1^t \quad (4.39-7)$$

$$E_{s322} = -Y_1 - Y_1^t - Q_1 \quad (4.39-8)$$

$$S_{x1} = XS_1 \quad (4.39-9)$$

$$S_{x2} = XS_2 \quad (4.39-10)$$

Proof:

$$E_s = \begin{bmatrix} E_{s11} & E_{s12} & -\tau\theta_c & S_1 & 0 & P & P & P\Gamma_o & G_s^t & -\varrho A_s^t W \\ \bullet & E_{s22} & -\tau Y_c & 0 & S_2 & 0 & 0 & 0 & G_{do}^t & -\varrho A_{do}^t W \\ \bullet & \bullet & -\tau W & 0 & 0 & 0 & 0 & 0 & 0 & 0 \\ \bullet & \bullet & \bullet & -\sigma I & 0 & 0 & 0 & 0 & 0 & 0 \\ \bullet & \bullet & \bullet & \bullet & -\kappa I & 0 & 0 & 0 & 0 & 0 \\ \bullet & \bullet & \bullet & \bullet & \bullet & -\kappa I & 0 & 0 & 0 & -W \\ \bullet & \bullet & \bullet & \bullet & \bullet & \bullet & -\sigma I & 0 & 0 & -W \\ \bullet & \bullet & \bullet & \bullet & \bullet & \bullet & \bullet & -\gamma^2 I & \Phi_o^t & -\varrho \Gamma_o^t W \\ \bullet & \bullet & \bullet & \bullet & \bullet & \bullet & \bullet & \bullet & -I & 0 \\ \bullet & \bullet & \bullet & \bullet & \bullet & \bullet & \bullet & \bullet & \bullet & -\varrho W \end{bmatrix} < 0 \quad (4.40-1)$$

where

$$E_{s11} = PA_s + A_s^t P + \theta + \theta^t + Q \quad (4.40-2)$$

$$E_{s12} = PA_{do} - \theta + Y^t \quad (4.40-3)$$

$$E_{s22} = -Y - Y^t - Q \quad (4.40-4)$$

$$S_1 = \sigma \alpha F^t \quad (4.40-5)$$

$$S_2 = \kappa \beta H^t \quad (4.40-6)$$

Since $A_s = A_o + B_o K_s$ and the time delay in our system is fixed and equal to ($\varrho = \tau$), then:

Since the Matlab LMI solver cannot solve any element that has two variables, we should eliminate W from our analysis. Thus \mathcal{E}_s (4.41) can be re-written as:

$$\mathcal{E}_{s1} = [I \ I \ I \ I \ I \ I \ I \ I \ I \ W^{-1}] \mathcal{E}_s [I \ I \ I \ I \ I \ I \ I \ I \ I \ W^{-1}]^t$$

$$= \begin{bmatrix} \mathcal{E}_{s11} & \mathcal{E}_{s12} & -\varrho \theta_c & S_1 & 0 & P & P & P\Gamma_o & G_o^t + K_s^t D_o^t & -\varrho A_o^t - \varrho K_s^t B_o^t \\ \bullet & \mathcal{E}_{s22} & -\varrho Y_c & 0 & S_2 & 0 & 0 & 0 & G_{do}^t & -\varrho A_{do}^t \\ \bullet & \bullet & -\varrho W & 0 & 0 & 0 & 0 & 0 & 0 & 0 \\ \bullet & \bullet & \bullet & -\sigma I & 0 & 0 & 0 & 0 & 0 & 0 \\ \bullet & \bullet & \bullet & \bullet & -\kappa I & 0 & 0 & 0 & 0 & 0 \\ \bullet & \bullet & \bullet & \bullet & \bullet & -\kappa I & 0 & 0 & 0 & -I \\ \bullet & \bullet & \bullet & \bullet & \bullet & \bullet & -\sigma I & 0 & 0 & -I \\ \bullet & \bullet & \bullet & \bullet & \bullet & \bullet & \bullet & -\gamma^2 I & \Phi_o^t & -\varrho \Gamma_o^t \\ \bullet & \bullet & \bullet & \bullet & \bullet & \bullet & \bullet & \bullet & -I & 0 \\ \bullet & \bullet & \bullet & \bullet & \bullet & \bullet & \bullet & \bullet & \bullet & -\varrho W^{-1} \end{bmatrix} < 0$$

(4.42)

Applying the congruent transformation to the \mathcal{E}_{s1} and defining $P = X^{-1}$ produce:

$$\mathcal{E}_2 = [X \ X \ X \ I \ I \ I \ I \ I \ I \ I] \mathcal{E}_{s1} [X \ X \ X \ I \ I \ I \ I \ I \ I \ I]^t$$

$$= \begin{bmatrix} X\mathcal{E}_{s11}X & X\mathcal{E}_{s12}X & -\varrho X\theta_c X & XS_1 & 0 & I & I \\ \bullet & X\mathcal{E}_{s22}X & -\varrho XY_c X & 0 & XS_2 & 0 & 0 \\ \bullet & \bullet & -\varrho XWX & 0 & 0 & 0 & 0 \\ \bullet & \bullet & \bullet & -\sigma I & 0 & 0 & 0 \\ \bullet & \bullet & \bullet & \bullet & -\kappa I & 0 & 0 \\ \bullet & \bullet & \bullet & \bullet & \bullet & -\kappa I & 0 \\ \bullet & \bullet & \bullet & \bullet & \bullet & \bullet & -\sigma I \\ \bullet & \bullet & \bullet & \bullet & \bullet & \bullet & \bullet \\ \bullet & \bullet & \bullet & \bullet & \bullet & \bullet & \bullet \\ \bullet & \bullet & \bullet & \bullet & \bullet & \bullet & \bullet \end{bmatrix}$$

$$\begin{bmatrix} \Gamma_o & X(G_o^t + K_s^t D_o^t) & X(-\varrho A_o^t - \varrho K_s^t B_o^t) \\ 0 & XG_{do}^t & -\varrho XA_{do}^t \\ 0 & 0 & 0 \\ 0 & 0 & 0 \\ 0 & 0 & 0 \\ 0 & 0 & -I \\ 0 & 0 & -I \\ -\gamma^2 I & \Phi_o^t & -\varrho \Gamma_o^t \\ \bullet & -I & 0 \\ \bullet & \bullet & -\varrho W^{-1} \end{bmatrix} < 0$$

$$\mathcal{E}_2 = \begin{bmatrix} X\mathcal{E}_{s11}X & X\mathcal{E}_{s12}X & -\varrho X\theta_c X & XS_1 & 0 & I & I \\ \bullet & X\mathcal{E}_{s22}X & -\varrho XY_c X & 0 & XS_2 & 0 & 0 \\ \bullet & \bullet & -\varrho XWX & 0 & 0 & 0 & 0 \\ \bullet & \bullet & \bullet & -\sigma I & 0 & 0 & 0 \\ \bullet & \bullet & \bullet & \bullet & -\kappa I & 0 & 0 \\ \bullet & \bullet & \bullet & \bullet & \bullet & -\kappa I & 0 \\ \bullet & \bullet & \bullet & \bullet & \bullet & \bullet & -\sigma I \\ \bullet & \bullet & \bullet & \bullet & \bullet & \bullet & \bullet \\ \bullet & \bullet & \bullet & \bullet & \bullet & \bullet & \bullet \\ \bullet & \bullet & \bullet & \bullet & \bullet & \bullet & \bullet \end{bmatrix}$$

$$\begin{bmatrix} \Gamma_o^t & XG_o^t + XK_s^t D_o^t & -\varrho XA_o^t - \varrho XK_s^t B_o^t \\ 0 & XG_{do}^t & -\varrho XA_{do}^t \\ 0 & 0 & 0 \\ 0 & 0 & 0 \\ 0 & 0 & 0 \\ 0 & 0 & -I \\ 0 & 0 & -I \\ -\gamma^2 I & \Phi_o^t & -\varrho \Gamma_o^t \\ \bullet & -I & 0 \\ \bullet & \bullet & -\varrho W^{-1} \end{bmatrix} < 0$$

$$\mathcal{E}_2 = \begin{bmatrix} X\mathcal{E}_{s11}X & X\mathcal{E}_{s12}X & -\varrho X\theta_c X & XS_1 & 0 & I & I \\ \bullet & X\mathcal{E}_{s22}X & -\varrho XY_c X & 0 & XS_2 & 0 & 0 \\ \bullet & \bullet & -\varrho XWX & 0 & 0 & 0 & 0 \\ \bullet & \bullet & \bullet & -\sigma I & 0 & 0 & 0 \\ \bullet & \bullet & \bullet & \bullet & -\kappa I & 0 & 0 \\ \bullet & \bullet & \bullet & \bullet & \bullet & -\kappa I & 0 \\ \bullet & \bullet & \bullet & \bullet & \bullet & \bullet & -\sigma I \\ \bullet & \bullet & \bullet & \bullet & \bullet & \bullet & \bullet \\ \bullet & \bullet & \bullet & \bullet & \bullet & \bullet & \bullet \\ \bullet & \bullet & \bullet & \bullet & \bullet & \bullet & \bullet \end{bmatrix}$$

$$\begin{bmatrix} \Gamma_o^t & XG_o^t + \mathcal{Y}^t D_o^t & -\varrho XA_o^t - \varrho \mathcal{Y}^t B_o^t \\ 0 & XG_{do}^t & -\varrho XA_{do}^t \\ 0 & 0 & 0 \\ 0 & 0 & 0 \\ 0 & 0 & 0 \\ 0 & 0 & -I \\ 0 & 0 & -I \\ -\gamma^2 I & \Phi_o^t & -\varrho \Gamma_o^t \\ \bullet & -I & 0 \\ \bullet & \bullet & -\varrho W^{-1} \end{bmatrix} < 0$$

(4.43-1)

where

$$\mathcal{Y}^t = K_s^t X^t = K_s^t X \quad (4.43-2)$$

Define $W = \varepsilon X^{-1}$ (or $W^{-1} = \varepsilon^{-1} X$), \mathcal{E}_2 in LMI (4.43) can be renamed as \mathcal{E}_3 and rewrite as follow:

$$\mathcal{E}_3 = \begin{bmatrix} \mathcal{E}_{s311} & \mathcal{E}_{s312} & -\varrho X \Theta_c X & X S_1 & 0 & I & I \\ \bullet & \mathcal{E}_{s322} & -\varrho X \Upsilon_c X & 0 & X S_2 & 0 & 0 \\ \bullet & \bullet & -\varrho \varepsilon X & 0 & 0 & 0 & 0 \\ \bullet & \bullet & \bullet & -\sigma I & 0 & 0 & 0 \\ \bullet & \bullet & \bullet & \bullet & -\kappa I & 0 & 0 \\ \bullet & \bullet & \bullet & \bullet & \bullet & -\kappa I & 0 \\ \bullet & \bullet & \bullet & \bullet & \bullet & \bullet & -\sigma I \\ \bullet & \bullet & \bullet & \bullet & \bullet & \bullet & \bullet \\ \bullet & \bullet & \bullet & \bullet & \bullet & \bullet & \bullet \\ \bullet & \bullet & \bullet & \bullet & \bullet & \bullet & \bullet \end{bmatrix}$$

$$\begin{bmatrix} \Gamma_o & X G_o^t + \mathcal{Y}^t D_o^t & -\varrho X A_o^t - \varrho \mathcal{Y}^t B_o^t \\ 0 & X G_{do}^t & -\varrho X A_{do}^t \\ 0 & 0 & 0 \\ 0 & 0 & 0 \\ 0 & 0 & 0 \\ 0 & 0 & -I \\ 0 & 0 & -I \\ -\gamma^2 I & \Phi_o^t & -\varrho \Gamma_o^t \\ \bullet & -I & 0 \\ \bullet & \bullet & -\varrho \varepsilon^{-1} X \end{bmatrix} < 0 \quad (4.44-1)$$

where

$$\begin{aligned} \mathcal{E}_{s311} &= X \mathcal{E}_{s11} X = X [P A_s + A_s^t P^t + \Theta_c + \Theta_c^t + Q] X \\ &= A_s X + X A_s^t + X \Theta_c X + X \Theta_c^t X + X Q X \end{aligned} \quad (4.44-2)$$

$$\mathcal{E}_{s312} = X \mathcal{E}_{s12} X = X [P A_{do} - \Theta + \Upsilon^t] X = A_{do} X - X \Theta_c X + X \Upsilon_c^t X \quad (4.44-3)$$

$$\mathcal{E}_{s322} = X \mathcal{E}_{s22} X = X [-\Upsilon_c - \Upsilon_c^t - Q] X = -X \Upsilon_c X - X \Upsilon_c^t X - X Q X \quad (4.44-4)$$

Since $A_s = A_o + B_o K_s$ and $G_s = G_o + D_o K_s$

Then $A_s X = A_o X + B_o K_s X = A_o X + B_o \mathcal{Y}$

Let

$$\theta_1 = X\theta_c X$$

$$Q_1 = XQX$$

$$\gamma_1 = X\gamma_c X$$

Then

$$\mathcal{E}_{s311} = A_s X + X A_s^t + \theta_1 + \theta_1^t + Q_1 = A_o X + B_o \mathcal{Y} + X A_o^t + \mathcal{Y}^t B_o^t + \theta_1 + \theta_1^t + Q_1$$

$$\mathcal{E}_{s312} = A_{do} X - \theta_1 + \gamma_1^t$$

$$\mathcal{E}_{s322} = -\gamma_1 - \gamma_1^t - Q_1$$

$$\text{Let } S_{x1} = X S_1 \text{ and } S_{x2} = X S_2$$

Then the LMI can be rewritten as follows:

$$\mathcal{E}_3 = \begin{bmatrix} \mathcal{E}_{s311} & \mathcal{E}_{s312} & -\varrho \theta_1 & S_{x1} & 0 & I & I \\ \bullet & \mathcal{E}_{s322} & -\varrho \gamma_1 & 0 & S_{x2} & 0 & 0 \\ \bullet & \bullet & -\varrho \varepsilon X & 0 & 0 & 0 & 0 \\ \bullet & \bullet & \bullet & -\sigma I & 0 & 0 & 0 \\ \bullet & \bullet & \bullet & \bullet & -\kappa I & 0 & 0 \\ \bullet & \bullet & \bullet & \bullet & \bullet & -\kappa I & 0 \\ \bullet & \bullet & \bullet & \bullet & \bullet & \bullet & -\sigma I \\ \bullet & \bullet & \bullet & \bullet & \bullet & \bullet & \bullet \\ \bullet & \bullet & \bullet & \bullet & \bullet & \bullet & \bullet \\ \bullet & \bullet & \bullet & \bullet & \bullet & \bullet & \bullet \end{bmatrix}$$

$$\begin{bmatrix} \Gamma_o & X G_o + \mathcal{Y}^t D_o^t & -\varrho X A_o^t - \varrho \mathcal{Y}^t B_o^t \\ 0 & X G_{do}^t & -\varrho X A_{do}^t \\ 0 & 0 & 0 \\ 0 & 0 & 0 \\ 0 & 0 & 0 \\ 0 & 0 & -I \\ 0 & 0 & -I \\ -\gamma^2 I & \Phi_o^t & -\varrho \Gamma_o^t \\ \bullet & -I & 0 \\ \bullet & \bullet & -\varrho \varepsilon^{-1} X \end{bmatrix} < 0$$

This completes the proof.

4-8 Dynamic Output Feedback Control Scheme

To continue our design of the stabilizing scheme using the dynamic output feedback for the NLTD system (4.11), we will consider the following theorem:

Theorem 3:

Given scalar ϱ and matrix $W > 0$, the LNDT system with the dynamic output control $u(t) = K_c x_e(t)$ is delay independent asymptotically stable with \mathcal{L}_2 performance bound γ if there exist symmetric positive definite weighting matrices P, Q, S, W ; appropriate relaxation parameter matrices injected to facilitate the delay dependence analysis $\Theta \in \mathfrak{R}^{n \times n}, Y \in \mathfrak{R}^{n \times n}$; and scalars $\sigma > 0, \kappa > 0, \gamma > 0$ satisfying the following LMI:

$$\mathcal{E}_{dof} = \begin{bmatrix} \mathcal{E}_{h11} & \mathcal{E}_{h12} & -PBK_c & -\varrho\Theta & P \\ \bullet & \mathcal{E}_{h22} & A_{do}^t S - C_{do}^t V^t & -\varrho Y & 0 \\ \bullet & \bullet & SA_o + A_o^t S - VC_o - C_o^t V^t & 0 & 0 \\ \bullet & \bullet & \bullet & -\varrho W & 0 \\ \bullet & \bullet & \bullet & \bullet & -\sigma I \\ \bullet & \bullet & \bullet & \bullet & \bullet \\ \bullet & \bullet & \bullet & \bullet & \bullet \\ \bullet & \bullet & \bullet & \bullet & \bullet \\ \bullet & \bullet & \bullet & \bullet & \bullet \end{bmatrix} \begin{bmatrix} P & P\Gamma_o & G_o^t + K_c^t D^t & -\varrho A_o^t W - \varrho K_c^t B^t W \\ 0 & 0 & G_{do}^t & -\varrho A_{do}^t W \\ 0 & S\Gamma_o - V\psi_o & -K_c^t D^t & \varrho K_c^t B^t W \\ 0 & 0 & 0 & 0 \\ 0 & 0 & 0 & -W \\ -\kappa I & 0 & 0 & -W \\ \bullet & -\gamma^2 I & \Phi_o^t & -\varrho \Gamma_o^t W \\ \bullet & \bullet & -I & 0 \\ \bullet & \bullet & \bullet & -\varrho W \end{bmatrix} < 0 \quad (4.45-1)$$

where

$$\mathcal{E}_{h11} = PA_o + A_o^t P + \Theta + \Theta^t + Q + \sigma \alpha^2 F^t F + PBK_c + K_c^t B^t P \quad (4.45-2)$$

$$\mathcal{E}_{h12} = PA_{do} - \Theta + Y^t \quad (4.45-3)$$

$$\mathcal{E}_{h22} = -Y - Y^t - Q + \kappa\beta^2 H^t H \quad (4.45-4)$$

$$V = SK_o \quad (4.45-5)$$

Proof:

As considered before for the NLTD system (4.11):

$$\dot{x}(t) = A_o x(t) + A_{do} x(t - \tau) + B_o u(t) + f_o(x(t), t) + h_o(x(t - \tau), t) + \Gamma_o w(t)$$

$$y(t) = C_o x(t) + C_{do} x(t - \tau) + F_o u(t) + \psi_o w(t)$$

$$z(t) = G_o x(t) + G_{do} x(t - \tau) + D_o u(t) + \Phi_o w(t)$$

When the input-output have no relation and not linked to each other, $F_o = 0$, then we can

rewrite the output equation as follow:

$$y(t) = C_o x(t) + C_{do} x(t - \tau) + \psi_o w(t) \quad (4.46)$$

We have to design an observer such that the state equations will be:

$$\dot{x}_e(t) = Ax_e(t) + Bu(t) + K_o(y(t) - C_o x_e(t)) \quad (4.47)$$

while the controller will have the following equation:

$$u(t) = K_c x_e(t) \quad (4.48)$$

Hence, from (4.11), (4.46), (4.47), and (4.48), the state equation of the system with the observer will be:

$$\begin{aligned} \dot{x}_e(t) &= Ax_e(t) + BK_c x_e(t) - K_o C_o x_e(t) + K_o C_o x(t) + K_o C_{do} x(t - \tau) + K_o \psi_o w(t) \\ &= (A + BK_c - K_o C_o) x_e(t) + K_o C_o x(t) + K_o C_{do} x(t - \tau) + K_o \psi_o w(t) \end{aligned} \quad (4.49)$$

Note that we will ignore $f_o(x(t), t)$ and $h_o(x(t - \tau), t)$ during the development of our analysis to simplify the derivations. Let us now start some system augmentation such that:

$$\bar{x}(t) = \begin{bmatrix} x(t) \\ x_e(t) \end{bmatrix} \quad (4.50-1)$$

$$\dot{\bar{x}}(t) = \bar{A} \bar{x}(t) + \bar{A}_d \bar{x}(t - \tau) + \bar{F}_o w(t) \quad (4.50-2)$$

$$z(t) = \bar{G}\bar{x}(t) + \bar{G}_d\bar{x}(t - \tau) + \bar{\Phi}_o w(t) \quad (4.50-3)$$

where

$$\bar{A} = \begin{bmatrix} A & BK_c \\ K_o C_o & A + BK_c - K_o C_o \end{bmatrix} \quad (4.50-4)$$

$$\bar{A}_d = \begin{bmatrix} A_{do} & 0 \\ K_o C_{do} & 0 \end{bmatrix} \quad (4.50-5)$$

$$\bar{\Gamma}_o = \begin{bmatrix} \Gamma_o \\ K_o \psi_o \end{bmatrix} \quad (4.50-6)$$

$$\bar{G} = [G_o \quad D_o K_c] \quad (4.50-7)$$

$$\bar{G}_d = [G_{do} \quad 0] \quad (4.50-8)$$

Suppose that we have the following state augmented equation for the system with the observer:

$$\hat{X}(t) = \begin{bmatrix} x(t) \\ x(t) - x_e(t) \end{bmatrix} = \begin{bmatrix} x(t) \\ e(t) \end{bmatrix} = T \begin{bmatrix} x(t) \\ x_e(t) \end{bmatrix} \quad (4.51)$$

where

$e(t)$ is the state estimation error

$$T \text{ is transformation matrix such that } T = T^{-1} = \begin{bmatrix} I & 0 \\ I & -I \end{bmatrix}$$

To get $\hat{X}(t)$ from (4.51):

$$\begin{aligned} \dot{\hat{X}}(t) &= \bar{A}\bar{x}(t) + \bar{A}_d\bar{x}(t - \tau) + \bar{\Gamma}_o w(t) \\ &= \bar{A}T^{-1}T\bar{x}(t) + \bar{A}_dT^{-1}T\bar{x}(t - \tau) + \bar{\Gamma}_o w(t) \end{aligned} \quad (4.52)$$

We have to multiply $\dot{\hat{X}}(t)$ by T

$$T\dot{\hat{X}}(t) = T\bar{A}T^{-1}T\bar{x}(t) + T\bar{A}_dT^{-1}T\bar{x}(t - \tau) + T\bar{\Gamma}_o w(t)$$

$$\dot{\hat{X}}(t) = T\bar{A}T^{-1}\hat{X}(t) + T\bar{A}_dT^{-1}\hat{X}(t - \tau) + T\bar{\Gamma}_o w(t)$$

$$= \hat{A}\hat{X}(t) + \hat{A}_d\hat{X}(t - \tau) + \hat{\Gamma}_o w(t) \quad (4.53-1)$$

where

$$\begin{aligned} \hat{A} &= T\bar{A}T^{-1} = \begin{bmatrix} I & 0 \\ I & -I \end{bmatrix} \begin{bmatrix} A & BK_c \\ K_o C_o & A + BK_c - K_o C_o \end{bmatrix} \begin{bmatrix} I & 0 \\ I & -I \end{bmatrix} \\ &= \begin{bmatrix} I & 0 \\ I & -I \end{bmatrix} \begin{bmatrix} A + BK_c & -BK_c \\ A + BK_c & -A - BK_c + K_o C_o \end{bmatrix} = \begin{bmatrix} A + BK_c & -BK_c \\ 0 & A - K_o C_o \end{bmatrix} \end{aligned} \quad (4.53-2)$$

$$\begin{aligned} \hat{A}_d &= T\bar{A}_dT^{-1} = \begin{bmatrix} I & 0 \\ I & -I \end{bmatrix} \begin{bmatrix} A_d & 0 \\ K_o C_{do} & 0 \end{bmatrix} \begin{bmatrix} I & 0 \\ I & -I \end{bmatrix} = \begin{bmatrix} I & 0 \\ I & -I \end{bmatrix} \begin{bmatrix} A_d & 0 \\ K_o C_{do} & 0 \end{bmatrix} \\ &= \begin{bmatrix} A_d & 0 \\ A_d - K_o C_{do} & 0 \end{bmatrix} \end{aligned} \quad (4.53-3)$$

$$\hat{\Gamma}_o = T\bar{\Gamma}_o = \begin{bmatrix} I & 0 \\ I & -I \end{bmatrix} \begin{bmatrix} \Gamma_o \\ K_o \psi_o \end{bmatrix} = \begin{bmatrix} \Gamma_o \\ \Gamma_o - K_o \psi_o \end{bmatrix} \quad (4.53-4)$$

We will apply the same methodology to get the controlled output equation, thus:

$$\begin{aligned} z(t) &= \bar{G}\bar{x}(t) + \bar{G}_d\bar{x}(t - \tau) + \bar{\Phi}_o w(t) \\ &= \bar{G}T^{-1}T\bar{x}(t) + \bar{G}_dT^{-1}T\bar{x}(t - \tau) + \bar{\Phi}_o w(t) \\ &= \bar{G}T^{-1}\hat{X}(t) + \bar{G}_dT^{-1}\hat{X}(t - \tau) + \bar{\Phi}_o w(t) \\ &= \hat{G}\hat{X}(t) + \hat{G}_dQ^{-1}\hat{X}(t - \tau) + \bar{\Phi}_o w(t) \end{aligned} \quad (4.54-1)$$

where

$$\hat{G} = \bar{G}T^{-1} = \begin{bmatrix} G_o & D_o K_c \end{bmatrix} \begin{bmatrix} I & 0 \\ I & -I \end{bmatrix} = \begin{bmatrix} G_o + D_o K_c & -D_o K_c \end{bmatrix} \quad (4.54-2)$$

$$\hat{G}_d = \bar{G}_dT^{-1} = \begin{bmatrix} G_{do} & 0 \end{bmatrix} \begin{bmatrix} I & 0 \\ I & -I \end{bmatrix} = \begin{bmatrix} G_{do} & 0 \end{bmatrix} \quad (4.54-3)$$

In summary, the new system can be represented as:

$$\dot{\hat{X}}(t) = \hat{A}\hat{X}(t) + \hat{A}_d\hat{X}(t - \tau) + \hat{\Gamma}_o w(t) \quad (4.55-1)$$

$$z(t) = \hat{G}\hat{X}(t) + \hat{G}_dQ^{-1}\hat{X}(t - \tau) + \bar{\Phi}_o w(t) \quad (4.55-2)$$

$$\dot{x}(t) = (A + BK_c)x(t) - BK_ce(t) + A_{do}x(t - \tau) + \Gamma_o w(t) + f_o + h_o \quad (4.56-1)$$

$$\dot{e}(t) = (A - K_o C_o)e(t) + (A_{do} - K_o C_{do})x(t - \tau) + (\Gamma_o - K_o \Phi_o)w(t) \quad (4.56-2)$$

Using the same development technique that has been used before for stability analysis:

$$\dot{V}_2(t) = \dot{V}_{o2}(t) + \dot{V}_{a2}(t) + \dot{V}_{m2}(t) \quad (4.57-1)$$

$$\begin{aligned} \dot{V}_{o2}(t) &= \dot{x}^t(t)Px(t) + x^t(t)P\dot{x}(t) = 2x^t(t)P\dot{x}(t) \\ &= 2x^t(t)P[(A + BK_c)x(t) - BK_ce(t) + A_{do}x(t - \tau) + \Gamma_o w(t) + f_o + h_o] \end{aligned} \quad (4.57-2)$$

It is clear that this result is the same as that have shown before for $\dot{V}_o(t)$ while equation (4.19) development, with new extra term $-2\alpha PBK_ce(t)$

$$\dot{V}_{a2}(t) = \varrho \dot{x}^t(t)W\dot{x}(t) - \int_{t-\varrho}^t (\dot{x}^t(s)W\dot{x}(s))ds \quad (4.57-3)$$

$$\dot{V}_{m2}(t) = x^t(t)Qx(t) - x^t(t - \tau)Qx(t - \tau) \quad (4.57-4)$$

Again, consider the NLTD System with $u(.) \equiv 0$, and let

$$\chi_2(t, s) = [x^t(t) \quad x^t(t - \tau) \quad e^t(t) \quad \dot{x}^t(s) \quad f_o^t \quad h_o^t]^t \quad (4.58-1)$$

$$\dot{V}_2(t) \leq \chi_2^t(t, s)\mathcal{E}_{h2}\chi_2(t, s) < 0 \quad (4.58-2)$$

then

$$\mathcal{E}_{h2} = \begin{bmatrix} \mathcal{E}_{h211} & \mathcal{E}_{h212} & -PBK_c & P & P \\ \bullet & \mathcal{E}_{h222} & 0 & 0 & 0 \\ \bullet & \bullet & 0 & 0 & 0 \\ \bullet & \bullet & 0 & -\sigma I & 0 \\ \bullet & \bullet & \bullet & \bullet & -\kappa I \end{bmatrix} < 0 \quad (4.59-1)$$

where

$$\mathcal{E}_{h211} = PA_o + A_o^t P + \Theta + \Theta^t + Q + \sigma \alpha^2 F^t F + PBK_c + K_c^t B^t P \quad (4.59-2)$$

$$\mathcal{E}_{h212} = PA_{do} - \theta + \gamma^t \quad (4.59-3)$$

$$\mathcal{E}_{h222} = -\gamma - \gamma^t - Q + \kappa\beta^2 H^t H \quad (4.59-4)$$

but the following term $(\varrho \dot{x}^t(t)W\dot{x}(t))$ was not included in \mathcal{E}_{h2} (4.58). We can represent the state equation from the original system (4.11) and the control law definitions as:

$$\begin{aligned} \dot{x}(t) &= (A + BK_c)x(t) + A_{do}x(t - \tau) - BK_c e(t) + \Gamma_o w(t) + f_o + h_o \\ &= [A + BK_c \quad A_{do} \quad -BK_c \quad 0 \quad 1 \quad 1] \begin{bmatrix} x(t) \\ x(t - \tau) \\ e(t) \\ \dot{x}(s) \\ f_o \\ h_o \end{bmatrix} \\ &= \tilde{A}\chi_2(t, s) \triangleq \tilde{A}\chi_2 \end{aligned} \quad (4.60-1)$$

The controlled output is found to be:

$$z(t) = (G_o + D_o K_c)x(t) - D_o K_c e(t) + A_d x(t - \tau) + \Phi_o w(t) \quad (4.60-2)$$

Note that, again, the term $-D_o K_c e(t)$ was not included in $\dot{V}_2(t)$ (4.58), thus have to include new term $(\dot{V}_e(t))$ into the stability LKF equation such that

$$\dot{V}_{2new}(t) = \dot{V}_{o2}(t) + \dot{V}_{a2}(t) + \dot{V}_{m2}(t) + \dot{V}_e(t) \quad (4.61-1)$$

where

$$V_e(t) = e^t(t)Se(t) \quad (4.61-2)$$

$$\begin{aligned} \dot{V}_e(t) &= \dot{e}^t(t)Se(t) + e^t(t)S\dot{e}(t) = 2e^t(t)S\dot{e}(t) \\ &= 2e^t(t)S((A - K_o C_o)e(t) + (A_{do} - K_o C_{do})x(t - \tau) + (\Gamma_o - K_o \Phi_o)w(t)) \\ &= e^t(t)(SA + A^t S - SK_o C_o - C_o^t K_o^t S)e(t) \\ &\quad + 2e^t(t)(SA_{do} - SK_o C_{do})x(t - \tau) + 2e^t(t)(S\Gamma_o - SK_o \Phi_o)w(t) \end{aligned} \quad (4.61-3)$$

Thus, using the same development procedure used in \mathcal{L}_2 gain analysis produces:

$$\dot{V}_{2new}(t) < \chi_2 \Xi_{dof} \chi_2 < 0 \quad (4.62)$$

Using the Schur Complement yield

$$\begin{bmatrix} \Xi_{h2} & \varrho \tilde{A}^t W \\ \varrho W \tilde{A} & \varrho W \end{bmatrix} < 0 \quad (4.63)$$

Since we have to find $\Xi_{dof} < 0$, then

$$\Xi_{dof} = \begin{bmatrix} \Xi_{h11} & \Xi_{h12} & -PBK_c & -\tau\theta & P \\ \bullet & \Xi_{h22} & A_{do}^t S - C_{do}^t K_o^t S & -\tau Y & 0 \\ \bullet & \bullet & SA_o + A_o^t S - SK_o C_o - C_o^t K_o^t S & 0 & 0 \\ \bullet & \bullet & \bullet & -\tau W & 0 \\ \bullet & \bullet & \bullet & \bullet & -\sigma I \\ \bullet & \bullet & \bullet & \bullet & \bullet \\ \bullet & \bullet & \bullet & \bullet & \bullet \\ \bullet & \bullet & \bullet & \bullet & \bullet \\ \bullet & \bullet & \bullet & \bullet & \bullet \end{bmatrix}$$

$$\begin{bmatrix} P & P\Gamma_o & G_o^t + K_c^t D^t & -\varrho A_o^t W - \varrho K_c^t B^t W \\ 0 & 0 & G_{do}^t & -\varrho A_{do}^t W \\ 0 & S\Gamma_o - SK_o \psi_o & -K_c^t D^t & \varrho K_c^t B^t W \\ 0 & 0 & 0 & 0 \\ 0 & 0 & 0 & -W \\ -\kappa I & 0 & 0 & -W \\ \bullet & -\gamma^2 I & \Phi_o^t & -\varrho \Gamma_o^t W \\ \bullet & \bullet & -I & 0 \\ \bullet & \bullet & \bullet & -\varrho W \end{bmatrix} < 0 \quad (4.64)$$

Since the Matlab LMI solver will be used to find the observer gain K_o , and our Ξ_{dof} have two unknown variables (S and K_o) multiplied by each other; we have to simplify our Ξ_{dof} such that it can be solved directly by the Matlab LMI solver, then we have to define new variable V such that

$$V = SK_o$$

$$\Rightarrow K_o = S^{-1}V$$

and

$$\varrho = \tau$$

We can now rewrite (4.64) as follow:

$$\mathcal{E}_{dof} = \begin{bmatrix} \mathcal{E}_{h11} & \mathcal{E}_{h12} & -PBK_c & -\varrho\Theta & P \\ \bullet & \mathcal{E}_{h22} & A_{do}^t S - C_{do}^t V^t & -\varrho Y & 0 \\ \bullet & \bullet & SA_o + A_o^t S - VC_o - C_o^t V^t & 0 & 0 \\ \bullet & \bullet & \bullet & -\varrho W & 0 \\ \bullet & \bullet & \bullet & \bullet & -\sigma I \\ \bullet & \bullet & \bullet & \bullet & \bullet \\ \bullet & \bullet & \bullet & \bullet & \bullet \\ \bullet & \bullet & \bullet & \bullet & \bullet \\ \bullet & \bullet & \bullet & \bullet & \bullet \end{bmatrix}$$

$$\begin{bmatrix} P & P\Gamma_o & G_o^t + K_c^t D^t & -\varrho A_o^t W - \varrho K_c^t B^t W \\ 0 & 0 & G_{do}^t & -\varrho A_{do}^t W \\ 0 & S\Gamma_o - V\psi_o & -K_c^t D^t & \varrho K_c^t B^t W \\ 0 & 0 & 0 & 0 \\ 0 & 0 & 0 & -W \\ -\kappa I & 0 & 0 & -W \\ \bullet & -\gamma^2 I & \Phi_o^t & -\varrho \Gamma_o^t W \\ \bullet & \bullet & -I & 0 \\ \bullet & \bullet & \bullet & -\varrho W \end{bmatrix} < 0$$

where

$$\mathcal{E}_{h11} = PA_o + A_o^t P + \Theta + \Theta^t + Q + \sigma\alpha^2 F^t F + PBK_c + K_c^t B^t P$$

$$\mathcal{E}_{h12} = PA_{do} - \Theta + Y^t$$

$$\mathcal{E}_{h22} = -Y - Y^t - Q + \kappa\beta^2 H^t H$$

This completes the proof.

Chapter 5

RESULTS AND CONCLUSIONS

5-1 Introduction

It is now well understood that the insulin-glucose regulation is one of the most complicated control topics since the system is nonlinear with time delay. We will start this chapter with patient data simulation using special software to show how the partial closed-loop controls for such kind of systems have many complications and should be used with a lot of cautions. Then, we will simulate Bergman model using MPC strategy. Later on, the following steps will be done in order to reach the thesis goal:

1. Simulate and check the \mathcal{L}_2 delay effects on the system stability for “type 1-diabetic patient” model with single time delay (2.11) for the LNDT system using Matlab LMI Solver.
2. State Feedback controller and Dynamic Output Controller theorem evaluation using Matlab LMI Solver. Then check the performance of each controller by conducting numerical simulations for the original model, model with noise, model with parameter variation, and model with meal disturbance.
3. Compare the results for both controllers.

Finally, we will draw the conclusions and suggest the future research topic.

5-2 Patient Data Simulation using AIDA Software

Simulation for real patient data was performed using AIDA freeware diabetes software blood glucose simulator program [124]. Figure 5.1 shows the AIDA data entry screen where details of the current case scenario regimen are displayed. Information about the dietary intake, insulin dosage regimen and blood glucose measurements are recorded in the same figure.

The screenshot displays the AIDA data entry screen with the following information:

Patient Information:
 Name: Day Wilson, Weight: 70.0 kg, Case Number: 0001, Date: 01/01/01

Text:
 This woman is on three injections of short and/or intermediate acting insulin each day, with a split-evening dose. She wants to start a family, but consistently has had quite high blood glucose levels in the early afternoon, despite numerous attempts to normalise her control in anticipation of becoming pregnant.

MEALS:

	Breakfast	Snack	Lunch	Snack	Supper	Snack
Time (hhmm):	0800	1000	1200	1550	1800	2230
Carbohydrate (g):	30	20	40	10	30	0

INSULIN INJECTIONS:

	Time (hhmm):	Number 1	Number 2	Number 3	Number 4
Humulin S dose (U):		8.75	17.5	22.5	
Humulin I dose (U):		3	4	0	
		12	8	10	

BLOOD GLUCOSE MEASUREMENTS:

Time (hhmm):	0600	1130	1330	1700	2200		
Glucose (mmol/l):	4.1	8.8	9.9	10.3	10.8		

HYPOLYCAEMIC EPISODES:

Time (hhmm):	Number 1	Number 2	Number 3	Number 4

CLINICAL VARIABLES:

RTG: 9.0 mmol/l, CCR: 100 ml/min

INSULIN DISTRIBUTION:

Hepatic (Sh): 0.4, Peripheral (Sp): 0.6

Figure 5.1: AIDA data entry screen.

As a result, two graphs will be shown, Figure 5.2, on the graphical simulator display. The upper graph will show the "observed" blood glucose readings (o) recorded via the data entry screen (blue and black lines), while the lower graph will provide a composite display of information regarding insulin and carbohydrate intake. It is clear that increasing the dose of the short- and intermediate-acting insulin injected before breakfast significantly improves this case blood glucose profile later in the day. Note that the blue plot in the Blood Glucose Level graph stands for the blood glucose before the insulin adjusts, while the black one is for after insulin adjust. Moreover, 1 mmol/l is equivalent to 18 mg/dl.

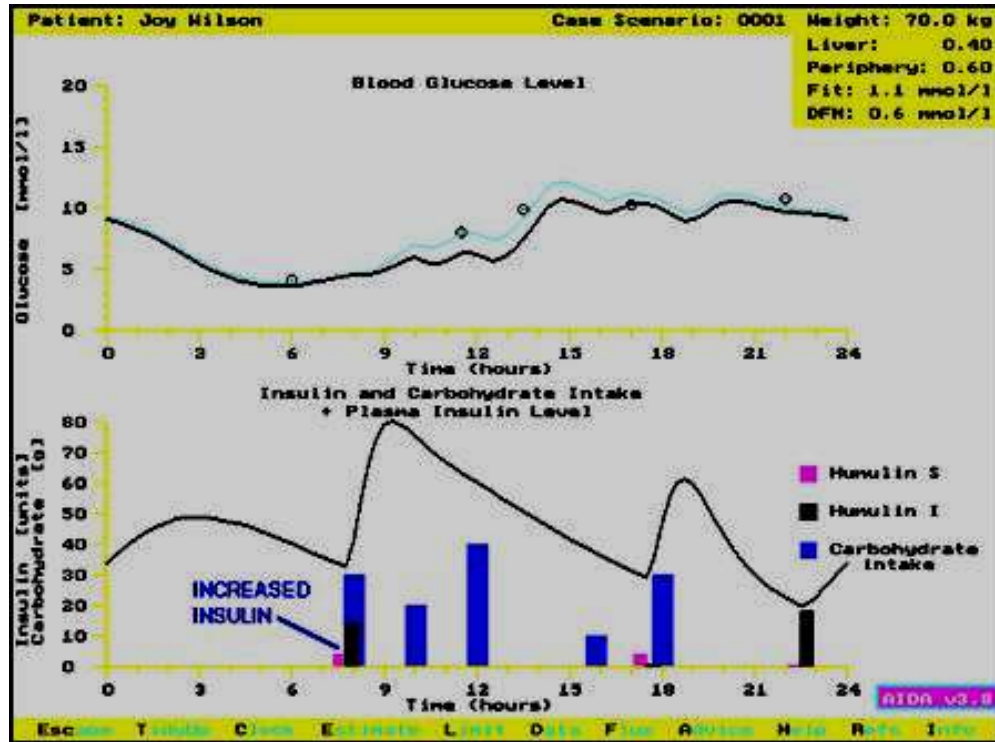


Figure 5.2: AIDA graphical simulator display: blue glucose graph before insulin increase, and the black is after.

It is clear now that any small variation of the insulin (type, dose, or time and number of injection), and carbohydrate (intake dose, intake time, or number of meals) will affect the blood glucose level. Thus we have to be careful when we use the partially close-loop control since it is easy not to maintain the blood glucose level in the Normoglycemia.

5-3 MPC Simulation for Bergman Model

Based on Bergman model (2.2) and its corresponding parameters Table 2.1, the system matrices can be easily calculated as follows:

$$A = \begin{bmatrix} 0.8670 & -352.0000 & -0.0467 & 0 & 4.6700 \\ 0 & 0.8680 & 0.0002 & 0 & 0 \\ 0 & 0 & 0.6290 & 0 & 0 \\ 0.5620 & -132.0000 & -0.0128 & 0.3390 & 1.7100 \\ 0 & 0 & 0 & 0 & 1.0000 \end{bmatrix}$$

$$B = \begin{bmatrix} -0.0069 & 0 \\ 0.0001 & 0 \\ 0.3340 & 0 \\ -0.0015 & 0 \\ 0 & 1 \end{bmatrix}$$

$$C = [0 \quad 0 \quad 0 \quad 1 \quad 0], \quad D = [0 \quad 0]$$

The MPC simulation of Bergman model using Matlab Simulink are shown in Figure 5.3.

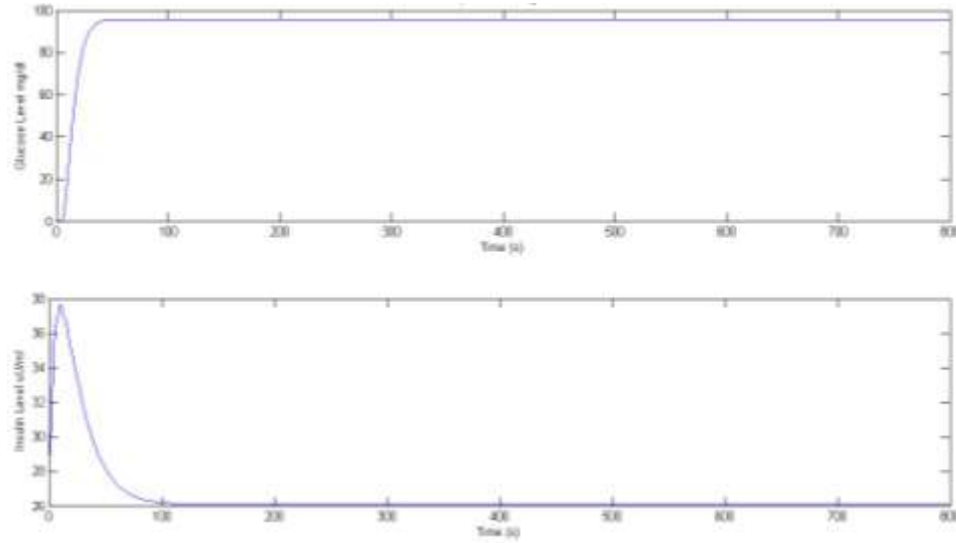


Figure 5.3: MPC Response for Bergman Model.

Thus, it is clear that the base insulin secretion level of 26.1 μ U/ml will maintain the blood glucose level at 95mg/dl. The glucose takes about 60 seconds to reach the Normoglycemia lower level (70 mg/dl).

5-4 New Stabilizing Methodology Results

We will start this section with the system matrices calculations for the single explicit time delay model (2.11). Note that, for simplicity and to avoid conflict, we will rename the following model parameters E_g , $1/t_1$, α , and β as G_{in} , d_i , α_1 , and β_1 respectively. Thus we can rewrite our model equation as:

$$\dot{G}(t) = \frac{dG(t)}{dt} = G_{\text{in}} - f_2(G(t)) - f_3(G(t))f_4(I(t)) + f_5(I(t - \tau)) \quad (5.1-1)$$

$$\dot{I}(t) = \frac{dI(t)}{dt} = f_1(G(t)) - d_i I(t) \quad (5.1-2)$$

where

$$f_1(G(t)) = \frac{R_m}{1 + \exp\left(\frac{\left(C_1 - \frac{G}{V_g}\right)}{a_1}\right)}$$

$$f_2(G) = U_b \left(1 - \exp\left(-\frac{G}{C_2 V_g}\right)\right)$$

$$f_3(G) = \frac{G}{C_3 V_g}$$

$$f_4(I) = U_o + \frac{U_m - U_o}{1 + \exp\left(-\beta_1 * \ln\left(\frac{I}{C_4 \left(\frac{1}{V_i} + \frac{1}{Et_i}\right)}\right)\right)}$$

$$f_5(I) = \frac{R_g}{1 + \exp\left(\alpha_1 * \left(\frac{I}{V_p} - C_5\right)\right)}$$

Thus using the standard linearization technique to add and subtract the linear parts, as illustrated in chapter 4, we will get the following:

At the operating point $\dot{G}(t) = 0$, hence we can calculate G_{in} as follow:

$$G_{\text{in}} = f_2(G(t)) + f_3(G(t))f_4(I(t)) - f_5(I(t - \tau)) = 7.71$$

$$\dot{f}_1(G(t)) = \frac{R_m}{V_g a_1} \frac{\exp\left(\frac{\left(C_1 - \frac{G}{V_g}\right)}{a_1}\right)}{\left(1 + \exp\left(\frac{\left(C_1 - \frac{G}{V_g}\right)}{a_1}\right)\right)^2}$$

$$\dot{f}_2(G) = \frac{U_b}{C_2 V_g} \exp\left(-\frac{G}{C_2 V_g}\right)$$

$$\dot{f}_3(G) = \frac{1}{C_3 V_g}$$

$$\dot{f}_4(I) = \frac{\frac{(U_o - U_m)\beta_1}{I} \ln\left(\frac{I_i}{C_4 \left(\frac{1}{V_i} + \frac{1}{Et_i}\right)}\right)}{\left(1 + \exp\left(-\beta_1 * \ln\left(\frac{I}{C_4 \left(\frac{1}{V_i} + \frac{1}{Et_i}\right)}\right)\right)\right)^2}$$

$$\dot{f}_5(I) = \frac{\frac{R_g \alpha_1}{V_p} \exp\left(\alpha_1 * \left(\frac{I}{V_p} - C_5\right)\right)}{\left(1 + \exp\left(\alpha_1 * \left(\frac{I}{V_p} - C_5\right)\right)\right)^2}$$

We can rewrite the system matrices as follow:

$$A_o = \begin{bmatrix} -\dot{f}_2(G) - \dot{f}_3(G)f_4(I) & -f_3(G)\dot{f}_4(I) \\ \dot{f}_1(G) & -d_i \end{bmatrix}, \quad A_{do} = \begin{bmatrix} 0 & \dot{f}_5(I) \\ 0 & 0 \end{bmatrix}$$

Thus the system matrices, based on Table 2.2 and $\varrho = \tau = 6 \text{ minutes} = 360 \text{ seconds}$, parameters found to be:

$$A_o = \begin{bmatrix} -0.0917 & 0.4221 \\ 0.0017 & -0.06 \end{bmatrix}, \quad A_{do} = \begin{bmatrix} 0 & 3.6462 \\ 0 & 0 \end{bmatrix}$$

The remaining matrices and scalars have been selected such that the stability is satisfied and the system is feasible:

$$G_o = [0.0001 \quad 0.0001], G_{do} = [0.1 \quad 0.1], C_o = [10 \quad 10]$$

$$\Gamma_o = \begin{bmatrix} 0.0001 \\ 0.0001 \end{bmatrix}, B_o = \begin{bmatrix} 10 \\ 10 \end{bmatrix}, F = \begin{bmatrix} 1 \\ 1 \end{bmatrix}, H = \begin{bmatrix} 1 \\ 1 \end{bmatrix}$$

$$\alpha = 0.001, \beta = 0.001, \Phi_o = 0.4, D_o = 1$$

The simulation time window was selected to be about six times the delay time such that the system response controllability can be checked. The system open-loop simulation, Figure 5.4, due to initial conditions, 92 mg/dl glucose and 23.74 μ U/ml insulin, shows that the system is uncontrolled since the peak of the output is endlessly increasing. We can see the effect of the time delay at $t = 360$ seconds.

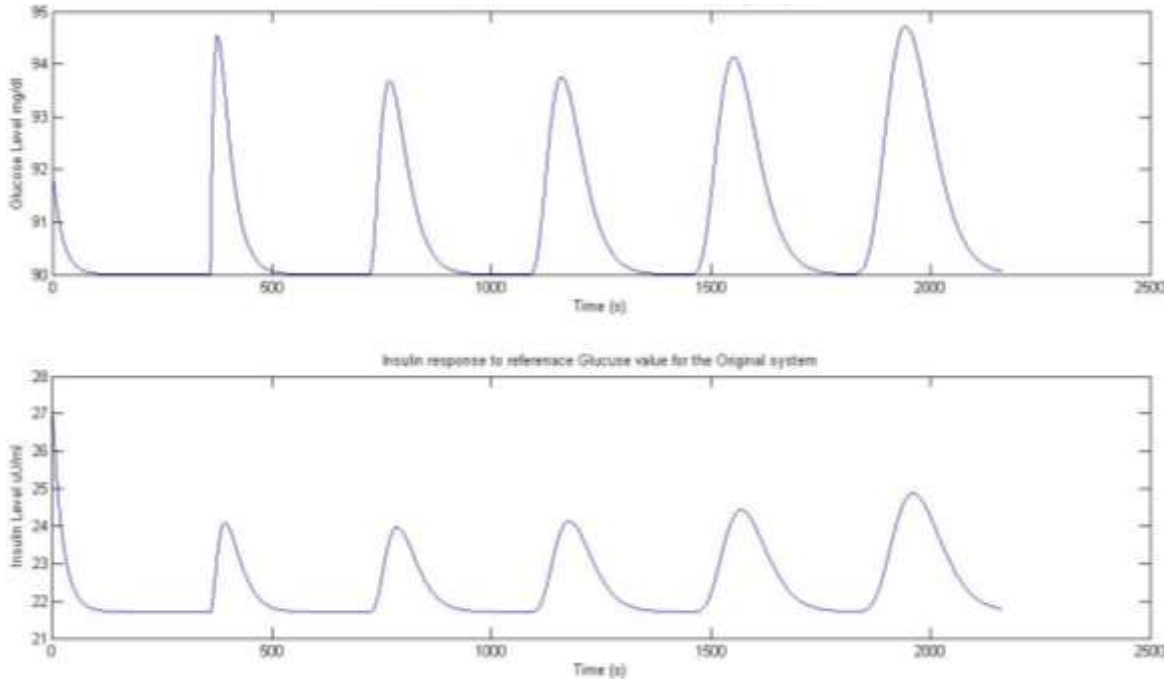


Figure 5.4: System open loop simulation with time delay at $t = 360$ sec

We will discuss the \mathcal{L}_2 gain analysis on the system stability, the State-Feedback, and the Dynamic Output Feedback results in the following sub-sections.

5-4-1 Stability Results based on \mathcal{L}_2 Gain Analysis

Using the Matlab LMI solver to test the system performance based on Theorem 1 found that the internal asymptotic stability for the open-loop system has been established and the system is feasible. Table 5.1 shows the results. Note that the disturbance rejection ratio level found here is comes from the LMI simulation not from the system itself.

Table 5.1: The time delay effect on the internal asymptotic stability parameters.

τ	5 min(300sec)	6 min(360sec)	15 min(900sec)
P	$\begin{bmatrix} 0.5986 & -1.0013 \\ -1.0013 & 21.6331 \end{bmatrix}$	$\begin{bmatrix} 0.8230 & -1.1061 \\ -1.1061 & 25.5422 \end{bmatrix}$	$\begin{bmatrix} 182.6 & -115.7 \\ -115.7 & 3377.5 \end{bmatrix}$
W	$\begin{bmatrix} 0.9418 & 1.8932 \\ 1.8932 & 392.9406 \end{bmatrix}$	$\begin{bmatrix} 1.1191 & 3.1504 \\ 3.1504 & 510.5266 \end{bmatrix}$	$\begin{bmatrix} 114 & 1268 \\ 1268 & 76844 \end{bmatrix}$
Q	$\begin{bmatrix} 0.0316 & -0.2849 \\ -0.2849 & 13.1526 \end{bmatrix}$	$\begin{bmatrix} 0.0332 & -0.2808 \\ -0.2808 & 14.9815 \end{bmatrix}$	$\begin{bmatrix} 2.0523 & -3.6632 \\ -3.6632 & 837.109 \end{bmatrix}$
θ	$\begin{bmatrix} -0.1882 & -0.3910 \\ -0.3910 & -77.5641 \end{bmatrix}$	$\begin{bmatrix} -0.1864 & -0.5382 \\ -0.5382 & -84.4236 \end{bmatrix}$	$\begin{bmatrix} -7.6 & -84.2 \\ -84.2 & -5116.6 \end{bmatrix}$
γ	$\begin{bmatrix} 0.1865 & 0.6223 \\ 0.6223 & 77.2630 \end{bmatrix}$	$\begin{bmatrix} 0.1848 & 0.6674 \\ 0.6674 & 84.1729 \end{bmatrix}$	$\begin{bmatrix} 7.4 & 80.9 \\ 80.9 & 5102.4 \end{bmatrix}$
σ	92.9773	100.9121	8036.5
κ	42496	62254	16228000
γ	85.891	104.0986	1622.6

Where, as stated in Theorem 1:

P, W, Q are symmetric positive define weighting matrices,

$\theta \in \mathbb{R}^{n \times n}, \gamma \in \mathbb{R}^{n \times n}$ are appropriate relaxation parameter matrices injected to facilitate the delay dependence analysis,

$\gamma > 0, \sigma > 0, \kappa > 0$ scalars that satisfy the stability LMI.

5-4-2 State-Feedback Results

Based on Theorem 2 to test the State-feedback scheme using the Matlab LMI solver, the system is feasible. Table 5.2 shows the results. Note that the disturbance rejection ratio level found here is comes from the LMI simulation not from the system itself.

Table 5.2: The time delay effect on the State feedback system parameters.

τ	5 min(300sec)	6 min(360sec)	15 min(900sec)
X	$\begin{bmatrix} 10.8117 & 0.3914 \\ 0.3914 & 0.4337 \end{bmatrix}$	$\begin{bmatrix} 6.5244 & 0.4422 \\ 0.4422 & 0.4703 \end{bmatrix}$	$\begin{bmatrix} 6.7867 & 0.1946 \\ 0.1946 & 0.2286 \end{bmatrix}$
y	$\begin{bmatrix} -0.6032 & -0.6091 \end{bmatrix}$	$\begin{bmatrix} -0.6649 & -0.6709 \end{bmatrix}$	$\begin{bmatrix} -0.1437 & -0.1432 \end{bmatrix}$
Q_1	$\begin{bmatrix} 6.1464 & 4.9830 \\ 4.9830 & 5.2130 \end{bmatrix}$	$\begin{bmatrix} 5.7650 & 5.4804 \\ 5.4804 & 5.7373 \end{bmatrix}$	$\begin{bmatrix} 1.6196 & 1.1448 \\ 1.1448 & 1.2449 \end{bmatrix}$
S_{x1}	$\begin{bmatrix} 0 & 0 \\ 0 & 0 \end{bmatrix}$	$\begin{bmatrix} 0 & 0 \\ 0 & 0 \end{bmatrix}$	$\begin{bmatrix} 0 & 0 \\ 0 & 0 \end{bmatrix}$
S_{x2}	$\begin{bmatrix} 0 & 0 \\ 0 & 0 \end{bmatrix}$	$\begin{bmatrix} 0 & 0 \\ 0 & 0 \end{bmatrix}$	$\begin{bmatrix} 0 & 0 \\ 0 & 0 \end{bmatrix}$
θ_1	$\begin{bmatrix} -0.0212 & -0.0002 \\ -0.0007 & -0.0001 \end{bmatrix}$	$\begin{bmatrix} -0.0109 & -0.0005 \\ -0.0007 & -0.0010 \end{bmatrix}$	$\begin{bmatrix} -0.0044 & -0.0001 \\ -0.0001 & -0.0000 \end{bmatrix}$
γ_1	$\begin{bmatrix} 0.0213 & 0.0008 \\ 0.0009 & 0.0000 \end{bmatrix}$	$\begin{bmatrix} -0.0109 & -0.0003 \\ -0.0009 & -0.0000 \end{bmatrix}$	$\begin{bmatrix} 0.0044 & 0.0001 \\ 0.0001 & 0.0000 \end{bmatrix}$
σ	3536.8	592.6953	1203.8
κ	37051	26181	1016.3
γ	2.6078	2.5930	2.5938
ε	0.01	0.01	0.01
K_s	$\begin{bmatrix} -0.0051 & -1.3998 \end{bmatrix}$	$\begin{bmatrix} -0.0056 & -1.4212 \end{bmatrix}$	$\begin{bmatrix} -0.0033 & -0.6236 \end{bmatrix}$
A_s	$\begin{bmatrix} -0.1428 & -13.5763 \\ -0.0494 & -14.0584 \end{bmatrix}$	$\begin{bmatrix} -0.1476 & -13.7895 \\ -0.0542 & -14.2716 \end{bmatrix}$	$\begin{bmatrix} -0.1246 & -5.8140 \\ -0.0312 & -6.2961 \end{bmatrix}$
G_s	$\begin{bmatrix} -0.0050 & -1.3997 \end{bmatrix}$	$\begin{bmatrix} -0.0055 & -1.4211 \end{bmatrix}$	$\begin{bmatrix} -0.0032 & -0.6235 \end{bmatrix}$

5-4-3 Dynamic Output Feedback Results

While evaluating the Dynamic Output Feedback scheme on various time delays, Theorem 3, using the Matlab LMI solver found the system is feasible and have the results that are shown in Table 5.3. The following system matrices were calculated based on 6 minutes (360 seconds) time delay. Note that the disturbance rejection ratio level found here is comes from the LMI simulation not from the system itself.

$$\hat{A} = \begin{bmatrix} -0.1476 & -13.7895 & 0.0559 & 14.2116 \\ -0.0542 & -14.2716 & 0.0559 & 14.2116 \\ 0 & 0 & -4.9371 & -4.4232 \\ 0 & 0 & 0.0131 & -0.0486 \end{bmatrix}$$

$$\hat{A}_d = \begin{bmatrix} -0.1476 & -13.7895 & 0.0559 & 14.2116 \\ -0.0542 & -14.2716 & 0.0559 & 14.2116 \\ 0 & 0 & -4.9371 & -4.4232 \\ 0 & 0 & 0.0131 & -0.0486 \end{bmatrix}$$

$$\hat{f}_o = \begin{bmatrix} 0.0001 \\ 0.0001 \\ -0.0484 \\ 0.0002 \end{bmatrix}, \quad B = \begin{bmatrix} 1 \\ 1 \\ 1 \\ 1 \end{bmatrix}$$

$$\hat{G} = [-0.0055 \quad -1.4211 \quad 0.0056 \quad 1.4212]$$

$$\hat{G}_d = [0.1000 \quad 0.1000 \quad 0 \quad 0]$$

$$C_{do} = [1 \quad 1 \quad 1 \quad 1]$$

$$D = 10$$

$$\psi_o = 0.1$$

Table 5.3: The time delay effect on the dynamic output feedback system parameters.

τ	5 min(300sec)	6 min(360sec)	15 min(900sec)
P	$\begin{bmatrix} 321 & -102 \\ -102 & 17637 \end{bmatrix}$	$\begin{bmatrix} 272 & -63 \\ -63 & 15628 \end{bmatrix}$	$\begin{bmatrix} 6.6809 & -11.6335 \\ -11.6335 & 446.4482 \end{bmatrix}$
S	$10^5 * \begin{bmatrix} 0.0020 & 0.0225 \\ 0.0225 & 8.3568 \end{bmatrix}$	$10^6 * \begin{bmatrix} 0.0001 & 0.0049 \\ 0.0049 & 1.8053 \end{bmatrix}$	
Q	$\begin{bmatrix} 30 & -11 \\ -11 & 25706 \end{bmatrix}$	$\begin{bmatrix} 19 & 28 \\ 28 & 23897 \end{bmatrix}$	$\begin{bmatrix} 0.7725 & -2.2940 \\ -2.2940 & 370.7177 \end{bmatrix}$
W	$\begin{bmatrix} 350.3 & -707.2 \\ -707.2 & 2747 \end{bmatrix}$	$\begin{bmatrix} 275 & -834.3 \\ -834.3 & 3866.2 \end{bmatrix}$	$\begin{bmatrix} 2.3 & -7.3 \\ -7.3 & 5385.9 \end{bmatrix}$
θ	$\begin{bmatrix} -83.9680 & 169.8482 \\ 83.6831 & -431.8009 \end{bmatrix}$	$\begin{bmatrix} -55.9847 & 169.8319 \\ 96.1857 & -526.5172 \end{bmatrix}$	$\begin{bmatrix} -0.2437 & 6.6349 \\ 1.0928 & -422.8641 \end{bmatrix}$
γ	$\begin{bmatrix} 38.3040 & -76.5804 \\ 178.0400 & -105.8813 \end{bmatrix}$	$\begin{bmatrix} 24.7507 & -78.3129 \\ 108.8353 & -189.1842 \end{bmatrix}$	$\begin{bmatrix} 0.0761 & -0.0609 \\ 2.1468 & 77.8972 \end{bmatrix}$
σ	34558	25511	986
κ	37051	26181	1016
γ	0.8551	0.8882	1.2909
K_c	$[-0.0051 \quad -1.3998]$	$[-0.0056 \quad -1.4212]$	$[-0.0033 \quad -0.6236]$
K_o	$\begin{bmatrix} 0.5561 \\ -0.0012 \end{bmatrix}$	$\begin{bmatrix} 0.4845 \\ -0.0011 \end{bmatrix}$	$\begin{bmatrix} 0.9702 \\ 0.0001 \end{bmatrix}$
V	$\begin{bmatrix} 110.1045 \\ 272.7860 \end{bmatrix}$	$\begin{bmatrix} 27.2542 \\ 306.6631 \end{bmatrix}$	$\begin{bmatrix} 15.7583 \\ -44.3827 \end{bmatrix}$

5-5 New Stabilizing Method Simulation Results

In this section, we will show the State Feedback and the Dynamic Output Feedback simulation response for the following cases:

- 1- Response to reference value without disturbance: 92 mg/dl glucose and 23.74 $\mu\text{U/ml}$ insulin.
- 2- Response to initial conditions without disturbance: 100 mg/dl glucose and 25.74 $\mu\text{U/ml}$ insulin.
- 3- Response to initial conditions with added white noise disturbance through I_o .

Table 5.4 shows the effect of the simulation sampling times on the system output level for the both control schemes. We have chosen the sampling time to be 0.1 second since the results were acceptable and comparable. Practically, we can use 0.1 second while implementing the realistic controller because of the availability of real-time glucose-monitor.

Table 5.4: The effect of sampling time on the system output for the State Feedback and the Dynamic Output Feedback.

Sampling time	State Feedback	Dynamic Output Feedback
0.01 second	Output level is controlled	Output level is controlled
0.1 second	Output level is controlled	Output level is controlled
0.2 second	Output level is uncontrolled	Output level is controlled
0.3 second	Output level is uncontrolled	Output level is uncontrolled
0.4 second	Output level is uncontrolled	Output level is uncontrolled

Moreover, the results of evaluating both control schemes for effect of the minimum and the maximum time delay, $\tau = 5$ minutes (300seconds) and $\tau = 15$ minutes (900seconds), show that using any of these two controllers will give satisfactory results. Thus, all the simulation results shown hereunder are based on $\tau = 6$ minutes (360seconds)

Figure 5.5 shows the system simulation response to reference value without disturbance. While Figure 5.6 shows the system simulation response to initial conditions without disturbance. The response for the system simulation to initial conditions with added, random, noise through I_o is shown in Figure 5.7. The comparative of State Feedback response for all the previous cases is shown in Figure 5.8. On the other hand, Figure 5.9 shows the comparative simulation response for the Dynamic Output Feedback. Finally, the response for all the above cases ($\tau = 5$ minutes , 6 minutes, and 15 minutes) are shown in Figure 5.10.

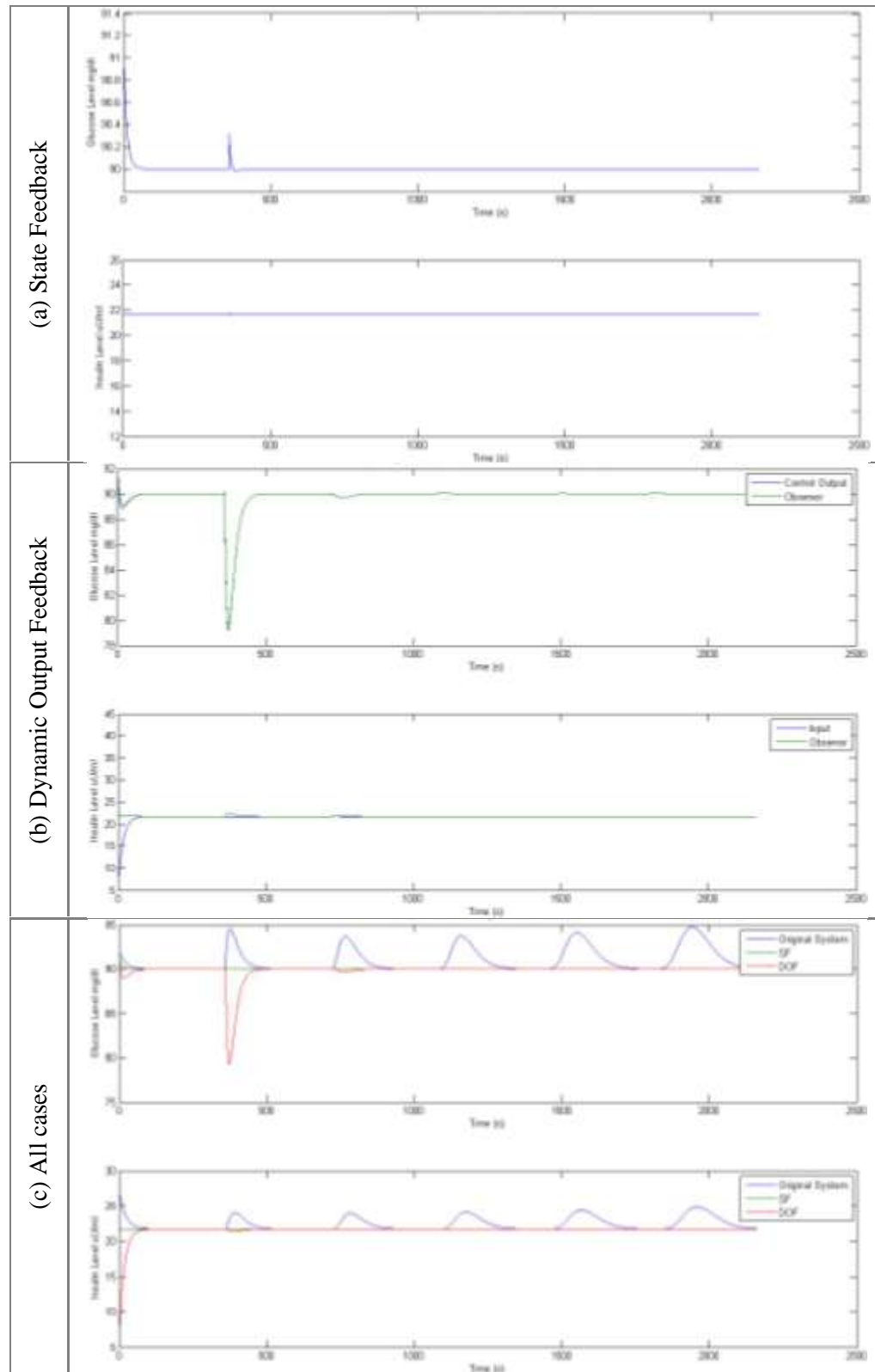


Figure 5.5: Response to reference value without disturbance.

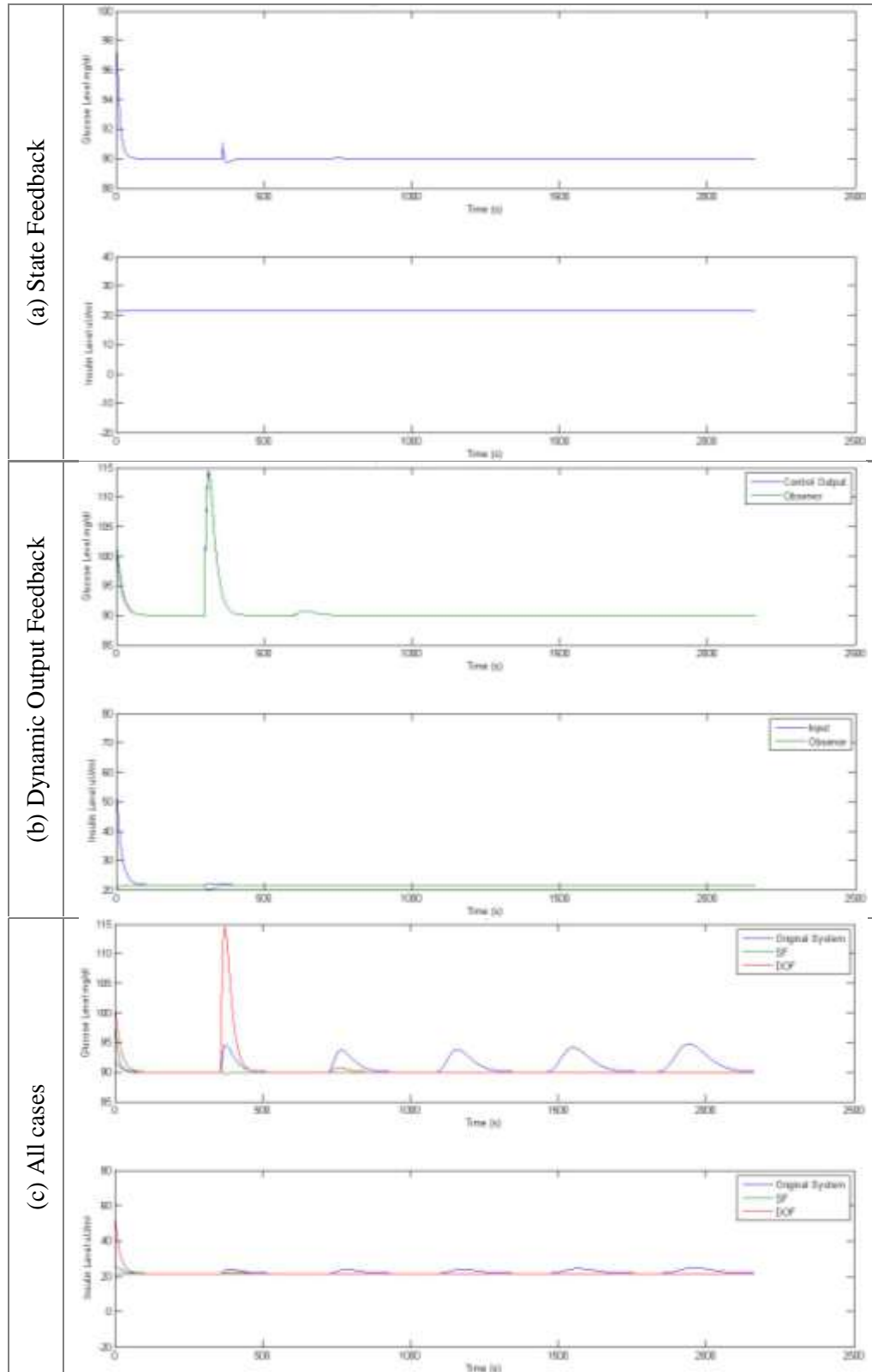
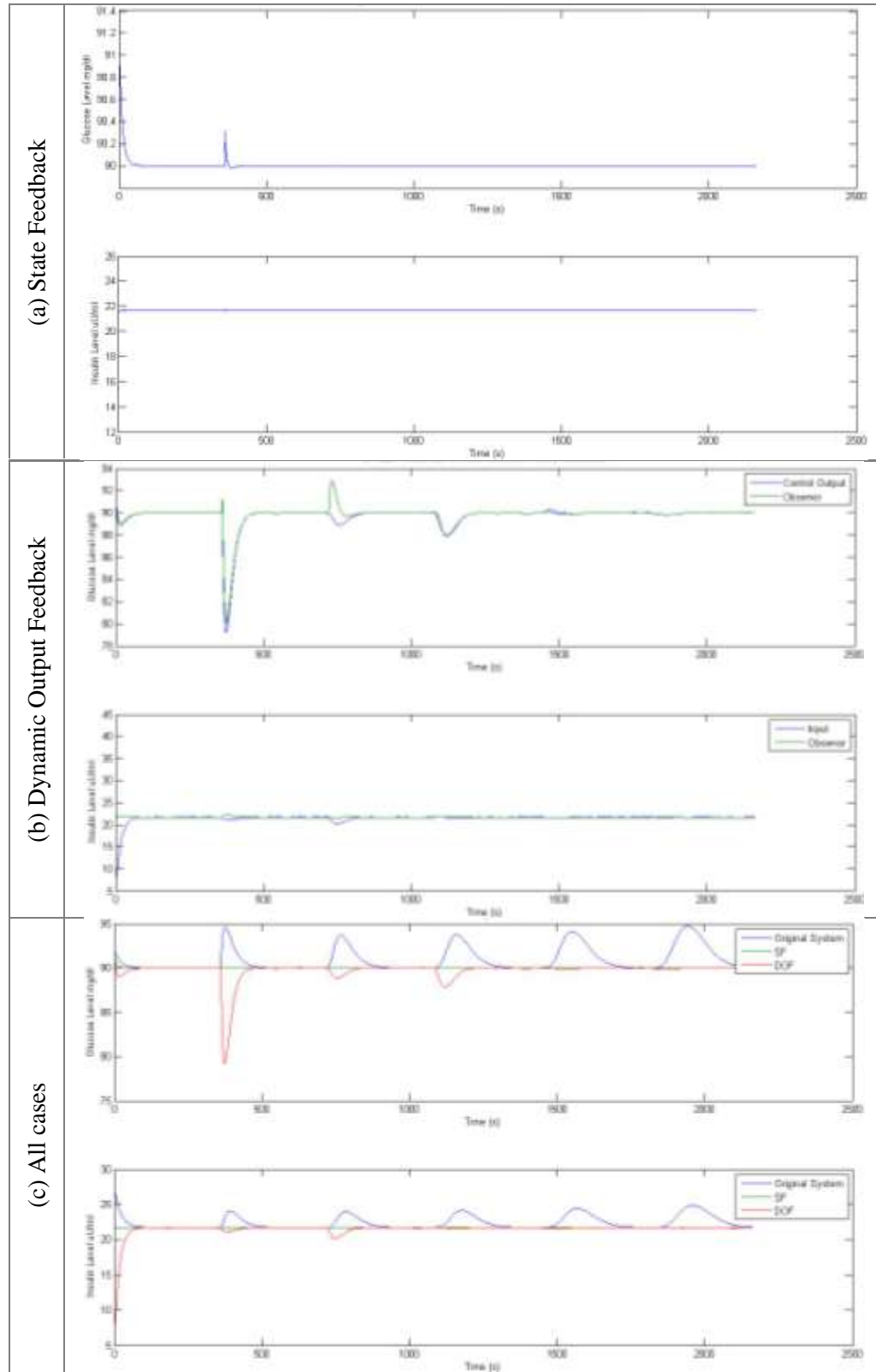


Figure 5.6: Response to initial conditions without disturbance.

Figure 5.7: Response to initial conditions with added disturbance through I_0

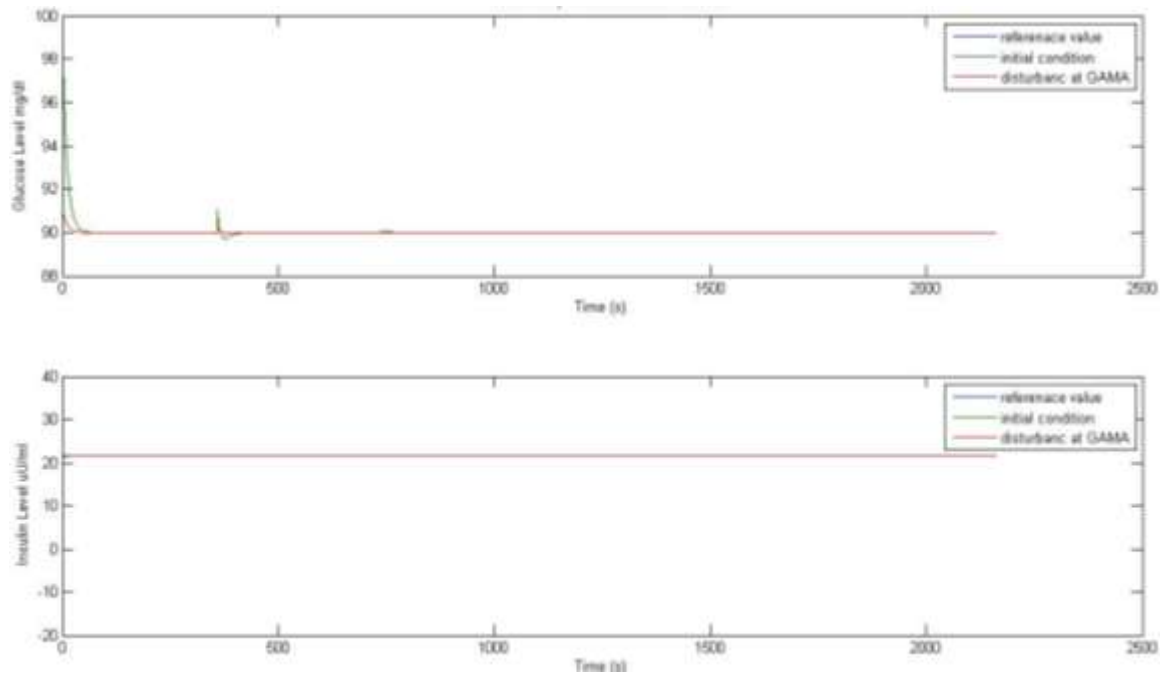


Figure 5.8: State feedback Response for the three cases.

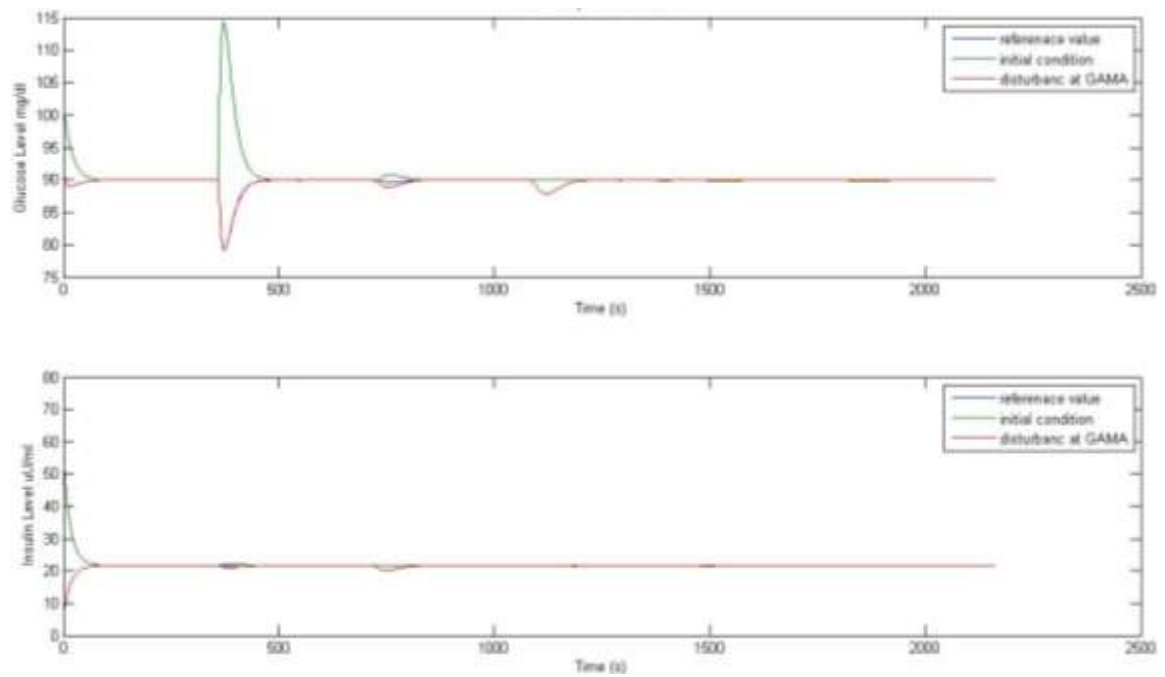


Figure 5.9: Dynamic Output feedback Response for the three cases.

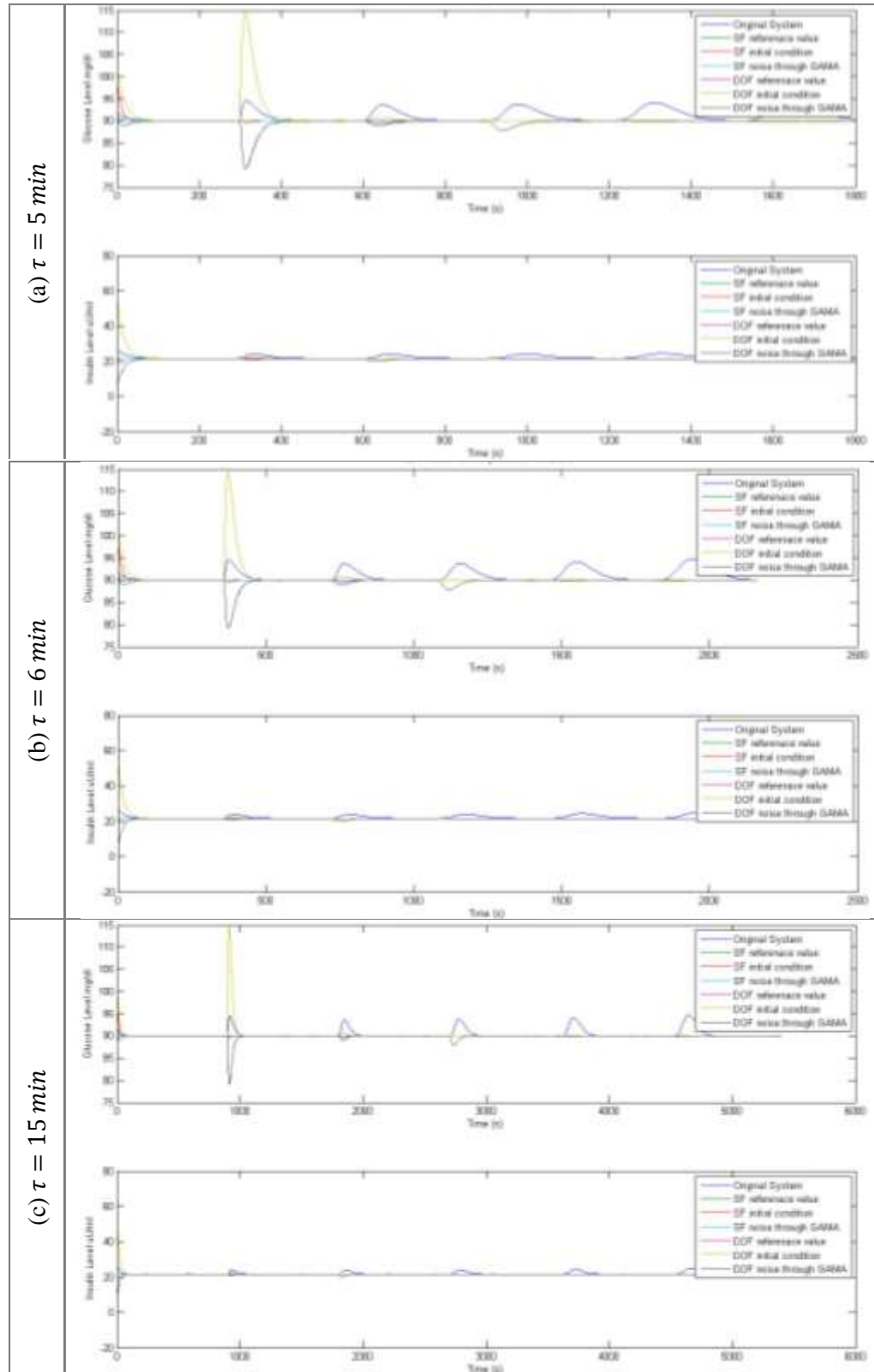


Figure 5.10: Response for all the cases.

5-6 Control Schemes Robustness and Sensitivity Analysis

Positive and negative meal disturbance signals, shown in Figure 5.11, were used to test the robustness of the system due to initial conditions. The positive disturbance consist of pluses of (100, 50, 20, and 10 mg/dl), while the negative one has only one pulse of 25 mg/dl. Each of the signals start at $t = 0$ seconds, and the pulse width is 5 seconds each. The system parameters have been varied by $\pm 50\%$, $\pm 25\%$ of the parameters value. The results of this sensitivity analysis and robustness test are shown in Table 5.5 and their corresponding figures.

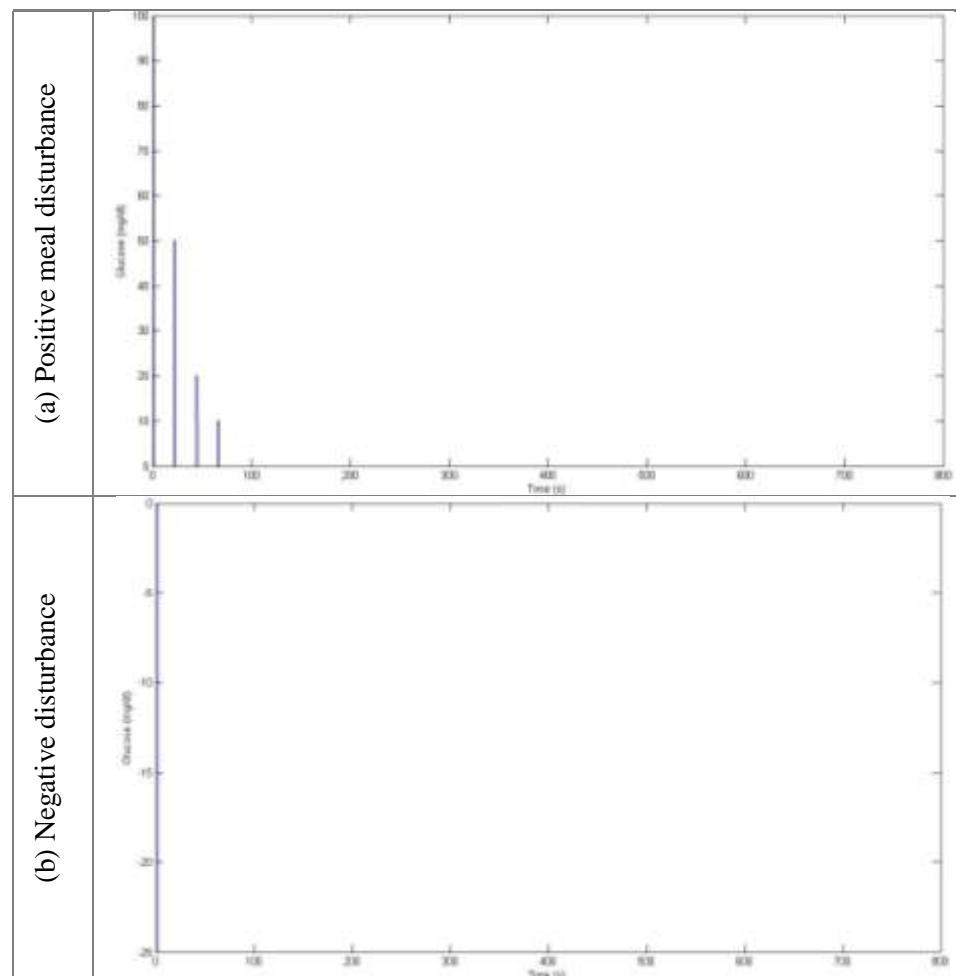


Figure 5.11: Meal disturbance signals.

Table 5.5: Sensitivity analysis and robustness test.

Variable	Effect on function	State Feedback		Dynamic Output Feedback	
		Parameter Variation	Meal Disturbance	Parameter Variation	Meal Disturbance
V_g	$f_1(G), f_2(G), f_3(G)$	Figure 5.12	Figure 5.13	Figure 5.14	Figure 5.15
R_m	$f_1(G)$	Negligible effects	Negligible effects	Negligible effects	Negligible effects
α_1	$f_1(G)$	Negligible effects	Negligible effects	Negligible effects	Negligible effects
C_1	$f_1(G)$	Minor Effects	Minor Effects	Minor Effects	Minor Effects
C_2	$f_2(G)$	No effect	No effect	No effect	No effect
U_b	$f_2(G)$	No effect	No effect	No effect	No effect
C_3	$f_3(G)$	Figure 5.16	Figure 5.17	Figure 5.18	Figure 5.19
V_p	$f_5(I)$	Figure 5.20	Figure 5.21	Figure 5.22	Figure 5.23
V_i	$f_4(I)$	No effect	Negligible effects	Figure 5.24	Figure 5.25
E	$f_4(I)$	No effect	Negligible effects	Figure 5.26	Figure 5.27
U_0	$f_4(I)$	No effect	Negligible effects	Negligible effects	Negligible effects
U_m	$f_4(I)$	Figure 5.28	Figure 5.29	Figure 5.30	Figure 5.31
β_1	$f_4(I)$	Negligible effects	Negligible effects	Figure 5.32	Figure 5.33
C_4	$f_4(I)$	No effect	Negligible effects	Figure 5.34	Figure 5.35
R_g	$f_5(I)$	Figure 5.36	Figure 5.37	Figure 5.38	Figure 5.39
α_1	$f_5(I)$	Negligible effects	Negligible effects	Figure 5.40	Figure 5.41
C_5	$f_5(I)$	Figure 5.42	Figure 5.43	Figure 5.44	Figure 5.45
t_i	$f_4(I)$	No effect	Negligible effects	Figure 5.46	Figure 5.47

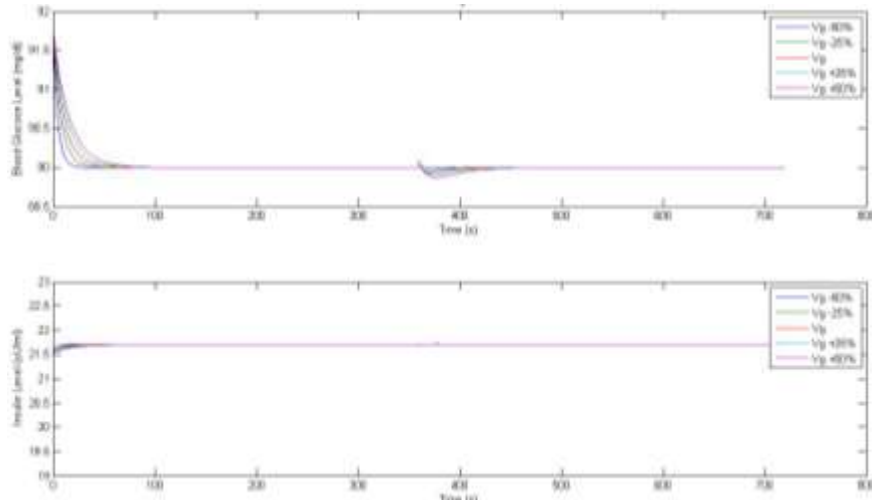


Figure 5.12: State feedback with V_g variation.

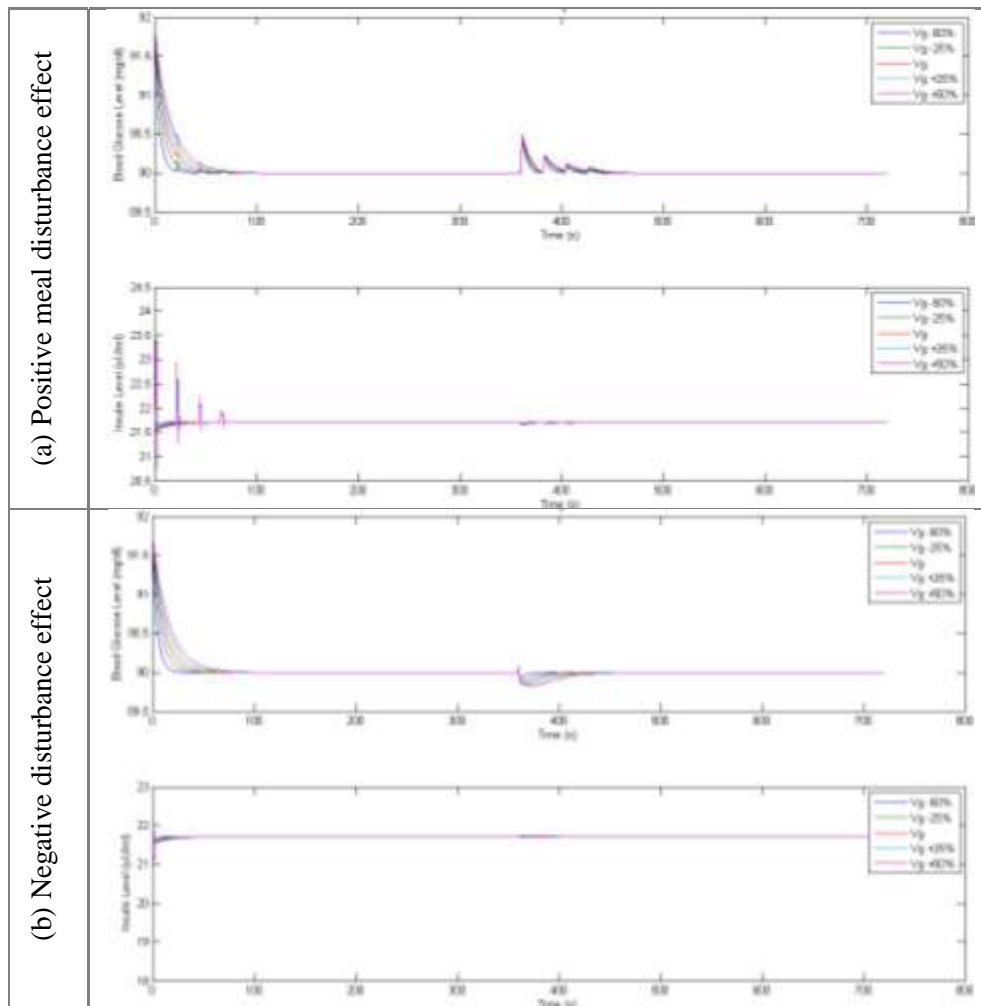


Figure 5.13: State feedback with V_g variation and meal disturbance.

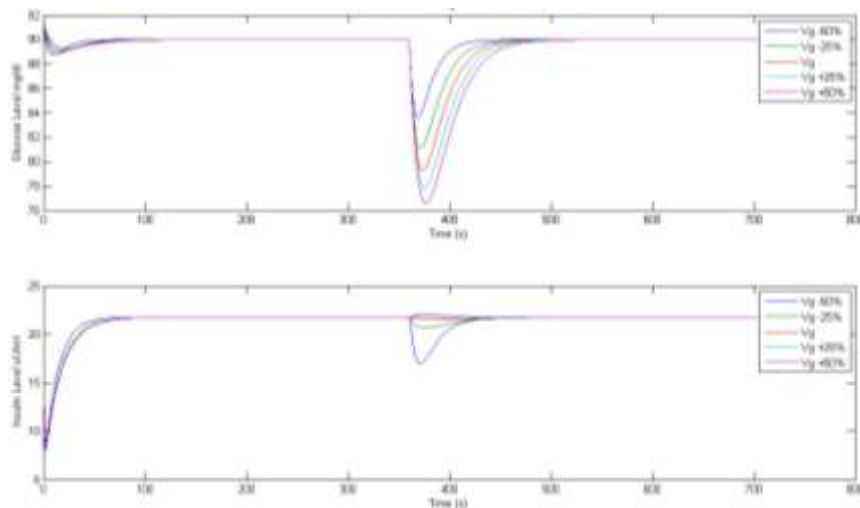


Figure 5.14: Dynamic Output feedback with V_g variation.

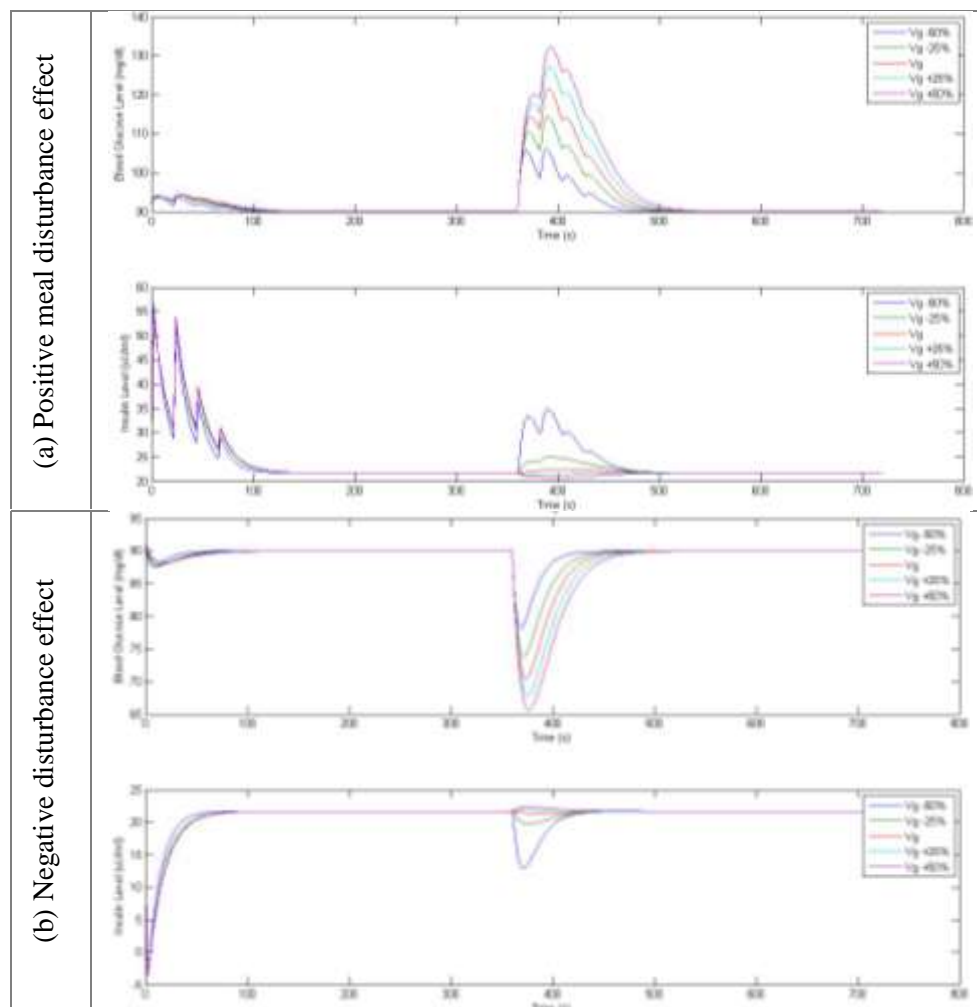
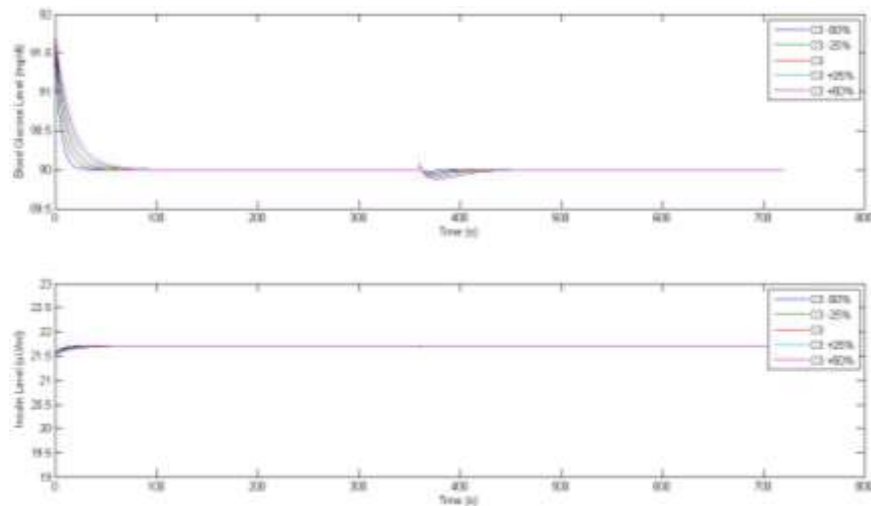
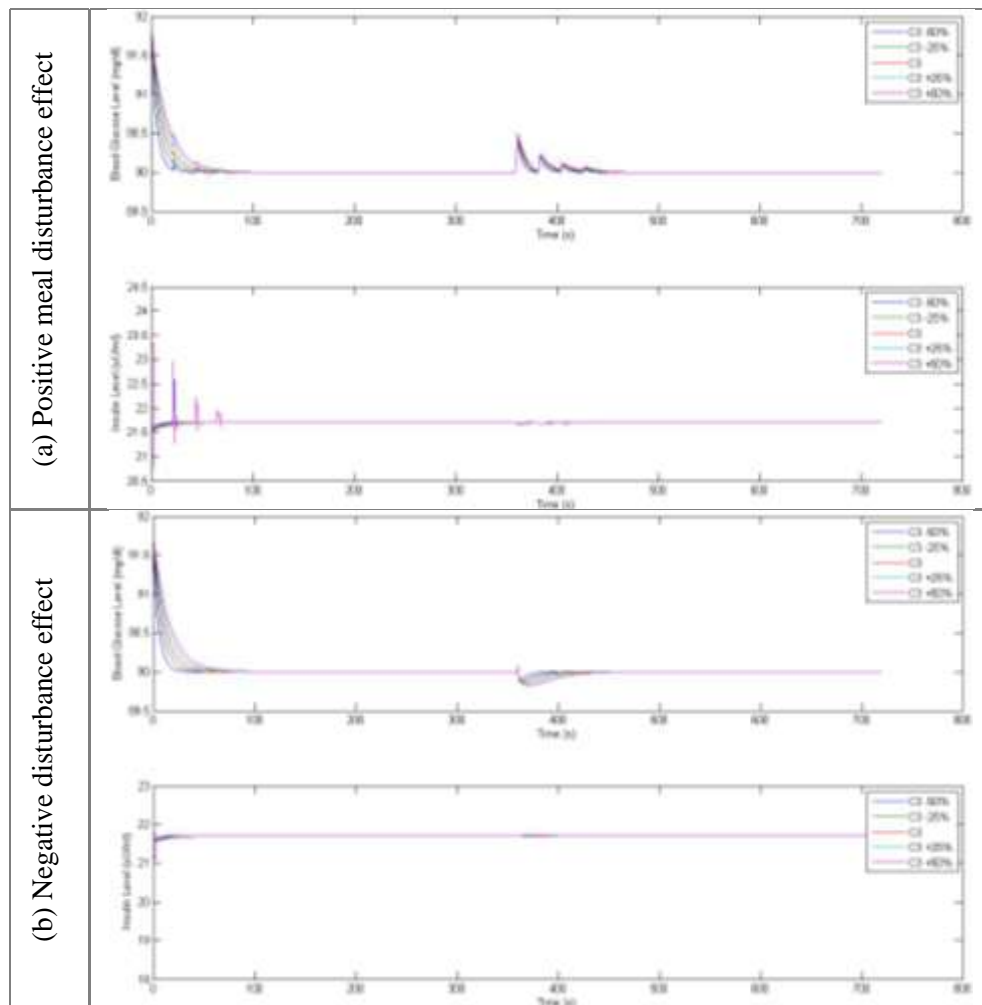


Figure 5.15: Dynamic output feedback with V_g variation and meal disturbance.

Figure 5.16: State feedback with C_3 variation.Figure 5.17: State feedback with C_3 variation and meal disturbance.

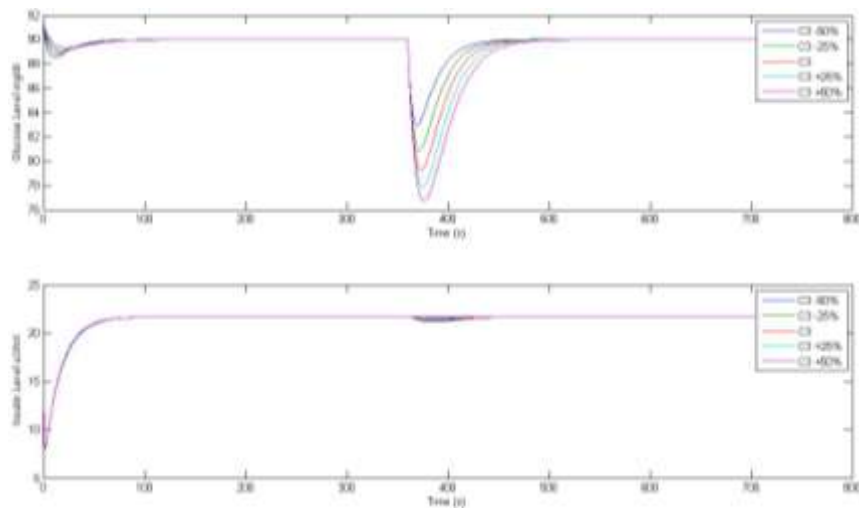


Figure 5.18: Dynamic Output feedback with C_3 variation.

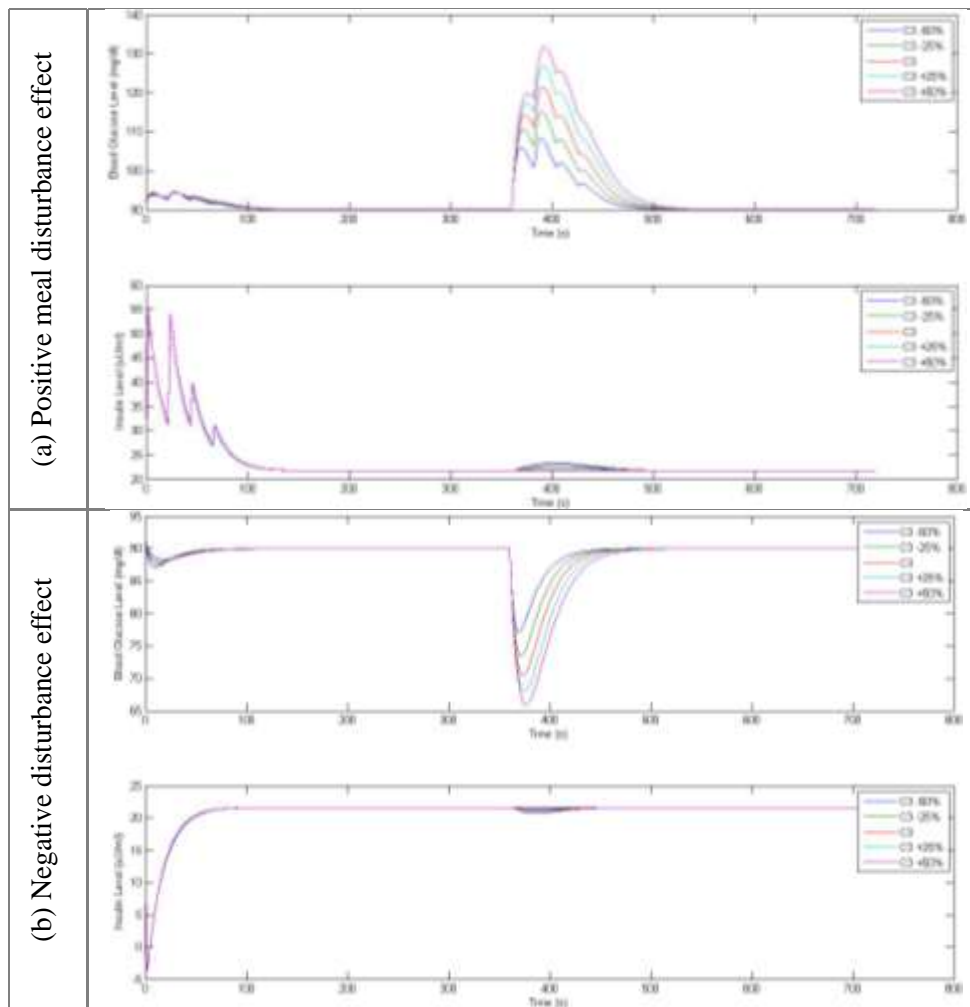
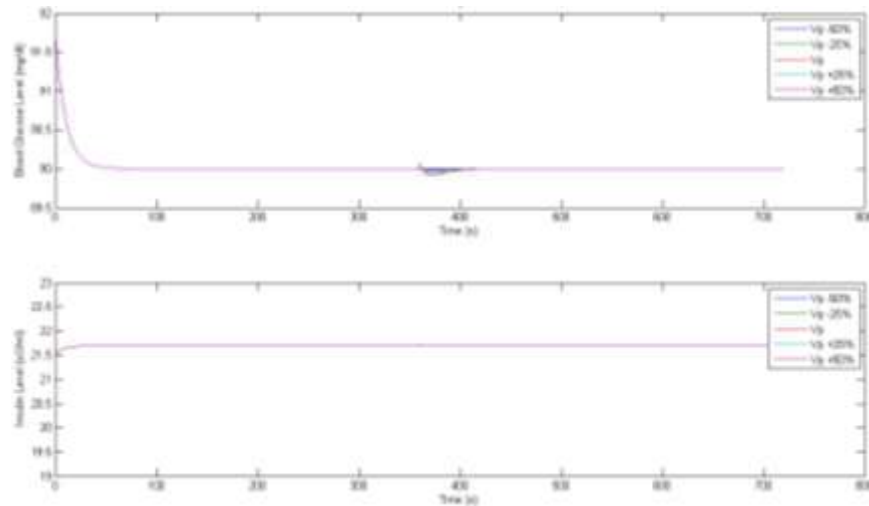
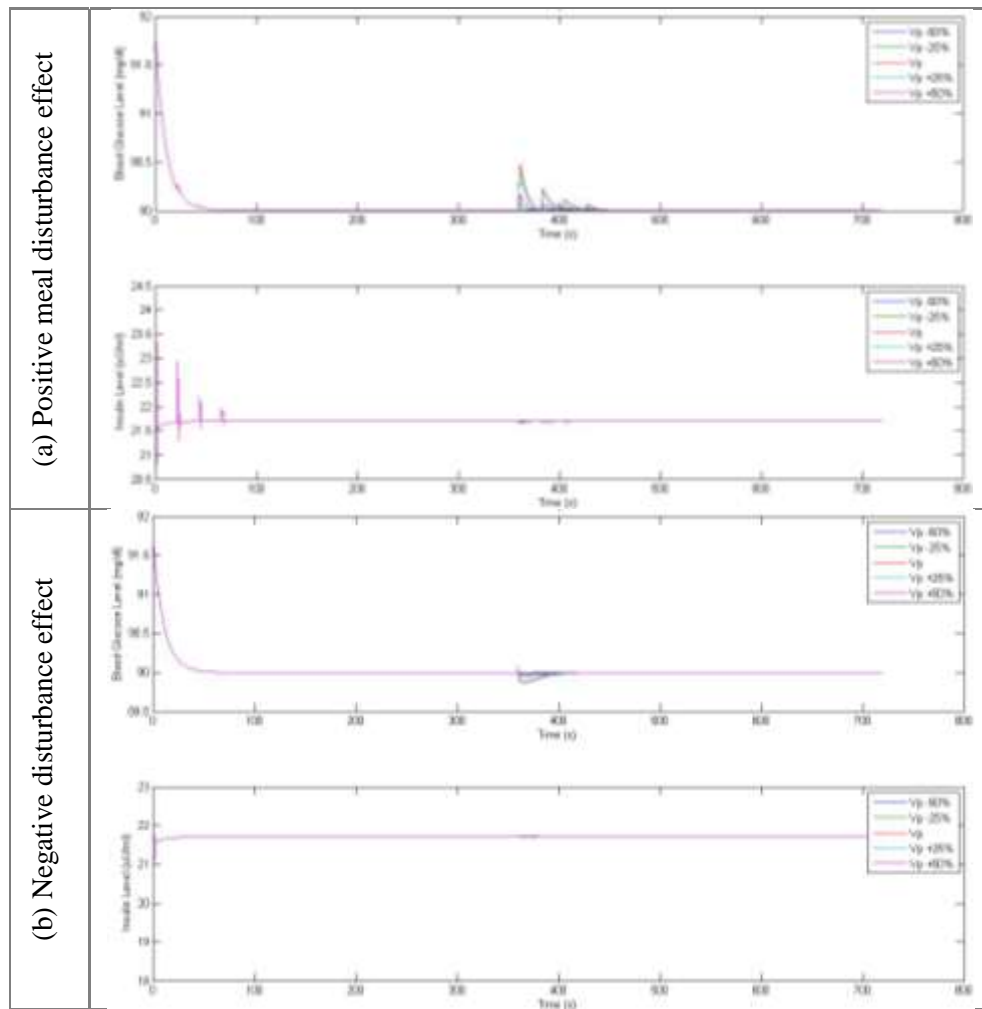


Figure 5.19: Dynamic output feedback with C_3 variation and meal disturbance.

Figure 5.20: State feedback with V_p variation.Figure 5.21: State feedback with V_p variation and meal disturbance.

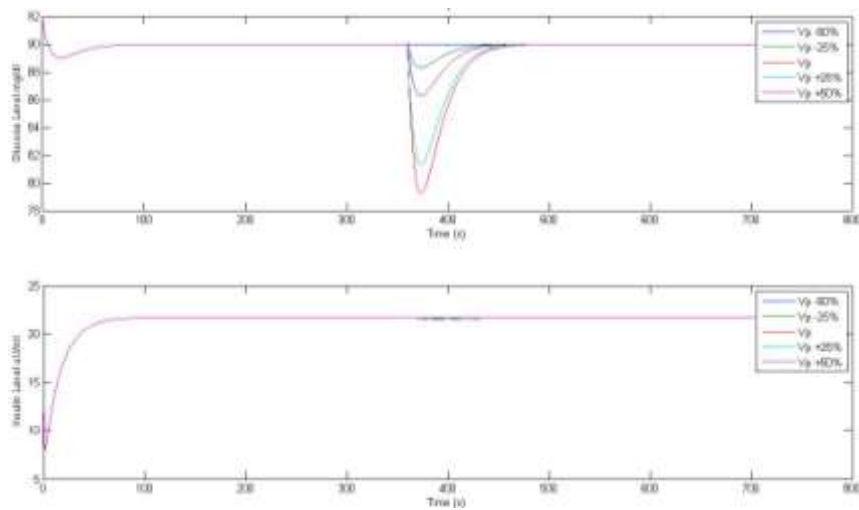


Figure 5.22: Dynamic Output feedback with V_p variation.

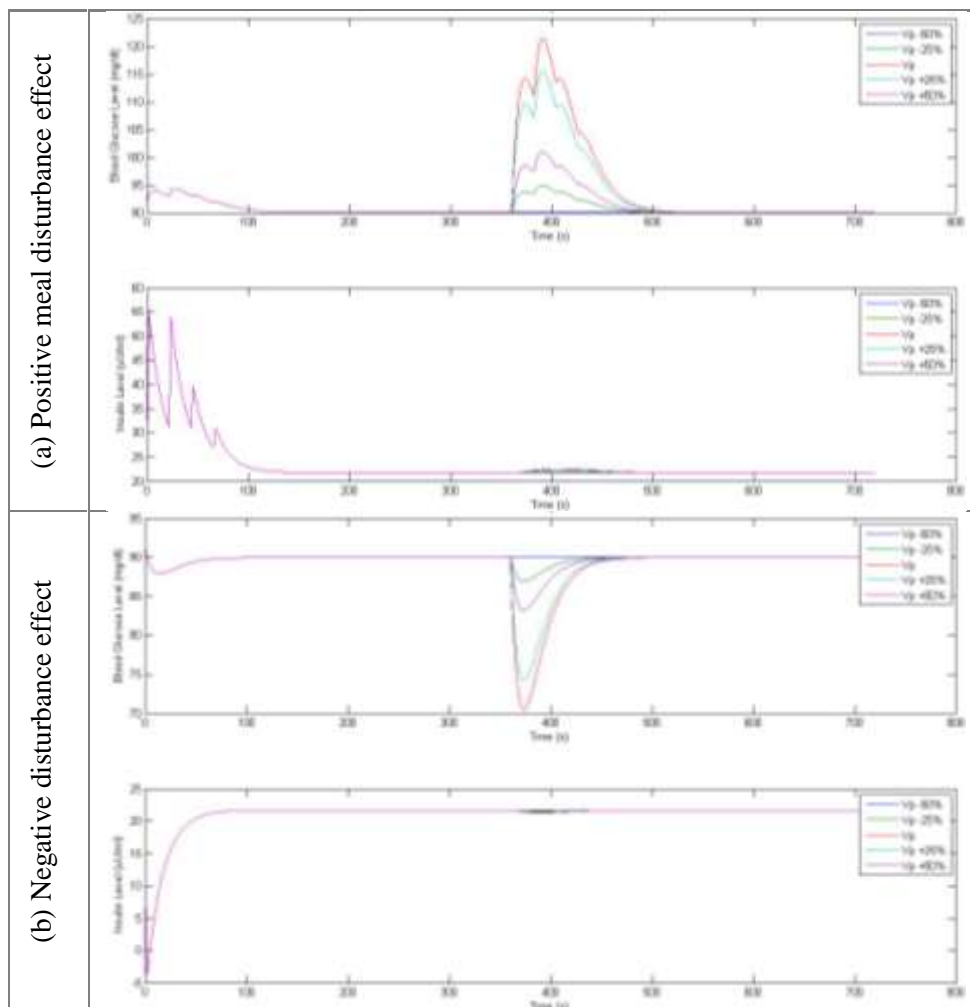


Figure 5.23: Dynamic output feedback with V_p variation and meal disturbance.

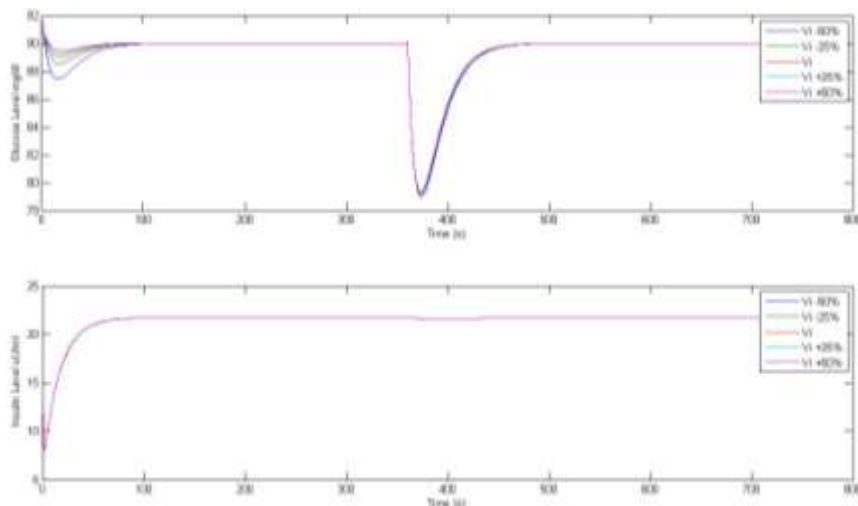


Figure 5.24: Dynamic Output feedback with V_i variation.

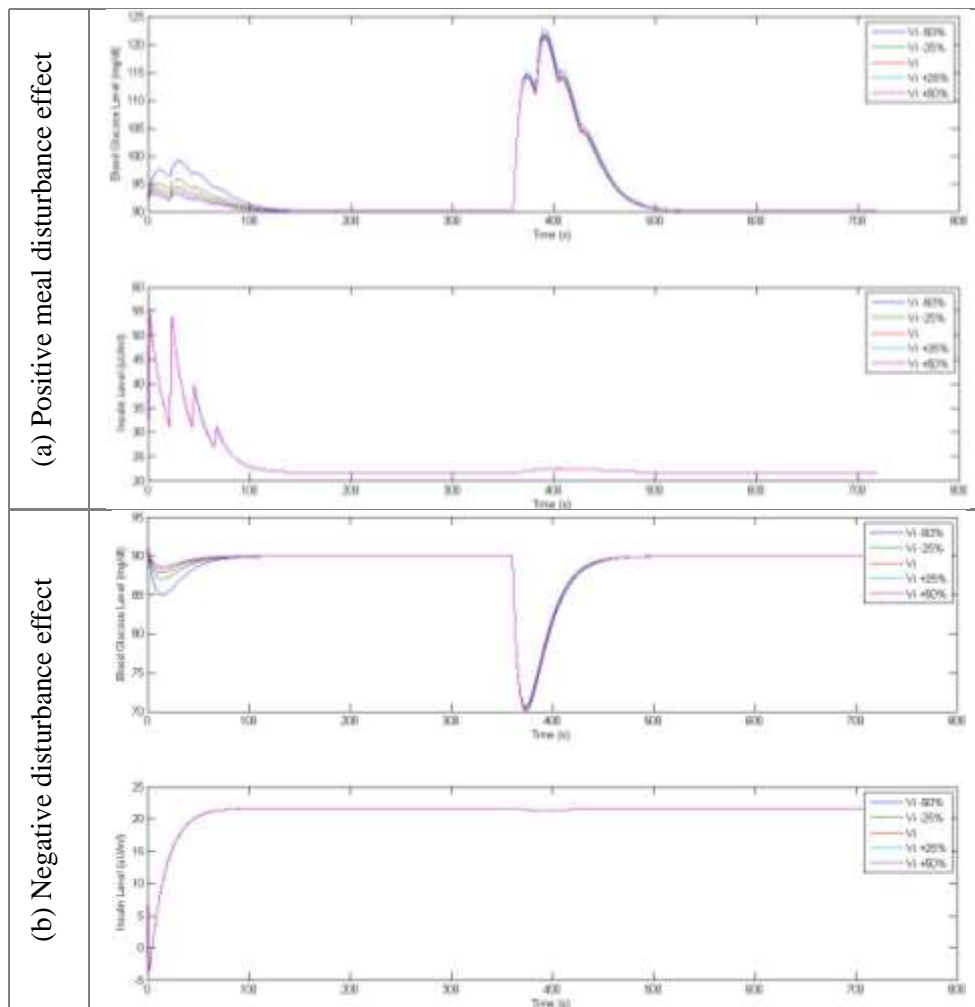


Figure 5.25: Dynamic output feedback with V_i variation and meal disturbance.

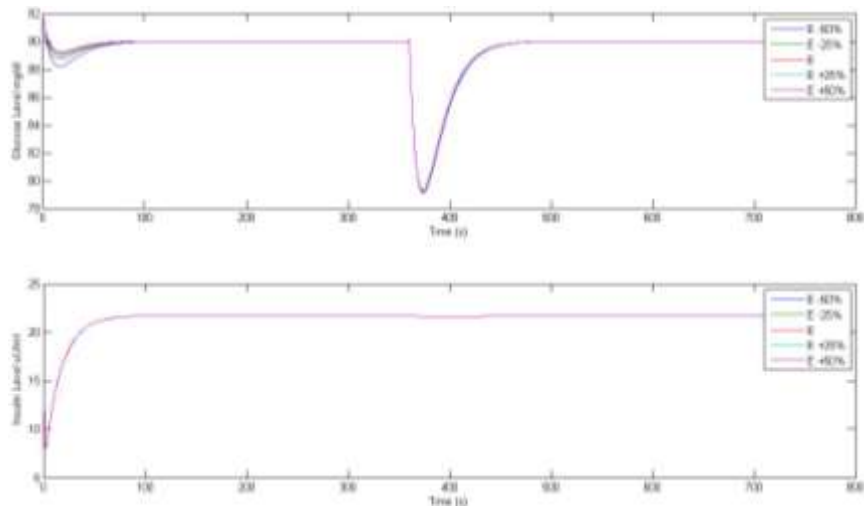


Figure 5.26: Dynamic Output feedback with E variation.

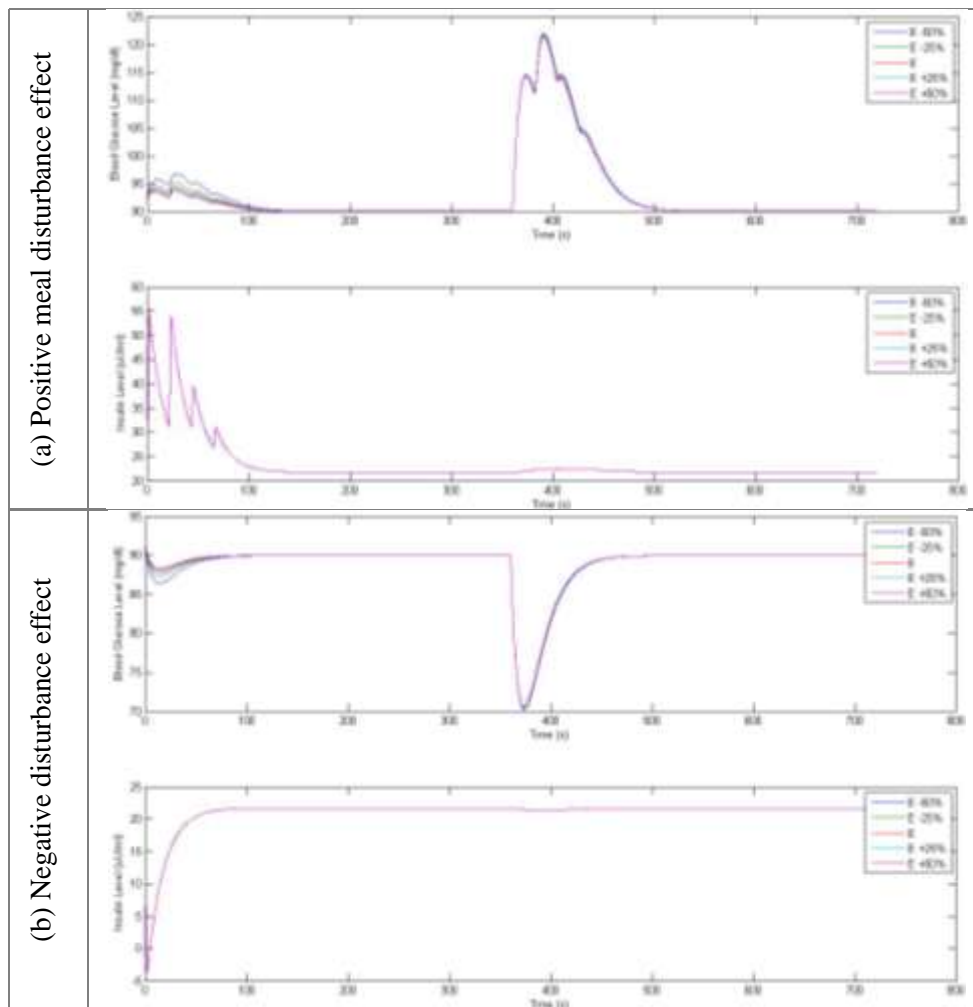
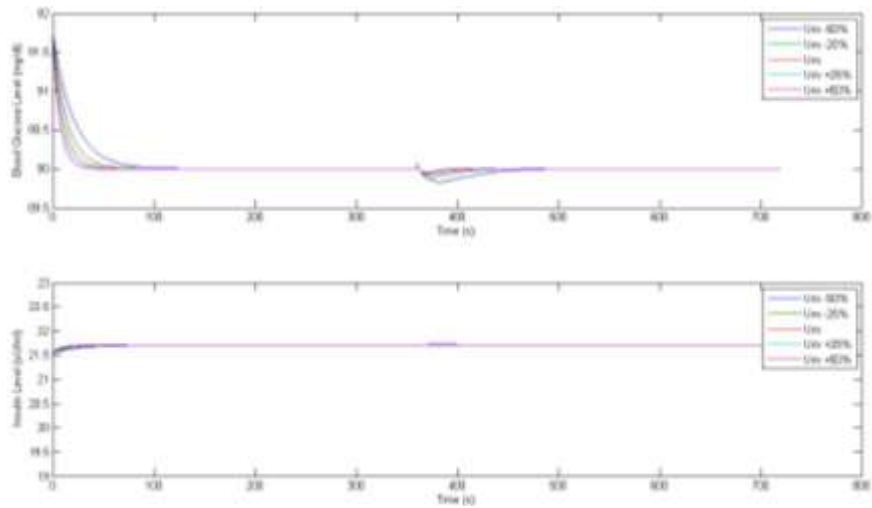
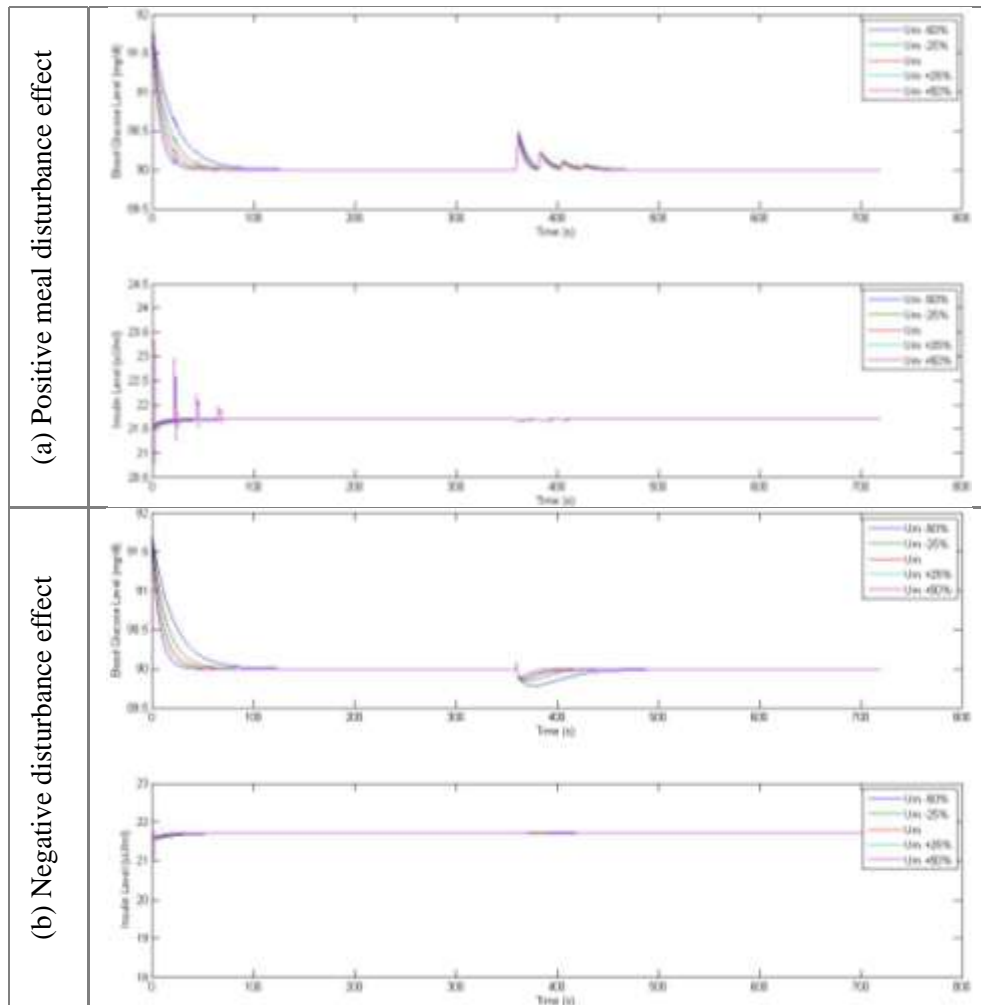


Figure 5.27: Dynamic output feedback with E variation and meal disturbance.

Figure 5.28: State feedback with U_m variation.Figure 5.29: State feedback with U_m variation and meal disturbance.

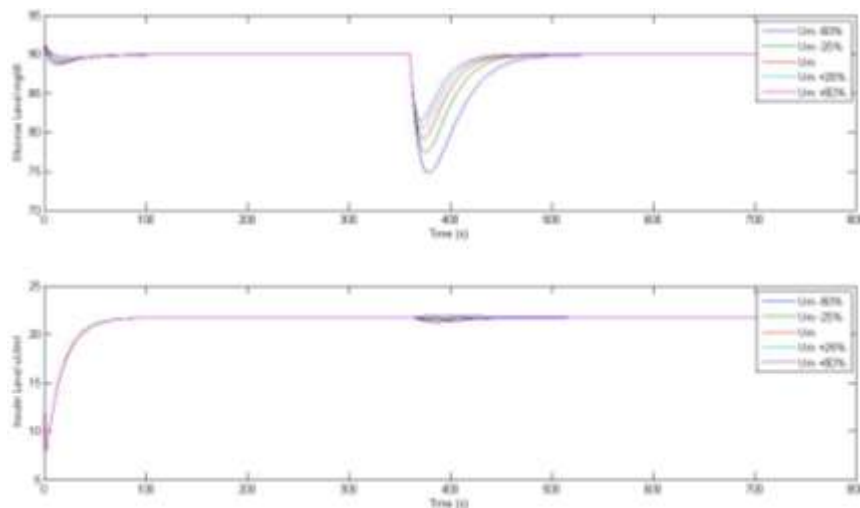


Figure 5.30: Dynamic Output feedback with U_m variation.

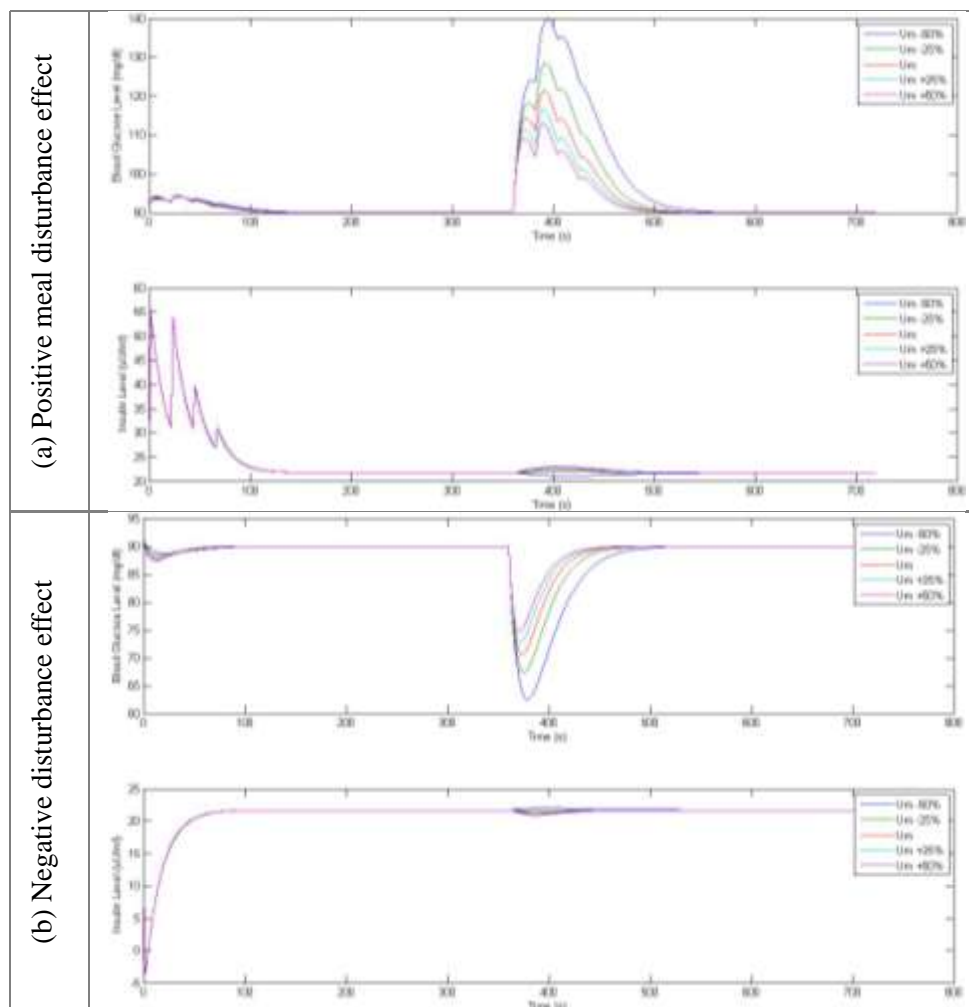


Figure 5.31: Dynamic output feedback with U_m variation and meal disturbance.

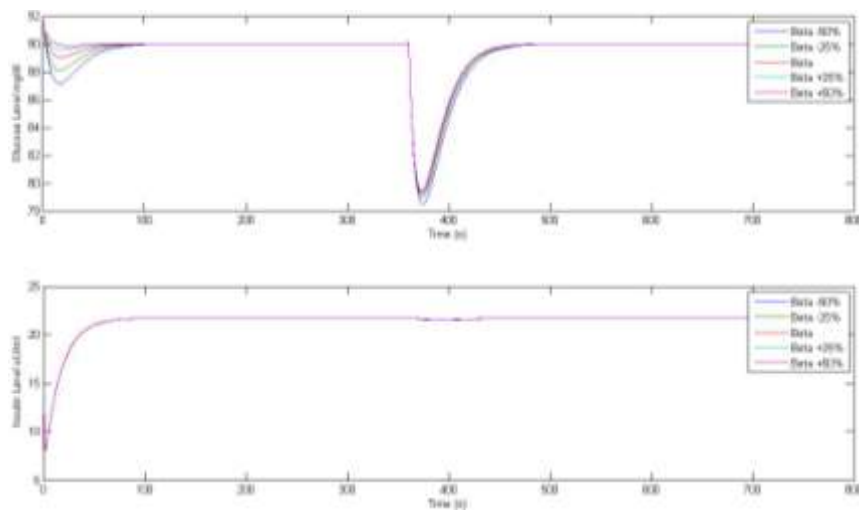


Figure 5.32: Dynamic Output feedback with β_1 variation.

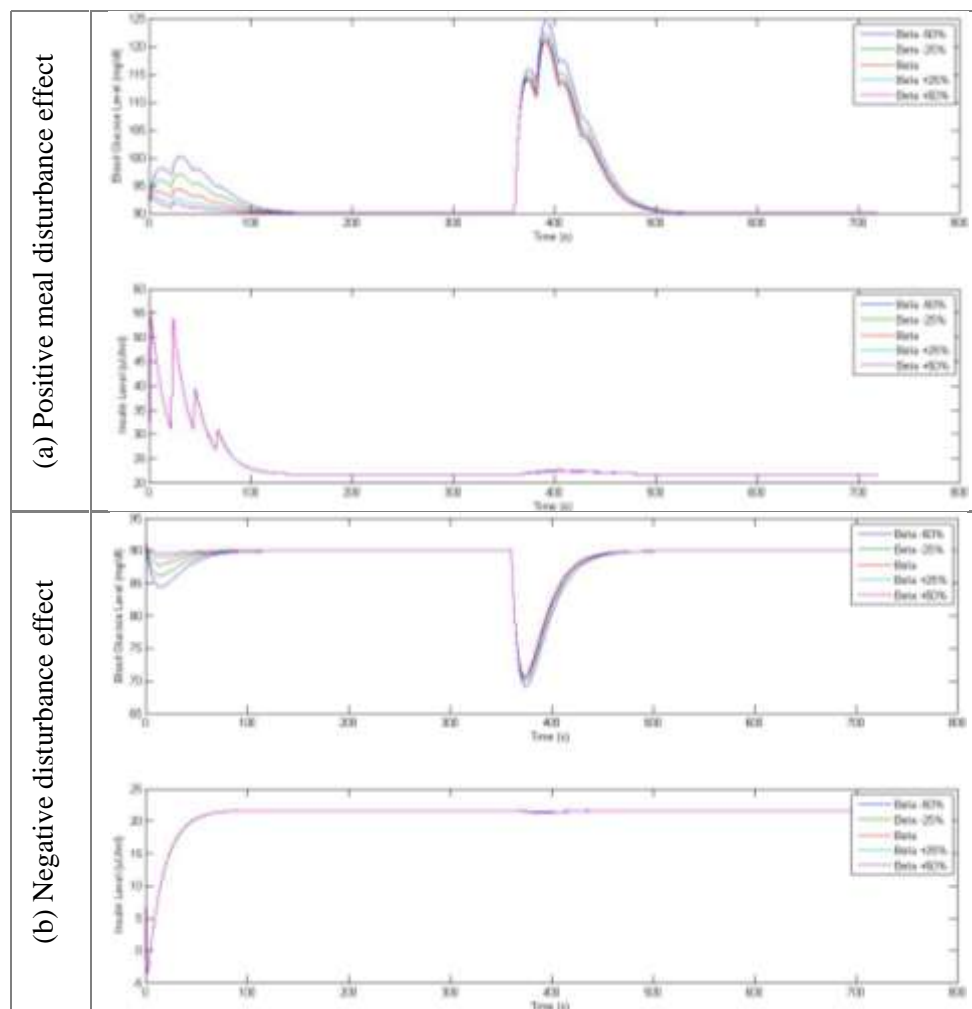
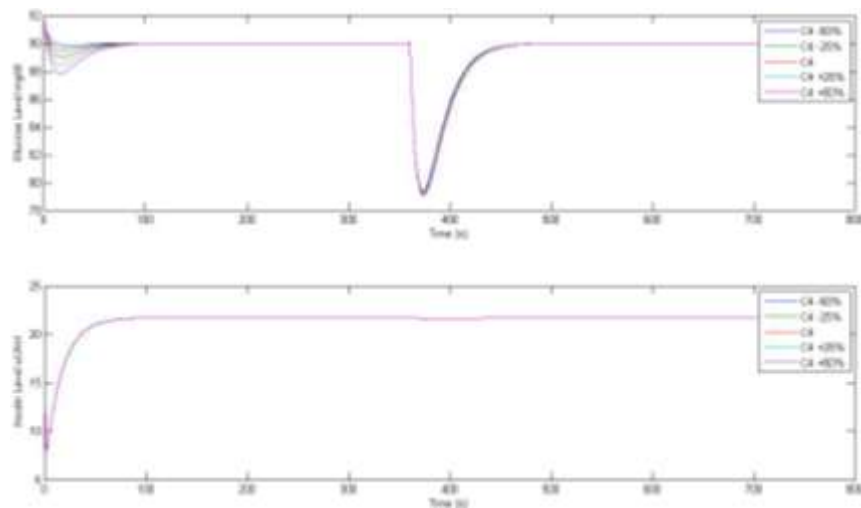
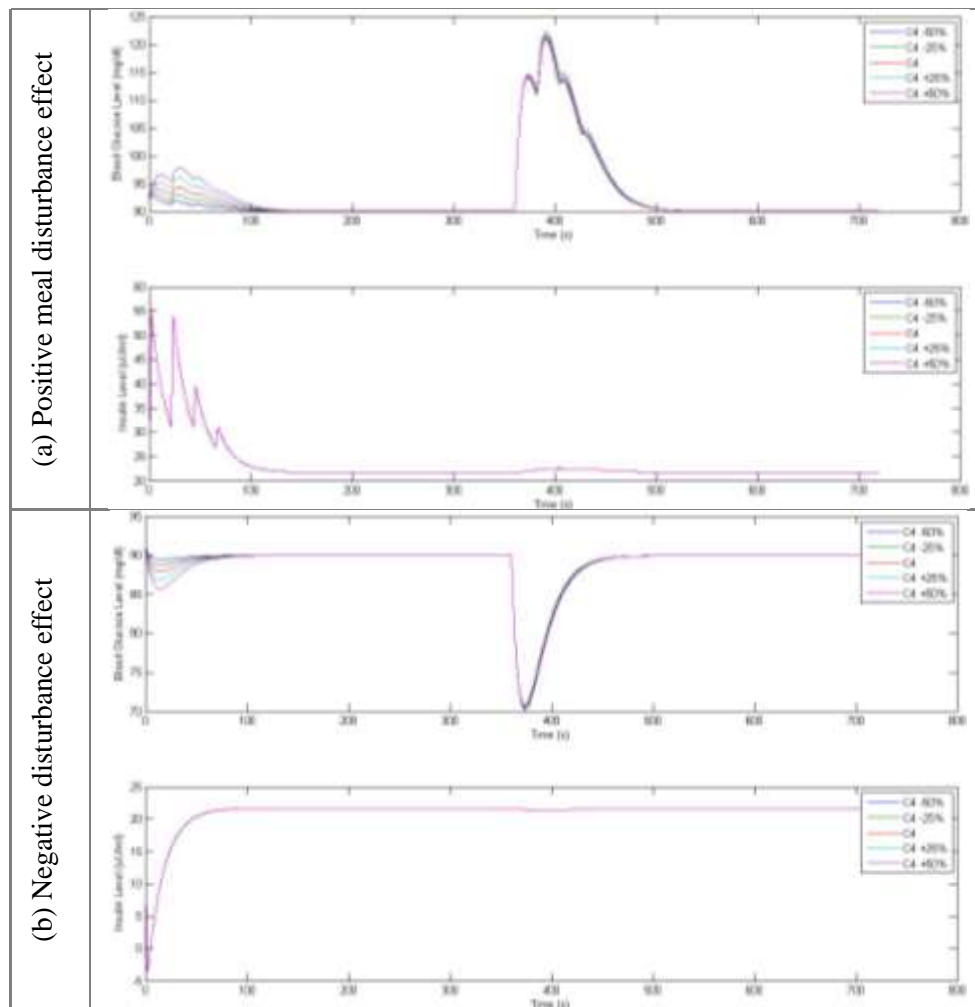
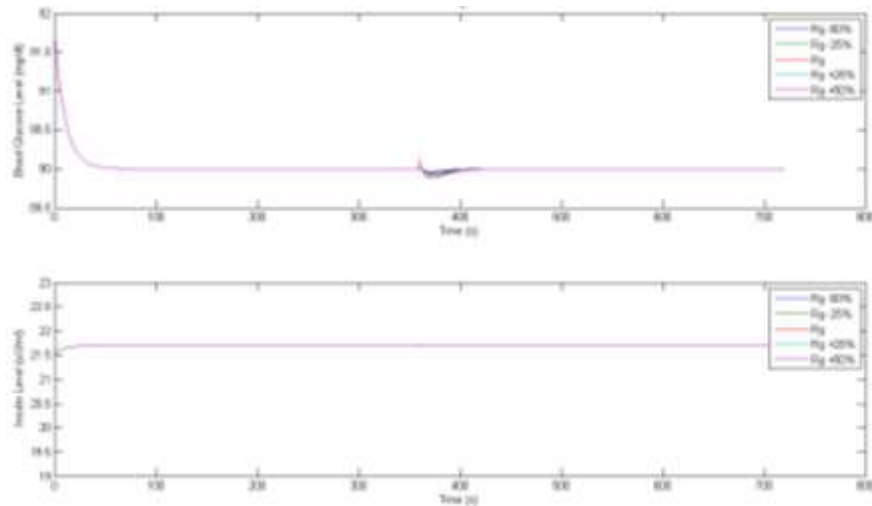
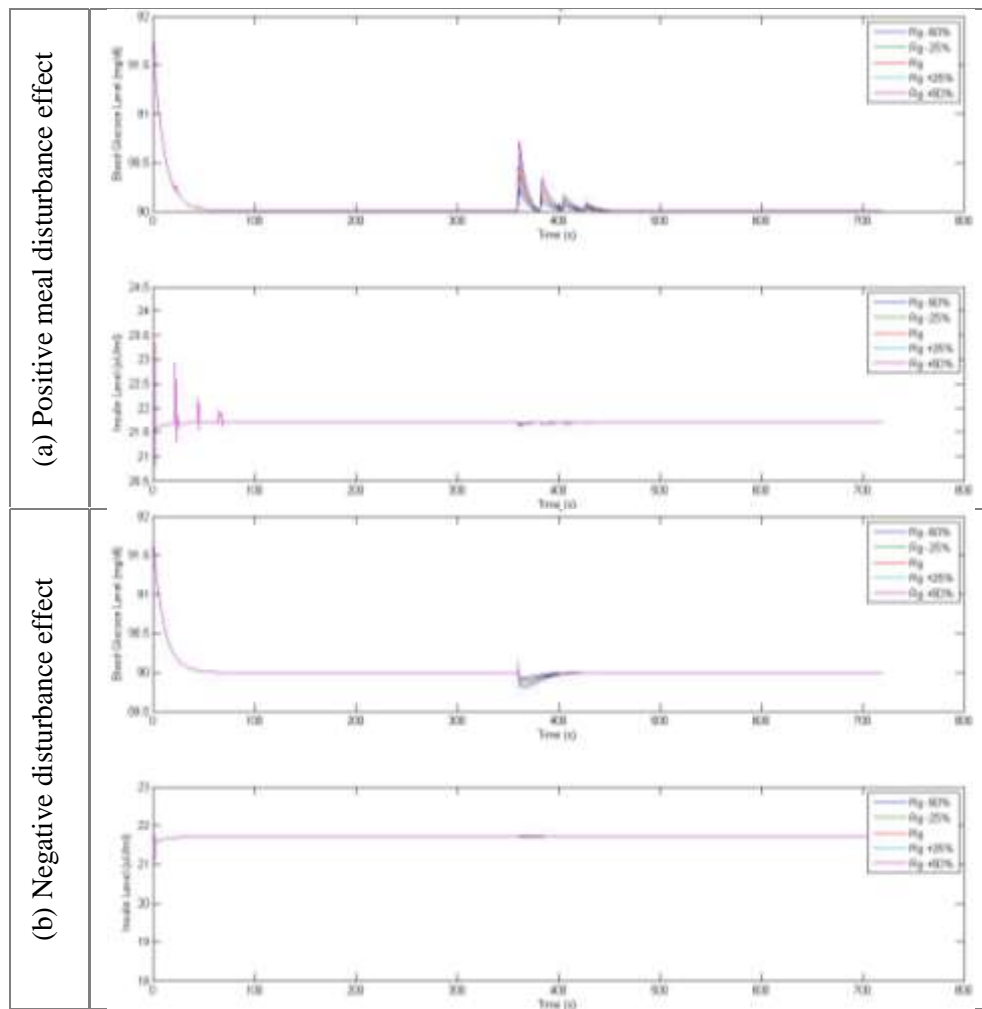


Figure 5.33: Dynamic output feedback with β_1 variation and meal disturbance.

Figure 5.34: Dynamic Output feedback with C_4 variation.Figure 5.35: Dynamic output feedback with C_4 variation and meal disturbance.

Figure 5.36: State feedback with R_g variation.Figure 5.37: State feedback with R_g variation and meal disturbance.

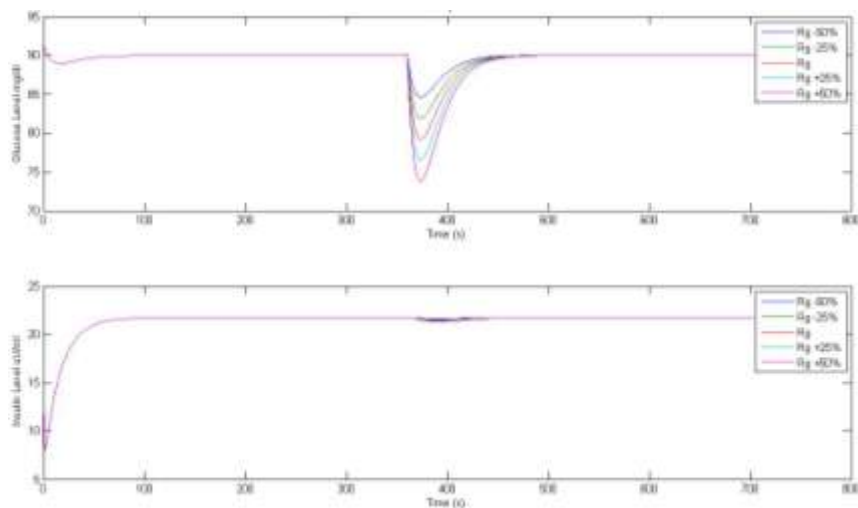


Figure 5.38: Dynamic Output feedback with R_g variation.

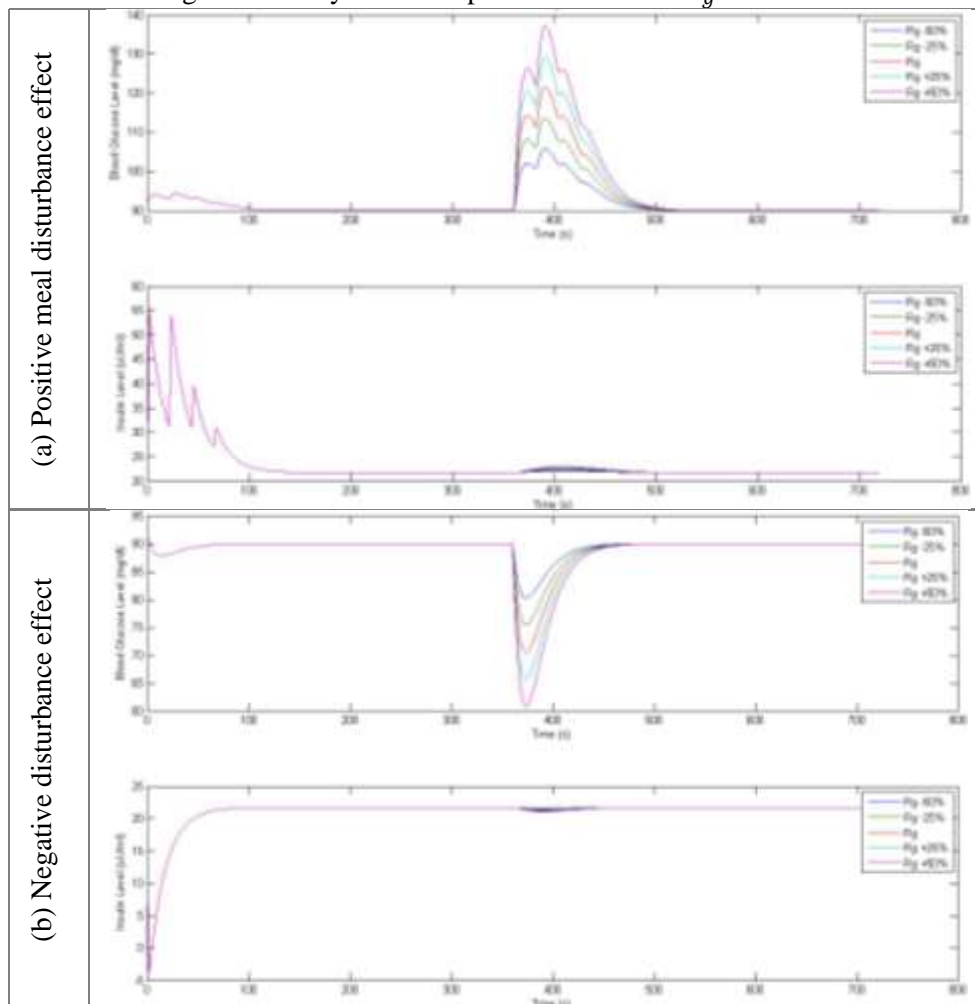
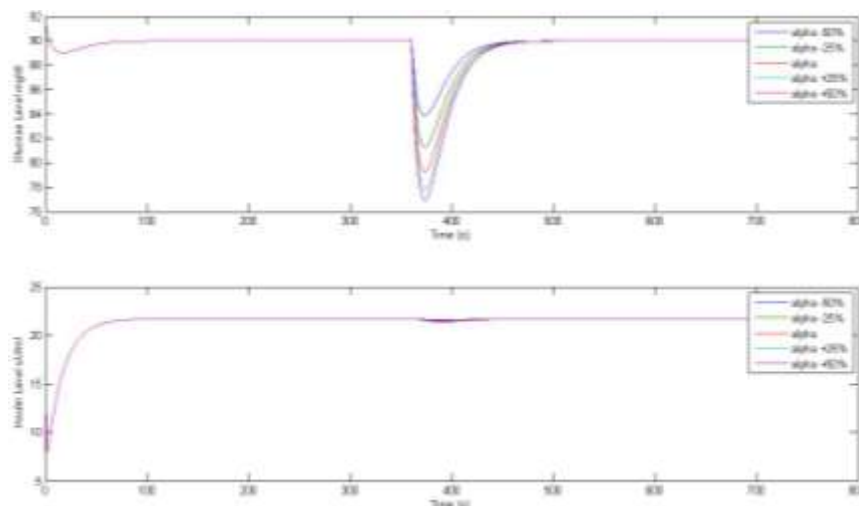
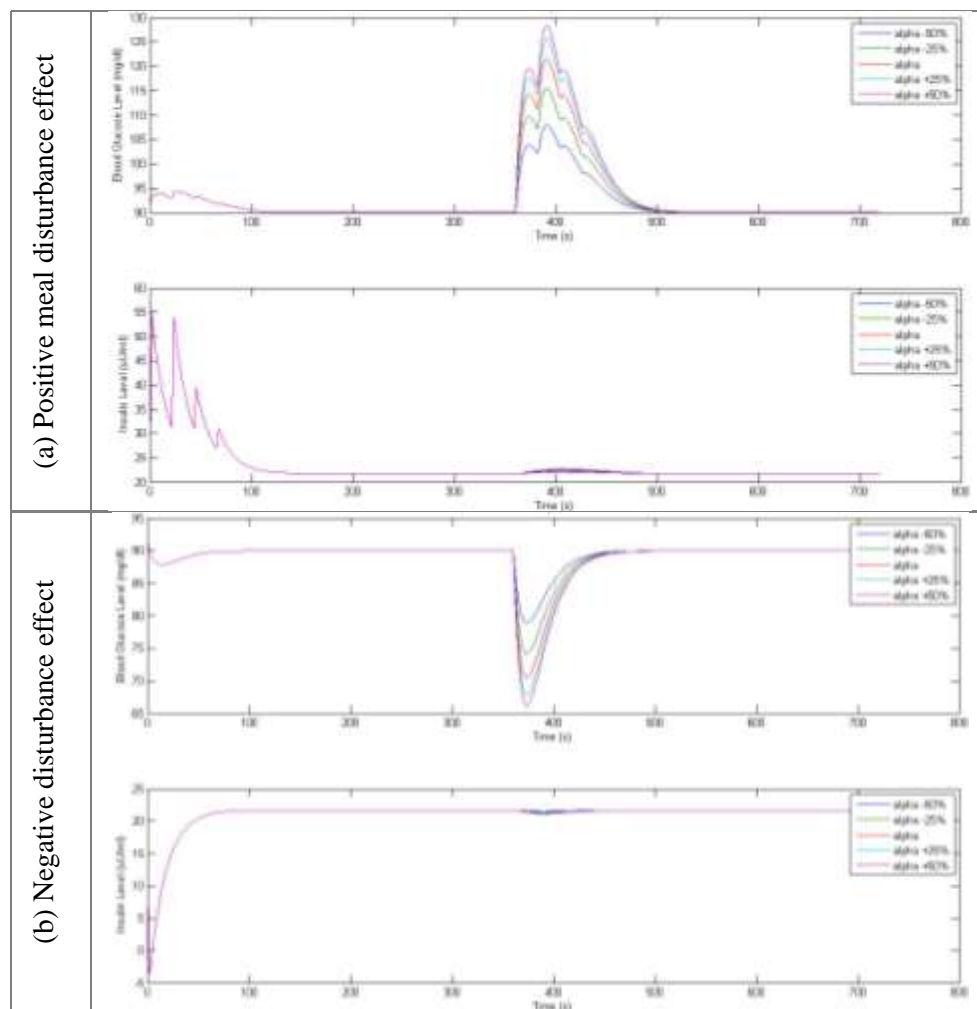
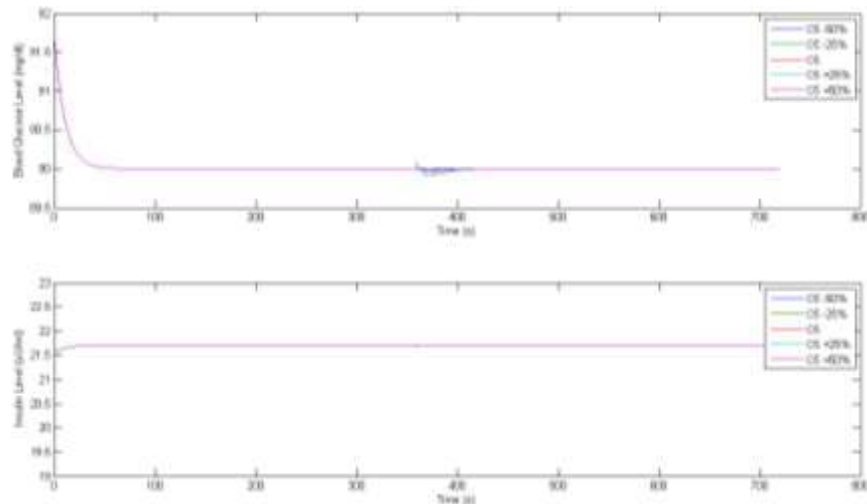
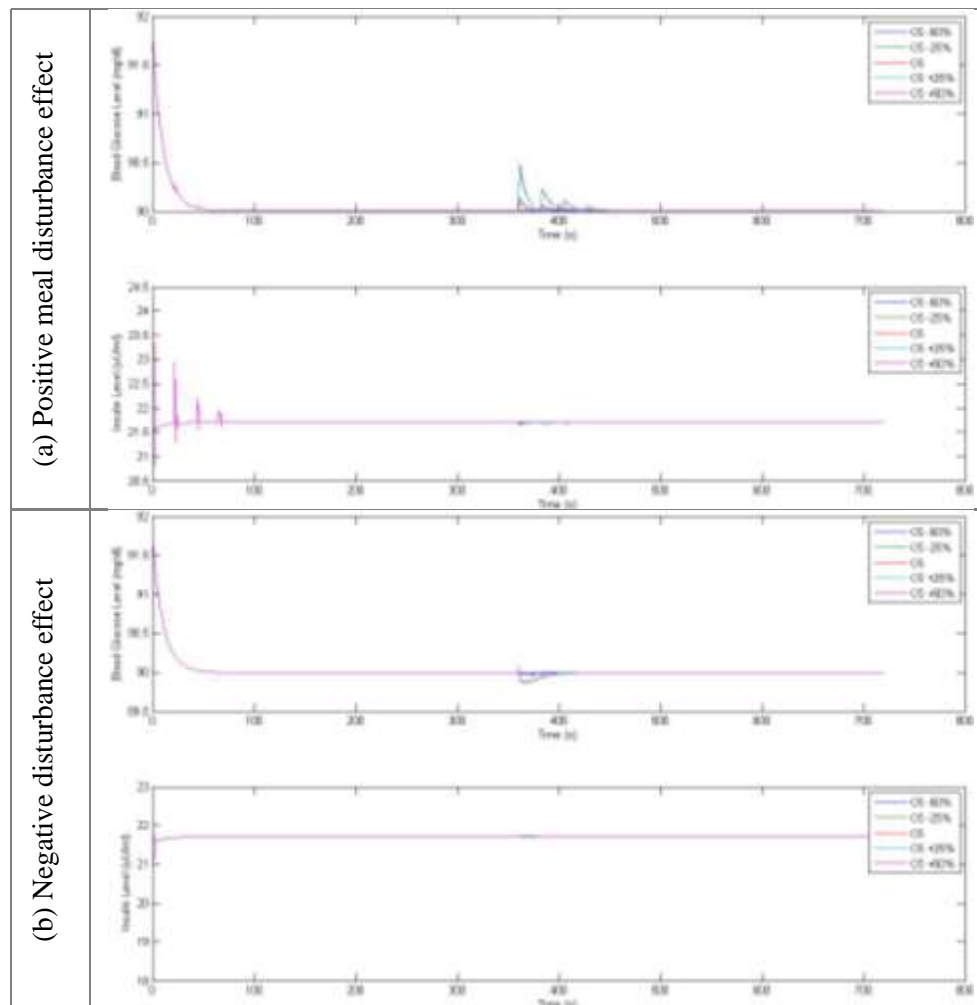


Figure 5.39: Dynamic output feedback with R_g variation and meal disturbance.

Figure 5.40: Dynamic Output feedback with α_1 variation.Figure 5.41: Dynamic output feedback with α_1 variation and meal disturbance.

Figure 5.42: State feedback with C_5 variation.Figure 5.43: State feedback with C_5 variation and meal disturbance.

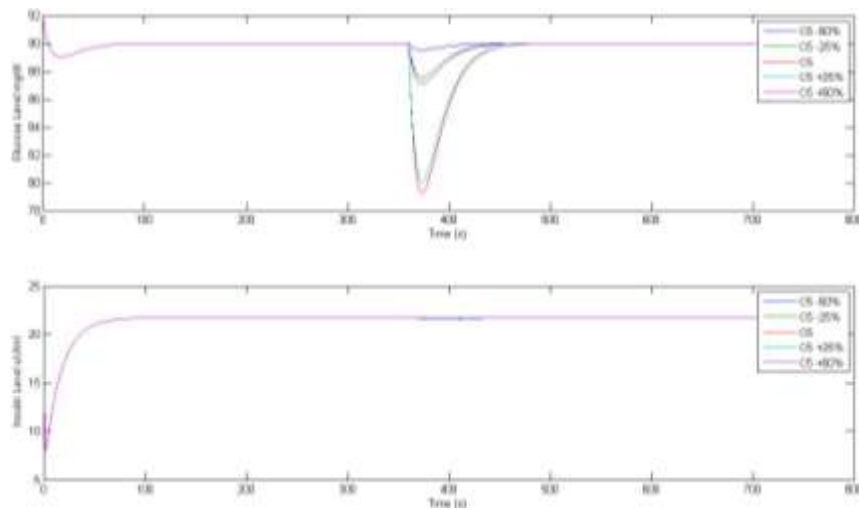


Figure 5.44: Dynamic Output feedback with C_5 variation.

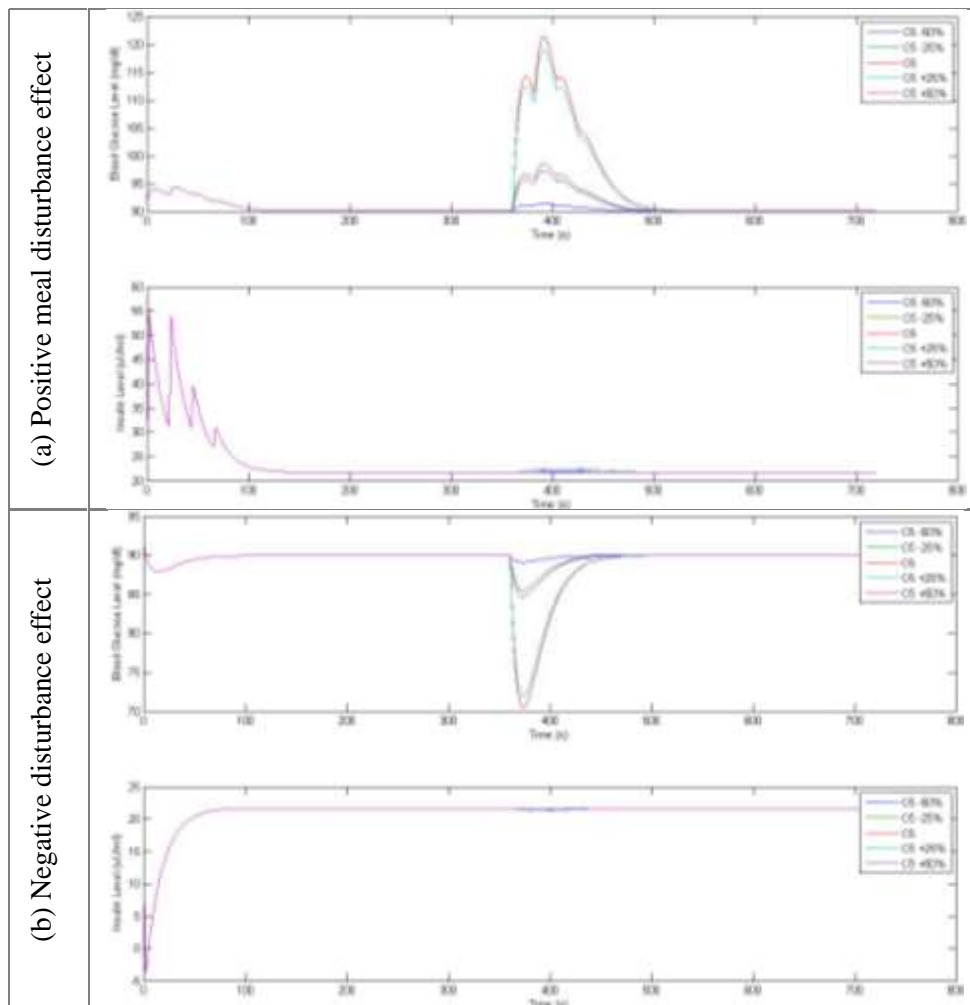


Figure 5.45: Dynamic output feedback with C_5 variation and meal disturbance.

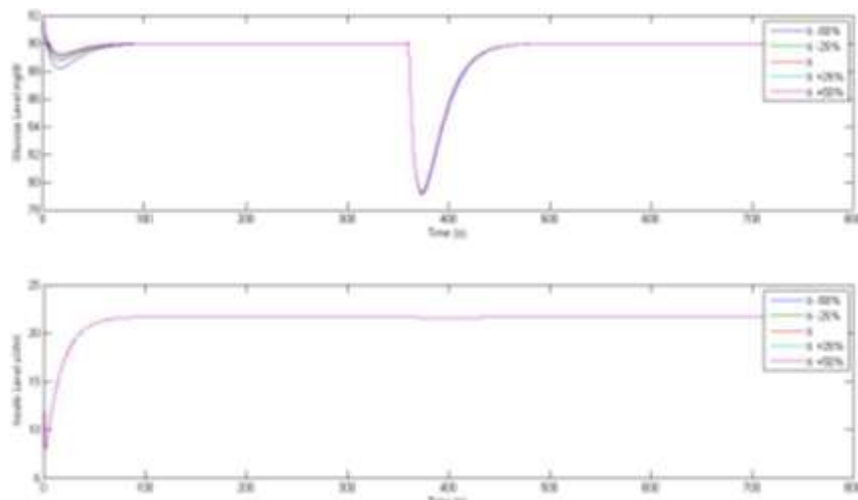


Figure 5.46: Dynamic Output feedback with t_i variation.

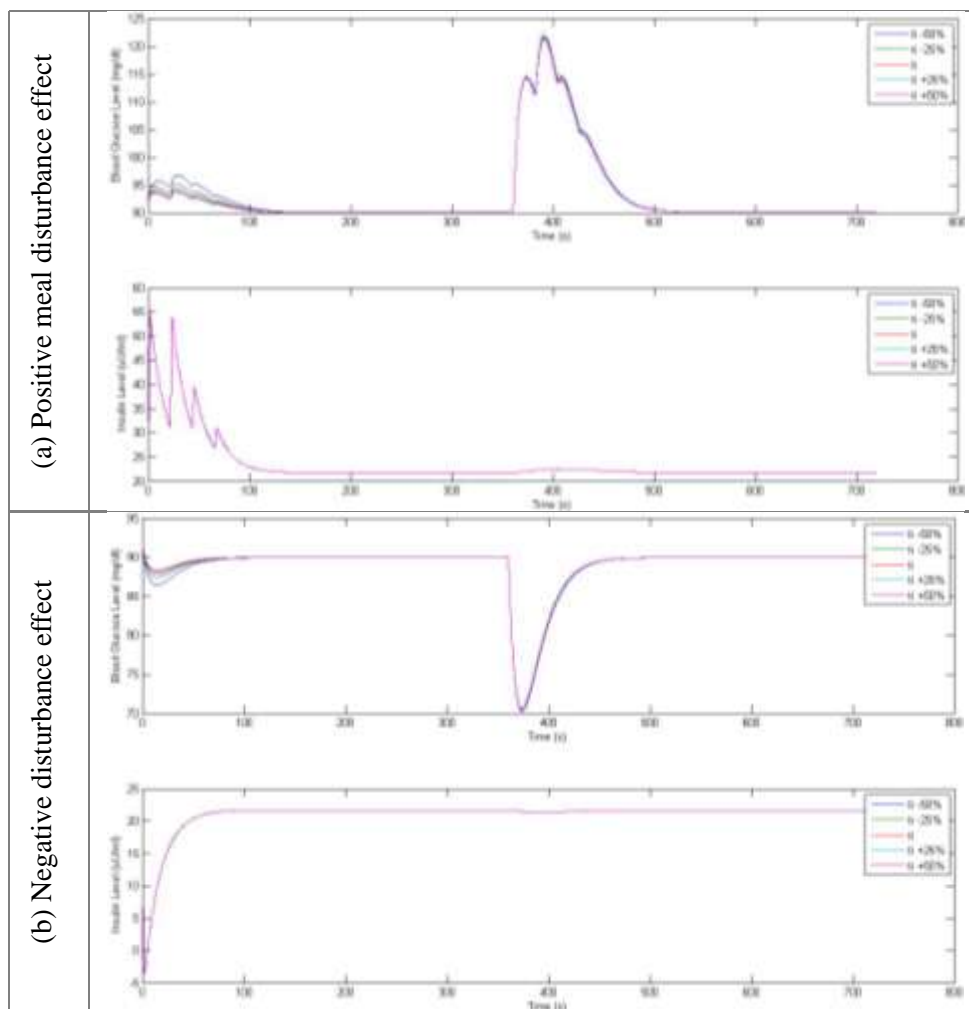


Figure 5.47: Dynamic output feedback with t_i variation and meal disturbance.

5-7 Discussion and Conclusions

It is not easy to use the partially close-loop strategy to control the blood glucose level for type 1 diabetic patient, since it is not easy to maintain the blood glucose level in the Normoglycemia range. Any small variation of the insulin (type, dose, time of injection), and/or carbohydrate (intake dose, intake time) will affect the blood glucose level.

Using Bergman model to control the blood glucose level using MPC technique can do the task. The basal insulin of $26.1\mu\text{U/ml}$ is higher than the nominal value ($22\mu\text{U/ml}$), but still acceptable. The problem of such model is the lack of the delay effect. Moreover, the MPC need for online model identification process that will make the system more complicated, and need to have more memory.

The new developed method for gain stabilizing shows that the internal asymptotic stability has been established and gives satisfactory results and the system found to be feasible for all time delays ($\tau = 5 - 15$ minutes).

The open-loop simulation for the system shows that the system output level is uncontrolled. Hence we have introduced new feedback strategies: State Feedback and the Dynamic Output Feedback. Both control strategies found to be feasible using 0.1 second sampling time for all time delays.

Using 6 minutes delay time we found that the disturbance rejection ratio level (γ) for the State Feedback is higher than 1 ($\gamma_{SF} = 2.5930$). Hence we have used Dynamic Output Feedback to this rejection ratio level ($\gamma_{DOF} = 0.8882$). Note that the disturbance rejection ratio level found here is comes from the LMI simulation not from the system itself.

The State Feedback control gain (K_s), and the Dynamic Output Feedback control gains (K_c and K_o) found to have reasonable values. As conclusion: the use of any developed controller can stabilize the blood glucose level into the Normoglycemia range.

The insulin, input state, response for the State Feedback found to be much better than that for the Dynamic Output Feedback. The basal insulin of $21.71\mu\text{U/ml}$ is very close to the nominal value ($22\mu\text{U/ml}$).

Robustness test for the system for parameter variation and external disturbance have shown excellent results. The State Feedback control strategy has shown superior results over that of the Dynamic Output Feedback control. For this reason we have considered the worst case using the Dynamic Output Feedback strategy: the maximum output, blood glucose level, for the system under parameters U_m , R_g , (V_g or C_3) variation and positive disturbance was (140, 138, 132) mg/dl respectively, while the minimum output under the parameters U_m , R_g , (V_g or C_3) variation and negative disturbance was (62, 61, 66) mg/dl respectively.

To explain why the output was high, low, or no change due to some parameters variation, we have to consider the parameter itself and what it is the functional effect. This can be summarizes as:

- 1- R_m , a_1 , and C_1 are $f_1(G)$ parameters. $f_1(G)$ is pancreatic insulin production as controlled by the glucose concentration. Since Type-1 diabetic patient have problems with the pancreatic insulin production, thus the effect of $f_1(G)$ parameters variation have negligible and minor effects.

- 2- C_2 and U_b are $f_2(G)$ parameters. $f_2(G)$ is the insulin independent glucose consumption by the brain, nerve cells and others. This consumption is very much smaller than that due to glucose consumption by muscles during exercises or normal day work. Thus changing of these parameters have no effects on the blood glucose level.
- 3- V_i , β_1 , E , C_3 , C_4 , t_i , U_m , and V_g are $f_3(G)$ and $f_4(I)$ parameters. $f_3(G)f_4(I)$ is a nonlinear term that stands for the relation of insulin-dependent glucose-utilization by muscle, fat cells and others. Since these functions are delay independent, any variation of these parameters has a direct effect on the glucose concentration at the transient time before the start of the delay. The system response after the delay have minor effects.
- 4- α_1 , R_g , C_5 , and V_p are $f_5(I)$ parameters. $f_5(I)$ characterize the hepatic glucose production. Changing any of these parameters will affect the conversion process of the stored sugar and fat into glucose. Afterward, the produced glucose will be sent to the blood which, in turn, affects blood glucose level. Since $f_5(I - \tau)$ is delay dependent function, it is clear from the figures that the effect of all these parameters is clear after the delay. The system response under parameters variation was identical for all the cases before the delay.

For all the cases, the input was able to control the output and keep it in the normal range during positive or negative disturbance. Consequently, varying the glucose concentration due to parameter variations will force the insulin concentration to vary in the same direction to compensate for these variations.

5-8 Future research topics

To improve the quality of this work and increase the blood glucose controller efficiency, State Feedback controller and/or Dynamic Output controller are suggested to be developed and tested for model with two time delays. Research and development of MPC for the models with time delay (one and/or two) is recommended.

This work was evaluated based on computer simulation only and not tested on any patient. For this reason, I suggest to start the cooperation between control people, diabetic research centers, pilot hospitals, Health care information technology centers, and voluntaries or patients. Public institutes and society organizations should provide the logistic support for such researches.

Diabetic research centers and mathematical research groups must work together such that they will be able to develop new models which are more accurate representing the real patient.

Control people have to do the following:

- 1- Develop new models using Identification techniques.
- 2- Design stable and robust controller for this new models.

Information technology will play important role to contributing to these activities by providing the real patient data and make it available for the above to research groups.

The functions of the pilot hospitals are:

- 1- Provide the clinical care for the patients under test.
- 2- Evaluate the controller results, stability, robustness, and accuracy.

NOMENCLATURE

$x(t)$: the state vector ($\in \mathfrak{R}^n$)

$y(t)$ the measured output vector($\in \mathfrak{R}^p$)

$u(t)$: the control input vector ($\in \mathfrak{R}^m$)

$w(t)$:the disturbance input vector ($\in \mathfrak{R}^q$) which belongs to $\mathcal{L}_2 [0, \infty)$

$w(\phi)$:the initial conditions ($\in \mathfrak{R}^q$)

$z(t)$: the controlled output vector ($\in \mathfrak{R}^q$)

t : time

τ : the fixed time-delay factor

ϕ : a differentiable vector-valued function on $[-\tau, 0]$

A_o : the System matrix ($\in \mathfrak{R}^{n \times n}$)

A_{do} : the delayed states matrix ($\in \mathfrak{R}^{n \times n}$)

B_o : the inputs matrix ($\in \mathfrak{R}^{n \times m}$)

G_o : the disturbance matrix ($\in \mathfrak{R}^{q \times n}$)

D_o : the matrix relates the inputs to the controlled outputs ($\in \mathfrak{R}^{q \times m}$)

Φ_o : the matrix that relates the disturbances to the controlled outputs ($\in \mathfrak{R}^{q \times q}$)

Γ_o : the matrix that relates the states to the controlled outputs ($\in \mathfrak{R}^{n \times q}$)

C_o : the matrix that relates the states to the outputs ($\in \mathfrak{R}^{p \times n}$)

C_{do} : the matrix that relates the delayed states to the outputs ($\in \mathfrak{R}^{p \times n}$)

F_o : the matrix that relates the inputs to the outputs ($\in \mathfrak{R}^{p \times m}$)

ψ_o : the matrix that relates the disturbances to the outputs ($\in \mathfrak{R}^{p \times q}$)

BIBLIOGRAPHY

1. **Roman H.** Management of diabetes using adaptive control. 2005, Vol. 19, pp. 309–325.
2. <http://www.diabetes.org/>. [Online]
3. <http://diabetes.niddk.nih.gov/dm/pubs/americanindian>. [Online]
4. **The Diabetic Control and Complications Trial Research Group.** The effect of intensive treatment of diabetes on the development and progression of long term complications in insulin-dependent diabetes mellitus. 1993, Vol. 329, pp. 977–986.
5. **Jiaxu L.** *The Dynamics Of Glucose-Insulin Endocrine Metabolic Regulatory System*. Arizona State University. 2004. A Dissertation Presented In Partial Fulfillment Of The Requirements For The Degree Doctor Of Philosophy.
6. **Rossetti L.** Glucose toxicity: the implications of hyperglycemia in the pathophysiology of diabetes mellitus. 1995, Vol. 18, pp. 255–260.
7. **Bergman N., Finegood T., and Kahn R.** The evolution of beta-cell dysfunction and insulin resistance in type 2 diabetes. 2002, Vol. 32, 3, pp. 35–45.
8. **Brian T., Keith P., Gerda D., Robert M., and Diane F.** A Model of β Cell Mass, Insulin, and Glucose Kinetics: Pathways to Diabetes. 2000, Vol. 206, pp. 605–619.
9. **Bonner-Weir S., Deery D., Leahy L., and Weir C.** Compensatory growth of pancreatic β -cells in adult rats after short-term glucose infusion. 1989, Vol. 38, pp. 49–53.
10. **Kizilel S., Garfinkel M., and Opara E.** *The Bioartificial Pancreas: Progress and Challenges*. s.l. : Mary Ann Liebert, Inc, 2005. Vol. 7.
11. **Doyle F., Jovanovic L., and Seborg D.** Opportunities for Control in Type 1 Diabetes. 2006.
12. **Haiyan W., Jiaxu L., and Yang K.** *Enhanced Modeling of The Glucose-Insulin System And Its Applications In Insulin Therapies*. Dedicated to Professor Ken Cooke.
13. **Sorensen T.** *A physiologic model of glucose metabolism in man and its use to design and assess improved insulin therapies for diabetes*. Chem. Eng., MIT. 1985. Ph.D. thesis.
14. **Tierney J., Tamada A., Potts O., Jovanovic L., Garg S., and the Cygnus Research Team.** Clinical evaluation of the GlucoWatch biographer: a continual,

- noninvasive glucose monitor for patients with diabetes. 2001, Vol. 16, pp. 621-629.
15. **Parker R., Doyle F., and Peppas N.** The Intravenous Route to Blood Glucose Control, A Review of Control Algorithms for Noninvasive Monitoring and Regulation in Type 1 Diabetic Patients. 2001, pp. 65-73.
 16. **Athena M., Jiaxu L., and Yang K.** Mathematical models and software tools for the glucose-insulin regulatory system and diabetes: an overview. 2006, Vol. 56, pp. 559-573.
 17. **Bertram R., Satin L., Zhang M., Smolen P., and Sherman A.** Calcium and glycolysis mediate multiple bursting modes in pancreatic islets. 2004, Vol. 87, pp. 3074-3087.
 18. **Poksen N., Hollingdal M., Juhl C., Butler P., Veldhuis D., and Schmitz O.** Pulsatile insulin secretion, regulation, and role in diabetes. 2002, Vol. 51, 1, pp. 245-254.
 19. **Simon C. and Brandenberger G.** Ultradian oscillations of insulin secretion in humans. 2002, Vol. 51, 1, pp. 258-261.
 20. **Sturis J., Polonsky S., Mosekilde E., and Van Cauter E.** Computer-model for mechanisms underlying ultradian oscillations of insulin and glucose. 1991, Vol. 260, pp. 801-809.
 21. **Bolie W.** Coefficients of normal blood glucose regulation. 1961, Vol. 16, pp. 783-788.
 22. **Bergman N., Ider Z., Bowden R., and Cobelli C.** Quantitative estimation of insulin sensitivity. 1979, Vol. 236, 6, pp. 667-677.
 23. **Martin C., Warram H., Krolewski S., Bergman N., Soeldner S., and Kahn R.** Role of glucose and insulin resistance in development of type 2 diabetes mellitus: results of a 25-year follow-up study. 1992, Vol. 340, pp. 925-929.
 24. **Bellazzi R., Nucci G., and Cobelli C.** The subcutaneous route to Insulin-Dependent Diabetes Therapy: closed-loop and partially closed-loop strategies in insulin dependent diabetes mellitus. *IEEE Eng. In Medicine and Biology Magazine*. 2001, pp. 54-64.
 25. **Daugherty K.** Review of Insulin Therapy. 2004, Vol. 17, 1, pp. 10-19.
 26. **Jaremko J. and Rorstad O.** Advances toward the implantable artificial pancreas for treatment of diabetes. 1998, Vol. 21, pp. 444-450.
 27. **Heise T., Weyer C., Serwas A., Heinrichs S., Osinga J., Roach P., Woodworth J., Gudat U., and Heinemann L.** Time-action profiles of novel premixed preparations of insulin lispro and NPL insulin. 1998, Vol. 21, pp. 800-803.

28. **Lalli C., Ciofetta M., Del Sindaco P., Torlone E., Pampanelli S., Compagnucci P., Cartechini M., Bartocci L., Brunetti P., and Bolli G.** Long-term intensive treatment of type 1 diabetes with the short-acting insulin analog lispro in variable combination with NPH insulin at mealtime. 1999, Vol. 22, pp. 468-477.
29. **Worthington D.** The use of models in the self-management of insulin dependent diabetes mellitus. 1990, Vol. 32, pp. 233-239.
30. **Lehmann E. and Deutsch T.** Compartmental models for glycemic prediction and decision-support in clinical diabetes care: Promise and reality. 1998, Vol. 52, pp. 193-205.
31. **Candas B. and Radziuk J.** An Adaptive Plasma Glucose Controller Based on a Nonlinear Insulin-Glucose Model. 1994, Vol. 41, 2, pp. 116-124.
32. **Kim A. and Malene H.** A Bayesian Approach to Bergman's Minimal Model. <http://research.microsoft.com/conferences/aistats2003/proceedings/183.pdf>.
33. **Pacini G. and Bergman N.** A computer program to calculate insulin sensitivity and pancreatic responsivity from the frequently sampled intravenous glucose tolerance test. 1986, Vol. 23, pp. 113 – 122.
34. **Bergman N.** Pathogenesis and prediction of diabetes mellitus: Lessons from integrative physiology. *Irving L. Schwartz Lecture, Mount Sinai J. Medicine*. 2002, Vol. 60, pp. 280–290.
35. **Engelborghs K., Lemaire V., Belair J., and Roose D.** Numerical bifurcation analysis of delay differential equations arising from physiological modeling. 2001, Vol. 42, pp. 361–385.
36. **Prager R., Wallace P., and Olefsky M.** In vivo kinetics of insulin action on peripheral glucose disposal and hepatic glucose output in normal and obese subjects. 1987, Vol. 78, pp. 472-481.
37. **Yang J., Hope D., Ader M., and Bergman N.** Insulin transport across capillaries is rate limiting for insulin action in dogs. 1989, Vol. 84, pp. 1620-1628.
38. **Poulin A., Steil M., Moore M., Ader M., and Bergman N.** Dynamics of glucose production and uptake are more closely related to insulin in hindlimb lymph than in thoracic duct lymph. 1994, Vol. 43, pp. 180-190.
39. **Jiaxu L., Yang K., and Clinton M.** Modeling the glucose–insulin regulatory system and ultradian insulin secretory oscillations with two explicit time delays. 2006.
40. **Bennett L. and Gourley A.** Asymptotic properties of a delay differential equation model for the interaction of glucose with the plasma and interstitial insulin. 2004, Vol. 151, pp. 189–207.

41. **Tolic I., Mosekilde E., and Sturis J.** Modeling the insulin-glucose feedback system: The significance of pulsatile insulin secretion. 2000, Vol. 207, pp. 361–375.
42. **Gaetano D. and Arino O.** Mathematical modeling of the intravenous glucose tolerance test. 2000, Vol. 40, pp. 136–168.
43. **Mukhopadhyay A., De Gaetano A., and Arino O.** Modeling the intra-venous glucose tolerance test: A global study for a single-distributed-delay model. 2004, Vol. 4, 2, pp. 407-417.
44. **Boutayeb A. and Derouich M.** Age structured models for diabetes in East Morocco. 2002, Vol. 58, pp. 215–229.
45. **Boutayeb A. and Twizell E.** An age structured model for complications of diabetes mellitus in Morocco. 2004, Vol. 12, pp. 77–87.
46. **Aslanidi O., Mornev O., Vesterager M., Sorensen M., and Christiansen P.** A model for glucose-induced wave propagation in pancreatic islets of Langerhans. 2002, Vol. 215, pp. 273–286.
47. **Wach P., Trajanoski Z., Kotanko P., and Skrabal F.** Numerical approximation of mathematical model for absorption of subcutaneously injected insulin. 1995, Vol. 33, 1, pp. 18-23.
48. **Keener P.** Diffusion induced oscillatory insulin secretion. 2001, Vol. 63, pp. 625–641.
49. **Maki W. and Keizer J.** Mathematical analysis of a proposed mechanism for oscillatory insulin secretion in perfused HIT-15 cells. 1995, Vol. 57, pp. 569–591.
50. **The Diabetes Control and Complication Trial Research Group.** Resource utilization and costs of care in the diabetes control and complication trial. 1995, Vol. 18, pp. 1468-1478.
51. **Shimoda S., Nishida K., Sakakida M., Konno Y., Ichinoshi K., Urkhara M., Nowak T., and Shichiri M.** Closed-loop subcutaneous insulin infusion algorithm with a short acting insulin analog for long-term clinical application of a wearable artificial endocrine pancreas. 1997, Vol. 8, pp. 197-211.
52. **Trajanoski Z., Brunner G., Schaupp L., Ellmerer M., Wach P., Pieber T., Kotanko P., and Skrabal F.** Open-flow microperfusion of subcutaneous adipose tissue for on-line continuous ex vivo measurement of glucose concentration. 1997, Vol. 20, pp. 1114-1121.
53. **Trajanoski Z. and Wach P.** Neural Predictive Controller for Insulin Delivery using the Subcutaneous Route. 1998, Vol. 45, pp. 1122-1134.

54. **Meyerhoff C., Bischof F., Sternberg F., Zier H., and Pfeiffer F.** On line continuous monitoring of subcutaneous tissue glucose in men by combining portable glucosensor with microdialysis. 1992, Vol. 35, pp. 1087-1092.
55. **Brange J., Owens D., Kang S., and Volund A.** Monomeric insulins and their experimental and clinical implications. 1990, Vol. 13, pp. 923-954.
56. **Lee S. and Lee J.** A model predictive control technique for batch processes and its application to temperature tracking control of an experimental batch reactor. 1999, Vol. 10, pp. 2175-2187.
57. **Zisser H., Jovanovic L., Doyle F., Ospina P., and Owens C.** Run-to-run control of meal related insulin dosing. 2005, Vol. 7, pp. 48-57.
58. **Owens C., Zisser H., Jovanovic L., Srinivasan B., Bonvin D., and Doyle F.** Run to-run control of blood glucose concentrations for people with type 1 diabetes mellitus. 2006 in press.
59. **Srinivasan B. and Primus J.** Run to run optimization via constraint control. 2000, pp. 797-802.
60. **Fabietti P., Massi Benedetti M., Bronzo F., Reboldi G., Sarti E., and Brunetti P.** Wearable system for acquisition, processing and storage of the signal from amperometric glucose sensors. 1991, Vol. 14, pp. 175-178.
61. **Brunetti P., Cobelli C., Cruciani P., Fabietti P., Filipucci F., Santeusano F., and Sarti E.** A simulation study on a self-tuning portable controller of blood glucose. 1993, Vol. 16, pp. 51-57.
62. **Alejandro G., Agustin C., Alexander P., and Tatiana P.** The Bergman's Insulin-Glucose Regulation Model: DNN-state Observer. July 23-28 2000.
63. **Khoo K.** Physiological Control Systems, Analysis, Simulation, and Estimation. 2000, pp. 190-196.
64. **Shichiri M., Sakakida M., Nishida K., and Shimoda S.** Enhanced, simplified glucose sensors: Long-term clinical application of wearable artificial pancreas. 1998, Vol. 22, pp. 32-42.
65. **Hashiguchi Y., Sakakida M., Nishida K., Uemura T., Kajiwarra K., and Shichiri M.** Development of a miniaturized glucose monitoring system by combining a needle-type glucose sensor with microdialysis sampling method. Long-term subcutaneous tissue glucose monitoring in ambulatory diabetic patients. *Diabetes Care*. 1994, Vol. 17, pp. 387-396.
66. **Kikuchi M., Machiyama E., Kabei N., Yamada A., and Sakurai Y.** Homeostat to control blood glucose level. 1978, pp. 541-545.
67. **Kikuchi M., Machiyama E., Kabei N., Yamada A., Sakurai Y., Hara Y., and Sano A.** Adaptive control system of blood glucose regulation. 1980, Vol. 80, pp. 96-100.

68. **Swan G.** An optimal control model of diabetes mellitus. 1982, Vol. 44, pp. 793-808.
69. **Fisher M. and Teo K.** Optimal insulin infusion resulting from a mathematical model of blood glucose dynamics. 1989, Vol. 36, pp. 479-486.
70. **Ollerton L.** Application of optimal control theory to diabetes mellitus. 1989, Vol. 50, pp. 2503-2522.
71. **Fisher E.** A semiclosed-loop algorithm for the control of blood glucose levels in diabetics. 1991, Vol. 38, pp. 57-61.
72. **Kienitz K. and Yoneyama T.** A controller for insulin pumps based on H-infinity theory. 1993, Vol. 40, pp. 1133-1137.
73. **Hovorka R., Canonico V., Chassin L., Haueter U., Massi-Benedetti M., Federic M.i, Pieber T., Schaller H., Schaupp L., Vering T., and Wilinska M.** Nonlinear model predictive control of glucose concentration in subjects with type 1 diabetes. 2004, Vol. 25, 4, pp. 905-920.
74. **Fisher U., Schenk W., Salzsieder E., Albrecht G., Abel P., and Freyse E.** Does physiological blood glucose control require an adaptive strategy. 1987, Vol. 34, pp. 575-582.
75. **Bequette W.** A critical assessment of algorithms and challenges in the development of a closed-loop artificial pancreas. 2005, Vol. 7, 1, pp. 28-47.
76. **Steil G., Panteleon A., and Rebrin K.** Closed-loop insulin delivery, the path to physiological glucose control. 2000, Vol. 56, pp. 125-144.
77. **Parker R. and Doyle F.** A model-based algorithm for blood glucose control in type 1 diabetic patients. 1999, Vol. 46, pp. 148-157.
78. **Hejlesen O., Andreassen S., Frandsen N., Sorensen T., Sando S., Hovorka R., and Cavan D.** Using a double blind controlled clinical trial to evaluate the function of a diabetes advisory system: A feasible approach. 1998, Vol. 52, pp. 165-173.
79. **Pearl J.** *Probabilistic Reasoning in Intelligent Systems*. New York : Morgan Kauffman, 1988.
80. **A. Zadeh.** Fuzzy sets. Information and control. 1965, Vol. 8, pp. 338-353.
81. **A. Zadeh.** Outline of a new approach to the analysis of complex systems. *IEEE Transactions on System*. 1973, Vol. 3, pp. 28-44.
82. **Davide D., Francesco T., Alessandra G., Enzo U., Roberto N., and Antonio P.** The control of blood glucose in the critical diabetic patient A neuro-fuzzy method. *Journal of Diabetes and Its Complications*. 2001, Vol. 15, pp. 80-87.
83. **Campos-Delgado D., Hernández-Ordoñez M., Femat R., and Gordillo-Moscoso A.** Fuzzy-Based Controller for Glucose Regulation in Type-1 Diabetic

- Patients by Subcutaneous Route. *IEEE TRANSACTIONS ON BIOMEDICAL ENGINEERING*. 2006, Vol. 53, 11, pp. 2201-2210.
84. **Ibbini M.** PI-fuzzy, logic controller for the regulation of blood glucose level in diabetic patients. *Med Eng Technol*. 2006, Vol. 30, 2, pp. 83–92.
 85. *Active Insulin Infusion Using Fuzzy-Based Closed-loop Control*. **Yasini Sh., Naghibi-Sistani M. B., and Karimpour A.** [ed.] IEEE. 2008. Proceedings of 3rd International Conference on Intelligent System and Knowledge Engineering. pp. 429-434.
 86. **Pascal G., Arkadi N., Alan .L., and Mahmoud C.** LMI Control Toolbox For Use with MATLAB User's Guide. 1.
 87. **Scherer C.** H_∞ Optimization without Assumptions on Finite or Infinite Zeros. *SIAM Journal of Control and Optimization*. 1992, Vols. 143–166, pp. 143–166.
 88. **Boyd S., El Ghaoui L., Feron E., and Balakrishnan V. .** Linear Matrix Inequalities in Systems and Control Theory. *SIAM books*. 1994.
 89. **Chilali M. and Gahinet P.** H_∞ Design with Pole Placement Constraints: an LMI Approach. *Proc. Conf. Dec. Contr.* 1994, pp. 553–558.
 90. **Khargonekar P. and Rotea M.A.** Mixed H_2/H_∞ Control: A Convex Optimization Approach. *IEEE Trans. Aut. Contr.* 1991, Vol. 39, pp. 824-837.
 91. **Boukas K. and Liu K.** Deterministic and Stochastic Time-delay Systems. *Birkhauser*. 2002.
 92. **M. S. Mahmoud.** Robust Control and Filtering for Time-Delay Systems. *Marcel-Dekker*. 2000.
 93. **J. P. Richard.** Time-Delay Sytems: An Overview of Some Recent Advances and Open Problems. *Automatica*. 2003, Vol. 39, 10, pp. 1667-1694.
 94. **Han Q.** "On Robust Stability of Neutral Systems with Time-Varying Discrete Delay and Norm-Bounded Uncertainty". *Automatica*. 2004, Vol. 40, 6, pp. 1087-1092.
 95. **M. S. Mahmoud.** Delay-Dependent Robust Stability and Stabilization for Systems with Mismatched Uncertainties. *IMA J. Mathematical Control and Information*. 2000, Vol. 17, pp. 309-323.
 96. **Hale J. K. and S. M. Verduyn Lunel.** Introduction to Functional Differential Equations. *Springer-Verlag*. 1993.
 97. **He Y., Wu M., She J., and Wang Y.** "Parameter-Dependent Lyapunov Functional for Stability of Time-Delay Systems with Polytopic Uncertainties". *IEEE Trans. Automat. Control*. 2004, Vol. 49, 5, pp. 828-832.
 98. **He Y., Wu M., and She J.** "Delay-Dependent Stability Criteria for Linear Systems with Multiple Time-Delays". *IEE Proc.- Control Theory Appl.* 2006, Vol. 153, 4, pp. 447-452.

99. **He Y., Wang Q., Xie L., and Lin C.** Further Improvement of Free-Weighting Matrices Technique for Systems with Time-Varying Delay. *IEEE Trans. Automat. Control.* 2007, Vol. 52, 2, pp. 293-299.
100. **Boyd S., El Ghaoui L., Feron E. and Balakrishnan V.** "Linear Matrix Inequalities in Control". *SIAM Studies in Applied Mathematics.* 1994.
101. **Fridman E. and Shaked U.** ". An Improved Stabilization Method for Linear Systems with Time-Delay. *IEEE Trans. Automa. Contr.* 2002, Vol. 47, pp. 1931-1937.
102. **Fridman E. and Shaked U.** "Delay-Dependent Stability and Hoo Control: Constant and Time-Varying Delays". *Int. J. Control.* 2003, Vol. 76, pp. 48-60.
103. **Gu K. Q.** ". Discretized Lyapunov Functional for Uncertain Systems with Multiple Time-Delay". *Int. J. Control.* 1999, Vol. 72, 16, pp. 1436-1445.
104. **Jiang X. and Han Q.** "Hoo Control for Linear Systems with Interval Time-Varying Delay. *Automatica.* 2005, Vol. 41, 12, pp. 2099-2106.
105. **Jiao, X. and Shen, T.** Adaptive Feedback Control of Nonlinear Time-Delay Systems: The LaSalle-Razumikhin-Based Approach. *IEEE Trans. Automat. Contro.* 2005, Vol. 50, 11, pp. 1909-1913.
106. **Jing, X. J., D. L. Tan and Y. C. Wang.** An LMI Approach to Stability of Systems with Severe Time-Delay. *IEEE Trans. Automa. Control.* 2004, Vol. 49, 7, pp. 1192-1195.
107. **Kharitonov, V. L. and A. P. Zhabko,.** Lyapunov-Krasovskii Approach to the Robust Stability Analysis of Time-Delay Systems. *Automatica.* 2003, Vol. 39, pp. 15-20.
108. **Kwon, W. H., J. W. Kang, Y. S. Lee and Y. S. Moon,.** A Simple Receding Horizon Control for State Delayed Systems and its Stability Criterion. *J. Process Control.* 2003, Vol. 13, pp. 539-551.
109. **Kim, J. H.** Delay and its Time-Derivative Dependent Robust Stability of Time-Delayed Linear Systems with Uncertainty. *IEEE Trans. Automa. Contr.* 2001, Vol. 46, 5, pp. 789-792.
110. **Lee, C. S. and G. Leitmann.** Continuous Feedback Guaranteeing Uniform Ultimate Boundedness for Uncertain Linear Delay Systems: An Application to River Pollution Control. *Computer and Mathematical Modelling.* 1988, Vol. 16, pp. 929-938.
111. **Lee, Y. S., Y. S. Moon, W. H. Kwon and P. G. Park.** Delay-Dependent H_∞ Control for Uncertain Systems with a State-Delay. *Automatica.* 2004, Vol. 40, pp. 65-72.

112. **Park, P.** A Delay-Dependent Stability Criterion for Systems with Uncertain Time-Invariant Systems. *IEEE Trans. Automa. Control.* 1999, Vol. 44, 4, pp. 876-879.
113. **Lehman, B., J. Bentsman, S. V. Lunel and E. I. Verriest.** Vibrational Control of Nonlinear Time-Lag Systems with Bounded Delay: Averaging Theory, Stability and Transient Behavior. *IEEE Trans. Automa. Control.* 1994, Vol. 39, 5, pp. 898-912.
114. **Li, X. and C. de Souza.** Criteria for Robust Stability and Stabilization of Test for Uncertain Linear Systems with State-Delay. *Automatica.* 1997, Vol. 33, pp. 1657-1662.
115. **Lin, Q. G. Wang and T. H. Lee.** A Less Conservative Robust Stability Test for Linear Uncertain Time-Delay Systems. *IEEE Trans. Automa. Control.* 2006, Vol. 51, pp. 87-91.
116. **Martinez, L. A. M., and C. H. Moog.** New Insights on the Analysis of Nonlinear Time-Delay Systems: Application to The Triangular Equivalence. *Systems & Control Letters.* 2007, Vol. 56, pp. 133-140.
117. **Wang, D., D. H. Zhou and Y. H. Jin.** Nonlinear State Predictor for a Class of Nonlinear Time-Delay Systems. *Int. J. Systems Sciences.* 2004, Vol. 35, 3, pp. 197-210.
118. **Weisheng, C. and L. Junmin.** Backstepping Tracking Control for Nonlinear Time-Delay Systems. *J. Systems Eng. and Electro.* 2006, Vol. 17, 4, pp. 846-852.
119. **Wu, M., Y. He, J. H. She and G. P. Liu.** Delay-Dependent Criteria for Robust Stability of Time-Varying Delay Systems. *Automatica.* 2004, Vol. 40, 8, pp. 1435-1439.
120. **Yanushevsky, R. T.** A Class of Nonlinear Time-Delay Systems and Related Optimal Problems. *Computers and Mathematics with Applications.* 1999, Vol. 37, 6, pp. 73-78.
121. **Zhang, X. M., M. Wu, J. H. She and Y. He.** Delay-Dependent Stabilization of Linear Systems with Time-Varying State and Input-Delays. *Automatica.* 2005, Vol. 41, 8, pp. 1405-1412.
122. **Zheng, F. and P. M. Frank.** Robust Control of Uncertain Distributed Delay Systems with Application to the Stabilization of Combustion in Rocket Motor Chambers. *Automatica.* 2002, Vol. 38, pp. 487-497.
123. **Zribi, M., M. S. Mahmoud, M. Karkoub and T. Li.** H_∞ -Controllers for Linearized Time-Delay Power Systems. *Proc. IEE Generation, Trans. and Distr.* 2000, Vol. 147, pp. 401-408.
124. **<http://www.2aida.org>.** [Online]

Vita

Name: Hosam Abdul Rahim Fareed Arabasy

Nationality: Jordanian

Date and Place of Birth: December 26th 1973, Kuwait

BSc Degree: Electronic (Biomedical) Engineering, Yarmouk University, Jordan 1998

MSc Degree: Systems (Control) Engineering, KFUPM, Saudi Arabia 2009

Emails: harabasy@gmail.com, harabasy@gawab.com, harabasy@hotmail.com

Present Address: Al-Bandariah, Al-Khobar, Saudi Arabia

Permanent Address: Al-Kamaliah, Suwailih, Jordan